Optimizing Mechanical Ventilation by Bedside Lung Monitoring Systems in Critically ill Patients

Ido G. Bikker

Optimizing Mechanical Ventilation by Bedside Lung Monitoring Systems in Critically ill Patients

Ido G. Bikker

Financial support for the printing of this thesis was kindly provided by:

Erasmus University Rotterdam
Department of Intensive Care, Erasmus MC
SFMN consultancy BV
Astellas Pharma BV
CoMedical
Dräger Medical GmbH
Eurocept BV
Pfizer Nederland
ProStrakan Pharma BV

ISBN: 978-94-6299-061-6

Printing: Ridderprint BV
Cover: Ridderprint / I.G. Bikker

Copyright: I.G. Bikker, Rotterdam 2015, The Netherlands.

Optimizing Mechanical Ventilation by Bedside Lung Monitoring Systems in Critically ill Patients

Optimalisatie van mechanische ventilatie met bedside long monitoring systemen in ernstig zieke patiënten

Proefschrift

ter verkrijging van de graad van doctor aan de
Erasmus Universiteit Rotterdam
op gezag van de
rector magnificus

Prof.dr. H.A.P. Pols

en volgens besluit van het College voor Promoties.
De openbare verdediging zal plaatsvinden op

woensdag 13 mei 2015 om 13.30 uur

Ido Geert Bikker
geboren te Noordeloos

Promotiecommissie

Promotor:	Prof.dr. D.A.M.P.J. Gommers
Overige Leden:	Prof.dr. R.J. Stolker
	Prof.dr. C. Ince
	Prof.dr. J. Kesecioglu

Table of contents

Chapter 1 **9**
General introduction

Chapter 2 **21**
End-expiratory lung volume during mechanical ventilation: a comparison with reference values and the effect of positive end-expiratory pressure in intensive care unit patients with different lung conditions
Bikker IG, van Bommel J, Reis Miranda D, Bakker J, Gommers D.
Crit Care 2008;12:R145.

Chapter 3 **35**
Measurement of end-expiratory lung volume in intubated children without interruption of mechanical ventilation
Bikker IG, Scohy TV, Bogers AJ, BakkerJ, Gommers D.
Intensive Care Med 2009 Oct;35(10):1749-53

Chapter 4 **47**
Alveolar recruitment strategy and PEEP improve oxygenation, dynamic compliance of respiratory system and end-expiratory lung volume in pediatric patients undergoing cardiac surgery for congenital heart disease
Scohy TV, Bikker IG, Hofland J, de Jong PL, Bogers AJ, Gommers D.
Paediatr Anaesth 2009 Oct 23

Chapter 5 **57**
Assessment of ventilation inhomogeneity during mechanical ventilation using a rapid-response oxygen sensor-based oxygen washout method
Bikker IG, Holland W, Specht P, Ince C, Gommers D.
Intensive Care Medicine Exp 2014 2:14

Chapter 6 **73**
Lung volume calculated from electrical impedance tomography in ICU patients at different PEEP levels
Bikker IG, Leonhardt S, Bakker J, Gommers D.
Intensive Care Med 2009 Aug;35(8):1362-7

Chapter 7 **87**
Bedside measurement of changes in lung impedance to monitor alveolar ventilation in dependent and non-dependent parts by electrical impedance tomography during a positive end-expiratory pressure trial in mechanically ventilated intensive care unit patients.
Bikker IG, Leonhardt S, Reis Miranda D, Bakker J, Gommers D.
Crit Care 2010;14(3):R100.

Chapter 8 **103**
Electrical impedance tomography measured at two thoracic levels can visualize the ventilation distribution changes at the bedside during a decremental positive end-expiratory lung pressure trial
Bikker IG, Preis C, Egal M, Bakker J, Gommers D.
Crit Care 2011;15(4):R193

Chapter 9 **121**
Global and regional parameters to visualize the 'best' PEEP during a PEEP trial in a porcine model with and without acute lung injury.
Bikker IG, Blankman P, Specht P, Bakker J, Gommers D.
Minerva Anestesiol 2013 Sep;79(9):983-92.

Chapter 10 **141**
End-expiratory lung volume-guided PEEP setting in mild acute respiratory distress syndrome: a randomized controlled trial
Blankman P, Bikker IG, Gommers D.
Submitted

Chapter 11 **155**
Summary and conclusions
Sammenvatting en conclusie

Dankwoord **167**

Curriculum Vitae **171**

Publications **173**

PhD Portfolio **175**

Chapter 1

General introduction

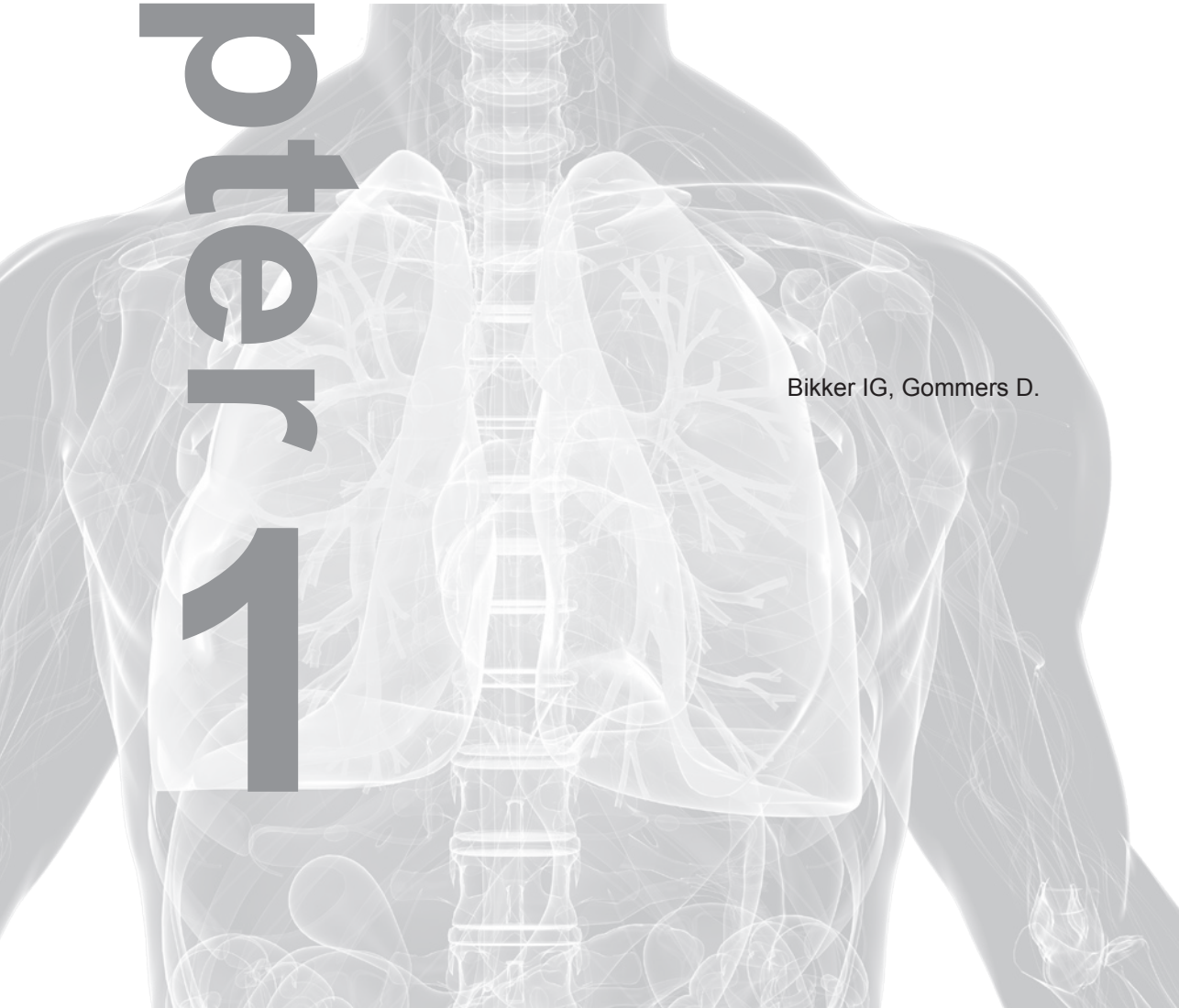

Bikker IG, Gommers D.

Mechanical ventilation and critical care

Since the original description of the acute respiratory distress syndrome (ARDS) in the Lancet by Ashbaugh et al. in 1967 (1), numerous studies have aimed to improve mechanical ventilation in order to prevent the associated ventilator-induced lung injury (VILI). In 2000, the landmark study of the ARDSnet group demonstrated that the application of tidal volumes of 6 ml/kg body weight resulted in a reduced mortality rate (2). This is now widely implemented as 'protective ventilation', not only in ARDS patients, but also in mechanically ventilated patients on both the operation room and the intensive care unit (ICU).

Brief history of mechanical ventilation

Descriptions of 'assisted' ventilation can be found over the centuries. The first reports of negative and positive pressure mechanical ventilation appeared in the early 1800s (3). In those days, the negative pressure ventilator was the modality most frequently used. This was first described in 1838 by John Dalziel, a Scottish physician. The patient was placed in sitting position in an airtight box, with only the head left outside. Subsequently, air was manually pumped in and out of the box to change the pressure within the box and in the patient's thoracic cage, thereby expanding the lungs while the patient was able to breathe room air. In 1928, the first iron lung was introduced by Drinker and was further improved in the following decades, and then widely used during the polio epidemics from the 1930s to 1960s. During this period, entire wards of patients were ventilated with these devices. Even prototypes of entire negative pressure operation rooms were designed. However, the equipment was very large, patients were difficult to reach, and effective ventilation with high airway pressure and application of positive end-expiratory airway pressure (PEEP) was not possible.

From the 1960s onwards, developments were primarily in the area of positive pressure ventilation. This was first described by Chaussier in 1780, as non-invasive ventilation with a bag and mask device. However, only after World War II did major developments start to take place. Tracheal intubation enabled the application of efficient ventilation with higher airway pressures and PEEP. ICUs emerged, requiring compact-sized ventilators. Moreover, the start of jet plane flight required and boosted the development of small intermittent positive pressure devices. Initially, ventilation was volume controlled and trigged by the ventilator

only. Patient triggering was developed during the 1970s with intermittent mandatory ventilation (IMV), which was later synchronized with the patient's efforts (SIMV). In 1981 the (still used) Servo 900C was developed, introducing pressure control and support ventilation, allowing the patient to initiate and change the breathing cycle. This was the beginning of the multitude of ventilatory modes which were introduced, especially after introduction of the microprocessor, enabling all sorts of respiratory and airflow patterns. Also, additional and more accurate monitoring options became available.

Ventilator-Induced Lung Injury (VILI)

During mechanical ventilation, increased airway pressures are often necessary to overcome additional forces from increased lung weight (e.g. edema, infiltrates), increased abdominal pressures, and the supine position. These factors result in inhomogeneous ventilation, as schematically shown in Figure 1. In region A the alveoli are collapsed during the entire ventilatory cycle, whereas low external pressure is exerted on alveoli in region B, which remain in an overstretched position. Region C represents alveoli which are normally ventilated. Tidal recruitment occurs between the regions of normally open and continuously atelectatic alveoli, leading to atelectotrauma. These alveoli collapse and open in a non-uniform way during each ventilatory cycle, generating high pressure and high shear forces on the fragile lung tissue. In 1970, using a mathematical model, Mead et al. demonstrated that a transpulmonary pressure of 30 cm H_2O would result in shear forces of 140 cm H_2O between the atelectatic and normal regions. Especially overdistended alveoli in which tidal recruitment occur, are at risk for VILI. In an atelectatic lung, an additional component of VILI is the occurrence of the 'baby lung' effect (4). Due to the widespread collapse of lung tissue, a currently advised tidal volume of 6 ml/kg will act as a tidal volume of 24 ml/kg with 75% lung collapse. This will result in excessive shear stress leading to alveolar epithelial disruption; this in turn leads to high permeability edema with increased lung weight and surfactant dysfunction, resulting in a further increase in atelectasis, eventually resulting in ARDS (5).

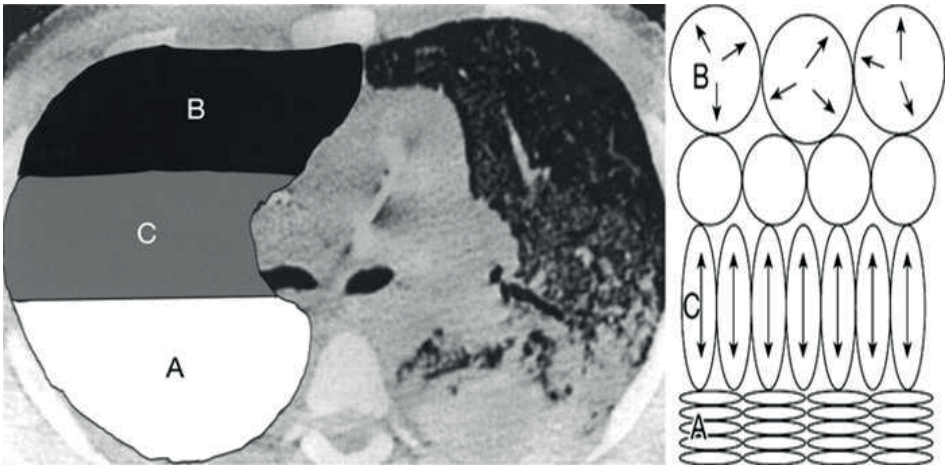

Figure 1. Schematic representation of lung regions during positive pressure mechanical ventilation.

Protective ventilation

In an editorial published in 1992, Lachmann postulated “the open lung concept (OLC)” (6), which aimed at opening collapsed alveoli in the lung by a critical inspiratory pressure and keeping them open by applying an adequate level of PEEP. After opening of collapsed lung tissue, ventilation should be with the lowest possible pressure amplitude and low tidal volumes (4-6 ml/kg) to minimize shear stress. The open lung is characterized by a low rate of intrapulmonary shunting and, clinically, can be evaluated by the PaO_2/FiO_2 ratio, which is also an important determinant in the diagnosis of ARDS (7). This strategy aims at minimizing shear stress with subsequent lower biotrauma and decreasing surfactant dysfunction, thereby lowering the required airway pressures. Several experimental studies demonstrated the beneficial effects of this strategy on lung function and histology (8). Amato et al. applied the OLC in a severe ARDS group and demonstrated a reduction in mortality (9). The effect of the OLC on the circulatory system was also studied by Dos Reis Miranda et al. (10;11). In cardiothoracic surgery patients, these authors studied the effect of lung recruitment on right ventricular afterload that can be impaired by increased airway pressures and lead to decreased cardiac output; they found no decrease in right ventricular afterload after full lung recruitment combined with low tidal volumes.

Current guidelines of protective ventilation in respiratory failure consist of a reduction of tidal volume to 6 ml/kg ideal body weight and a maximum plateau pressure of 30 cmH_2O. However the optimal level of PEEP remains unclear. In

2004 the ARDSnet studied lower vs. higher PEEP but were unable to demonstrate a benefit. Subsequently, two large clinical trials comparing high vs. low PEEP with fixed low tidal volume were unable to demonstrate a difference in mortality. However, a meta-analysis demonstrated a significant difference between the subgroups of ARDS, in favor of higher PEEP protocols in the severe ARDS group and lower PEEP levels in the mild ARDS group (12). Because higher PEEP may increase the risk of hyperinflation in the non-dependent lung region, a compromise must be found between PEEP-induced alveolar recruitment and prevention of hyperinflation. Also, Gattinoni et al. found extremely variable amounts of potential recruitable lung tissue on computer tomography (CT) scanning, which was strongly associated with the response to PEEP (13). Therefore, one should not use a so-called 'universal' level of PEEP, but rather the 'best' PEEP level that the individual patient needs at a specific time. This implies constant re-evaluation of the individual's ventilator settings, and the need for bedside lung monitoring to apply the 'best' PEEP.

Bedside lung monitoring techniques

Historically, mechanical ventilation is evaluated with respiratory variables such as respiratory compliance and variables of pulmonary gas exchange. Even CT has been used to evaluate lung regions. Although important information can be derived from these variables, they also have their limitations. For example, they are often non-specific, or not available due to the mode of mechanical ventilation used, or the size of the equipment. Monitoring lung function with blood gases requires minimal extrapulmonary shunt. Cressoni et al. demonstrated that variation in gas exchange cannot be used with sufficient confidence to assess anatomical lung recruitment in ARDS (14).

This initiated the search for additional or alternative lung monitoring equipment. Ideally, such a lung monitor should be safe, affordable, easy to use, small, precise, accurate, and always available. In this respect, techniques which are of interest include: bedside end-expiratory lung volume (EELV) measurements, lung electrical impedance tomography (EIT), lung inhomogeneity, lung ultrasound, and transpulmonary pressure calculation with esophageal pressure measurement (15). In this thesis some of these modalities were examined and efforts were made concerning their application in the clinical setting.

End-Expiratory Lung Volume (EELV) measurements

Functional residual capacity (FRC) is defined as the relaxed equilibrium volume of the lungs when there is no muscle activity, and no pressure difference between alveoli and the atmosphere. FRC is regularly determined at pulmonary function laboratories and is normally measured in sitting or standing position; it is gender, height and age dependent. It has been shown that FRC is decreased by 25% in healthy volunteers after changing from sitting to supine position during spontaneous breathing (16). This was confirmed by Hedenstierna and Edmark who observed that changing from sitting to supine position resulted in a decrease in FRC of 0.8-1 liter (17); if the patient is also sedated, FRC decreased further by an additional 0.4-0.5 liter. In critically ill patients receiving mechanical ventilation, the level of PEEP determines FRC and, therefore, it is considered more appropriate to use the term 'end-expiratory lung volume' (EELV). Measurements of EELV on the ICU have always been limited by the expensive and bulky equipment, as well as the use of tracer gases (16). Stenqvist and colleagues introduced a novel method to measure EELV without interrupting mechanical ventilation, based on a simplified and modified nitrogen multiple breath washout (NMBW) technique. This technique is integrated in the Engström ventilator (GE Healthcare, Madison, Wisconsin, USA) (18). The method requires a stepwise change in the inspired oxygen fraction (FiO_2) but without the need for supplementary tracer gases or specific additional monitoring equipment. In Chapter 2 we used the NMBW method integrated in the Carestation ventilator to measure EELV in an adult ICU population, because little information is available about EELV during mechanical ventilation. We studied 45 ICU patients with healthy and diseased lungs, and measurements were performed during a stepwise PEEP trial. EELV values were related to the patient's data on arterial oxygenation and respiratory compliance.

In children, decreased lung volume is of particular importance because of the lower elastic retraction forces and lower relaxation volume, which makes their lungs more prone to airway collapse (19). In Chapter 3 we evaluated the feasibility and precision of this NMBW technique in mechanically ventilated pediatric patients after cardiac surgery. Apart from the increased risk of airway collapse in children, in patients undergoing cardiac surgery, application of cardiopulmonary bypass with lung collapse will also increase the risk of airway collapse. Optimizing alveolar recruitment by the OLC and maintaining this recruited lung volume by adequate PEEP could be of particular benefit in this group, potentially reducing lung injury and an inflammatory reaction. In Chapter 4 we describe the effect of lung recruitment and PEEP on variables such as arterial oxygenation and respiratory

compliance in pediatric patients undergoing cardiac surgery for congenital heart disease.

Lung Ventilation Inhomogeneity

In an ideal healthy lung, all alveoli are ventilated simultaneously and more-or-less equally. However, in patients with lung abnormalities (such as chronic obstructive pulmonary disease) or in intubated patients with respiratory failure, alveoli are ventilated with different time constants. Airway size and function varies between lung regions. Inhomogeneity indices are often used in pulmonary function laboratories and can be improved after application of PEEP in pediatric anesthesia. However, use in the ICU has always been limited by the need of specialized equipment and tracer gases (20). Huygen et al. (21) and Gültuna et al. (22) worked on the development of inhomogeneity indices and indicator gas injectors based on SF6 for critically ill patients; however, implementation remained difficult due to the need for specialized equipment and gas containers at the bedside (21;23). In Chapter 5 we use the LUFU system that is available for non-invasive oxygen-based EELV measurements, and implemented inhomogeneity measurements. In that study we demonstrated the feasibility of previously described inhomogeneity indices based on oxygen washout.

Electrical Impedance Tomography

Electrical impedance tomography (EIT) is a non-invasive and radiation-free bedside imaging device that provides images of ventilation by measuring changes in electrical impedance. The technique is based on the injection of small currents and voltage (5 mA, 50 kHz) using electrodes on the skin surface (24). The measured impedance changes are translated in a cross-sectional picture of 32 by 32 pixels (Fig. 2). EIT visualizes the ventilation distribution and increases or decreases in the amount of air in a 5-10 cm thick slice of the thorax (25;26). All clinically available EIT systems use relative changes instead of absolute impedance values, due to the higher quality of the images (27). The difference between relative and absolute impedance can be explained by a case report, which also serves as an example for a possible application of this technique (28): during an experimental study, a pneumothorax developed accidentally in the right lung. A prominent increase of impedance was found in the ventral part of the right lung followed by a gradual decrease in ventilation-related impedance changes in the same region. Thereafter, the ventilation-related impedance changes of the right lung almost disappeared from the image because the thoracic cage was filled with air and tidal ventilation was impossible. If an EIT image had been made at that time

using absolute impedance, the right side of the image should have shown high impedance values because of the high air content, whereas relative impedance can detect only ventilation.

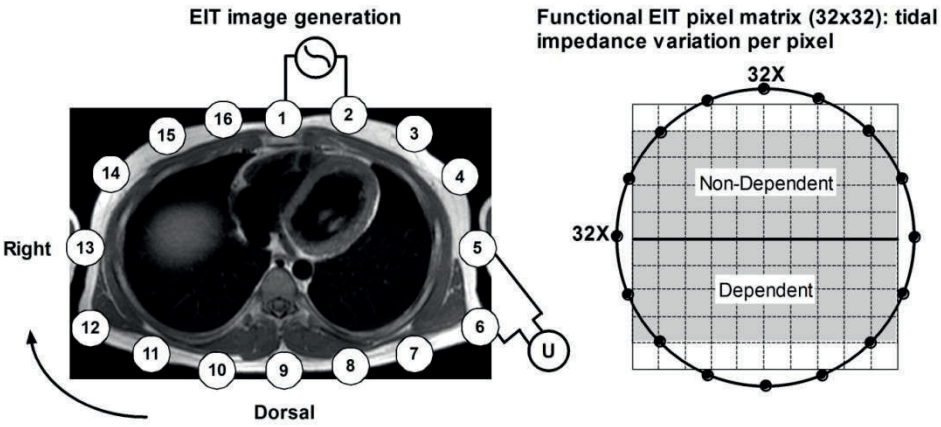

Figure 2. Schematic representation of EIT image generation. Left: cross-sectional CT picture with the placement of skin surface electrodes. Right: corresponding 32 pixels by 32 pixel matrix.

Different approaches are possible to analyze the vast amount of data generated by EIT measurements, including global and regional impedance changes, regional compliance calculations, center of gravity calculation, image subtraction, intratidal gas distribution, and even dividing the vascular component generating a ventilation/perfusion map.

Because EIT is very sensitive for air changes, earlier reports showed that the dynamic EIT at a single level could be used to calculate the global EELV changes (29;30). In Chapter 6 we studied the relation between EELV changes as measured by the nitrogen washout and EELV calculated from EIT in mechanically ventilated ICU patients.

Meier et al. introduced the subtraction of EIT images when altering the PEEP level (31). This enables a qualitative and quantitative assessment of regional change in ventilation after a PEEP change. In an experimental model, these authors showed that ventilation appeared and disappeared in certain lung regions when altering the PEEP level. In Chapter 7 we describe the use of regional compliance and use of subtraction of EIT images to provide a visual method for evaluating PEEP-induced improvement and loss of ventilation in dependent and non-dependent parts, just above the diaphragm, in patients with or without lung disorders.

EIT is almost always used at a single low thoracic level just above the diaphragm because this region is vulnerable to airway collapse, and also due to practical limitations. However, it is unlikely that lung inhomogeneity is only a ventral to dorsal process. Evidence from CT imaging suggests that there are different optimal PEEP values in the cranio-caudal direction to counteract the different superimposed pressures (32). In Chapter 8 we studied this phenomenon in adult ICU patients immediately after cardiothoracic surgery at two thoracic levels whilst they were undergoing a PEEP trial. EIT belts were placed just above the diaphragm and at the level of the armpits.

A more recent application, described by Lowhagen et al., is use of the high temporal resolution of EIT to assess intratidal gas distribution (ITV) in mechanically ventilated patients with ARDS (33). Intratidal regional gas distribution was analyzed by dividing the regional tidal impedance signal into eight isovolumetric parts. This visualizes the process of alveolar recruitment or alveolar distention within one breath and can be used for each pixel in the EIT map. In Chapter 9, using a porcine model of ARDS, we studied global and regional variables, including ITV, to identify which parameters should be used to describe ‘best’ PEEP. Another aim was to establish whether EIT parameters have additional value over the existing parameters in order to describe the 'best' PEEP.

In Chapter 10 we describe a single-site randomized controlled trial. We proposed and studied a protocol tailored to the individual patient based on EELV levels which, in our first study, were invariably decreased (34). This protocol aimed to restore EELV to predicted levels based on gender, height, age and body position, by changing PEEP levels. EIT was used to assess lung collapse and overdistention in the dependent and non-dependent lung regions at the PEEP levels applied.

Aim of the Thesis

The aim of this thesis is to guide PEEP settings during mechanical ventilation of patients in the ICU, with the use of EIT and/or specific equipment to measure FRC.

References

1. Ashbaugh DG, Bigelow DB, Petty TL, Levine BE. Acute respiratory distress in adults. *N Engl J Med* 1967; 7: 60-1.
2. ARDSnet. Ventilation with lower tidal volumes as compared with traditional tidal volumes for acute lung injury and the acute respiratory distress syndrome. The Acute Respiratory Distress Syndrome Network. *N Engl J Med* 2000; 342: 1301-8.
3. Kacmarek RM. The mechanical ventilator: past, present, and future. *Respir Care* 2011; 56: 1170-80.
4. Gattinoni L, Pesenti A. The concept of "baby lung". *Intensive Care Med* 2005; 31: 776-84.
5. Seeger W, Gunther A, Walmrath HD, Grimminger F, Lasch HG. Alveolar surfactant and adult respiratory distress syndrome. Pathogenetic role and therapeutic prospects. *Clin Investig* 1993; 71: 177-90.
6. Lachmann B. Open up the lung and keep the lung open. *Intensive Care Med* 1992; 18: 319-21.
7. Ranieri VM, Rubenfeld GD, Thompson BT, Ferguson ND, Caldwell E, Fan E, et al. Acute respiratory distress syndrome: the Berlin Definition. *JAMA* 2012; 307: 2526-33.
8. van Kaam AH, Dik WA, Haitsma JJ, De JA, Naber BA, van Aalderen WM, et al. Application of the open-lung concept during positive-pressure ventilation reduces pulmonary inflammation in newborn piglets. *Biol Neonate* 2003; 83: 273-80.
9. Amato MB, Barbas CS, Medeiros DM, Magaldi RB, Schettino GP, Lorenzi-Filho G, et al. Effect of a protective-ventilation strategy on mortality in the acute respiratory distress syndrome. *N Engl J Med* 1998; 338: 347-54.
10. Reis Miranda D, Gommers D, Struijs A, Meeder H, Schepp R, Hop W, et al. The open lung concept: effects on right ventricular afterload after cardiac surgery. *Br J Anaesth* 2004; 93: 327-32.
11. Reis Miranda D, Klompe L, Mekel J, Struijs A, van Bommel J, Lachmann B, et al. Open lung ventilation does not increase right ventricular outflow impedance: An echo-Doppler study. *Crit Care Med* 2006; 34: 2555-60.
12. Briel M, Meade M, Mercat A, Brower RG, Talmor D, Walter SD, et al. Higher vs lower positive end-expiratory pressure in patients with acute lung injury and acute respiratory distress syndrome: systematic review and meta-analysis. *JAMA* 2010; 303: 865-73.
13. Gattinoni L, Caironi P, Cressoni M, Chiumello D, Ranieri VM, Quintel M, et al. Lung recruitment in patients with the acute respiratory distress syndrome. *N Engl J Med* 2006; 354: 1775-86.
14. Cressoni M, Caironi P, Polli F, Carlesso E, Chiumello D, Cadringher P, et al. Anatomical and functional intrapulmonary shunt in acute respiratory distress syndrome. *Crit Care Med* 2007; 36: 669-75.
15. Blankman P, Gommers D. Lung monitoring at the bedside in mechanically ventilated patients. *Curr Opin Crit Care* 2012; 18: 261-6.
16. Ibanez J, Raurich JM. Normal values of functional residual capacity in the sitting and supine positions. *Intensive Care Med* 1982; 8: 173-7.
17. Hedenstierna G, Edmark L. The effects of anesthesia and muscle paralysis on the respiratory system. *Intensive Care Med* 2005; 31: 1327-35.
18. Olegard C, Sondergaard S, Houltz E, Lundin S, Stenqvist O. Estimation of functional residual capacity at the bedside using standard monitoring equipment: a modified nitrogen washout/washin technique requiring a small change of the inspired oxygen fraction. *Anesth Analg* 2005; 101: 206-12.

19. Mansell A, Bryan C, Levison H. Airway closure in children. *J Appl Physiol* 1972; 33: 711-4.

20. Schibler A, Henning R. Positive end-expiratory pressure and ventilation inhomogeneity in mechanically ventilated children. *Pediatr Crit Care Med* 2002; 3: 124-8.

21. Huygen PE, Gultuna I, Ince C, Zwart A, Bogaard JM, Feenstra BW, et al. A new ventilation inhomogeneity index from multiple breath indicator gas washout tests in mechanically ventilated patients. *Crit Care Med* 1993; 21: 1149-58.

22. Gultuna I, Huygen PE, Jabaaij C, Holland WP, Ince C, Bruining HA. A simple device to inject indicator gas for wash-out tests during mechanical ventilation. *Intensive Care Med* 1992; 18: 304-8.

23. Huygen PE, Feenstra BW, Holland WP, Ince C, Stam H, Bruining HA. Design and validation of an indicator gas injector for multiple gas washout tests in mechanically ventilated patients. *Crit Care Med* 1990; 18: 754-9.

24. Bikker IG, Leonhardt S, Bakker J, Gommers D. Lung volume calculated from electrical impedance tomography in ICU patients at different PEEP levels. *Intensive Care Med* 2009; 35: 1362-7.

25. Hedenstierna G. Using electric impedance tomography to assess regional ventilation at the bedside. *Am J Respir Crit Care Med* 2004; 169: 777-8.

26. Putensen C, Wrigge H, Zinserling J. Electrical impedance tomography guided ventilation therapy. *Curr Opin Crit Care* 2007; 13: 344-50.

27. Costa EL, Lima RG, Amato MB. Electrical impedance tomography. *Curr Opin Crit Care* 2009; 15: 18-24.

28. Preis C, Luepschen H, Leonhardt S, Gommers D. Experimental case report: development of a pneumothorax monitored by electrical impedance tomography. *Clin Physiol Funct Imaging* 2009; 29: 159-62.

29. Erlandsson K, Odenstedt H, Lundin S, Stenqvist O. Positive end-expiratory pressure optimization using electric impedance tomography in morbidly obese patients during laparoscopic gastric bypass surgery. *Acta Anaesthesiol Scand* 2006; 50: 833-9.

30. Hinz J, Hahn G, Neumann P, Sydow M, Mohrenweiser P, Hellige G, et al. End-expiratory lung impedance change enables bedside monitoring of end-expiratory lung volume change. *Intensive Care Med* 2003; 29: 37-43.

31. Meier T, Luepschen H, Karsten J, Leibecke T, Grossherr M, Gehring H, et al. Assessment of regional lung recruitment and derecruitment during a PEEP trial based on electrical impedance tomography. *Intensive Care Med* 2008; 34: 543-50.

32. Caironi P, Cressoni M, Chiumello D, Ranieri M, Quintel M, Russo SG, et al. Lung Opening and Closing During Ventilation of Acute Respiratory Distress Syndrome. *Am J Respir Crit Care Med* 2009.

33. Lowhagen K, Lundin S, Stenqvist O. Regional intratidal gas distribution in acute lung injury and acute respiratory distress syndrome--assessed by electric impedance tomography. *Minerva Anestesiol* 2010; 76: 1024-35.

34. Bikker IG, van BJ, Reis MD, Bakker J, Gommers D. End-expiratory lung volume during mechanical ventilation: a comparison with reference values and the effect of positive end-expiratory pressure in intensive care unit patients with different lung conditions. *Crit Care* 2008; 12: R145.

Chapter 2

End-expiratory lung volume during mechanical ventilation: a comparison with reference values and the effect of positive end-expiratory pressure in intensive care unit patients with different lung conditions

Bikker IG, van Bommel J, Reis Miranda D, Bakker J, Gommers D.

Crit Care 2008;12:R145.
Erratum: Crit Care 2009; 13:430

Abstract

Introduction:
Functional residual capacity (FRC) reference values are obtained from spontaneous breathing patients, and are measured in the sitting or standing position. During mechanical ventilation FRC is determined by the level of positive end-expiratory pressure (PEEP), and it is therefore better to speak of end-expiratory lung volume. Application of higher levels of PEEP leads to increased end-expiratory lung volume as a result of recruitment or further distention of already ventilated alveoli. The aim of this study was to measure end-expiratory lung volume in mechanically ventilated intensive care unit (ICU) patients with different types of lung pathology at different PEEP levels, and to compare them with predicted sitting FRC values, arterial oxygenation, and compliance values.

Methods:
End-expiratory lung volume measurements were performed at PEEP levels reduced sequentially (15, 10 and then 5 cmH_2O) in 45 mechanically ventilated patients divided into three groups according to pulmonary condition: normal lungs (group N), primary lung disorder (group P), and secondary lung disorder (group S).

Results:
In all three groups, end-expiratory lung volume decreased significantly ($p < 0.001$) while PEEP decreased from 15 to 5 cmH_2O, whereas the ratio of arterial oxygen tension to inspired oxygen fraction did not change. At 5 cmH_2O PEEP, end-expiratory lung volume was 31, 20, and 17 ml/kg predicted body weight in groups N, P, and S, respectively. These measured values were only 66%, 42%, and 34% of the predicted sitting FRC. A correlation between change in end-expiratory lung volume and change in dynamic compliance was found in group S ($p < 0.001$; $R_2 = 0.52$), but not in the other groups.

Conclusions:
End-expiratory lung volume measured at 5 cmH_2O PEEP was markedly lower than predicted sitting FRC values in all groups. Only in patients with secondary lung disorders were PEEP-induced changes in end-expiratory lung volume the result of derecruitment. In combination with compliance, end-expiratory lung volume can provide additional information to optimize the ventilator settings.

Introduction

Monitoring end-expiratory lung volume (EELV) might be a valuable tool to optimize respiratory settings in mechanical ventilation (1). However, determining EELV at the bedside in critically ill patients is not without difficulties. EELV can be measured using computed tomography (2,3), but this technique is not available for routine application at the bedside. Traditionally, EELV measurement techniques are based on dilution of tracer gases, such as sulfur hexafluoride washout (4), closed circuit helium dilution (5), or open circuit multibreath nitrogen washout (6). All of these techniques still need expensive and/or complex instrumentation and are in general not suitable for routine EELV measurements in the ICU. An alternative is the simplified helium dilution method, using a rebreathing bag with a helium mixture. However, an important disadvantage of this technique is that it requires interruption of mechanical ventilation for a short period of time (7). Recently, Stenqvist and colleagues (8) introduced a novel method to measure EELV without interruption of mechanical ventilation, based on a simplified and modified nitrogen multiple breath washout (NMBW) technique, which is integrated into a mechanical ventilator. This method requires a step change in the inspired oxygen fraction (FiO_2), without the need for supplementary tracer gases or specialized additional monitoring equipment (8).

Functional residual capacity (FRC) during spontaneous breathing is normally measured in the sitting or standing position and is length and age dependent. It has been shown that FRC is decreased by 25% in spontaneous breathing healthy volunteers after changing from the sitting to the supine position (9).

In critically ill patients receiving mechanical ventilation, FRC is determined by the level of positive end-expiratory pressure (PEEP), and it is therefore better to speak of EELV. Application of higher levels of PEEP leads to increased EELV values as a result of recruitment or further distention of already ventilated alveoli. To differentiate between recruitment and distention, EELV changes are combined with compliance values.

In this study, we used the modified NMBW technique to measure EELV at three different PEEP levels in mechanically ventilated patients with either non acute respiratory failure or with a primary or secondary lung disorder. The results were compared with reference predicted FRC values, arterial oxygenation, and dynamic compliance.

Materials and methods

The study population consisted of a convenient sample of 45 sedated and mechanically ventilated patients. For all patients, chest radiographs and, if available, computed tomography scans were retrospectively evaluated and related to clinical history and data to divide the patients into three groups: patients without acute respiratory failure (group N), those with respiratory failure due to primary lung disorders (group P), and those with respiratory failure due to secondary lung disorders (group S). With the approval of the local institutional human investigations committee, and after obtaining written informed consent, patients were enrolled in this study within 48 hours after intubation. Exclusion criteria were as follows: pneumothorax, pneumectomy, lung transplantation, and severe cardiovascular instability. Also, severe airflow obstruction due to chronic obstructive pulmonary disease (defined as forced expired volume in 1 second or vital capacity below predicted value minus 2 standard deviations) and patients with major inhomogeneous alveolar ventilation, as indicated by a significant upslope in phase III of the capnogram, were excluded. This was because gas wash out/in time could possibly be too short and end-tidal carbon dioxide could become unstable, potentially leading to errors in EELV measurement. We were unable to include patients with severe acute respiratory distress syndrome requiring a PEEP of 20 cm H_2O in our protocol because a pressure limitation of the COVX module (GE Healthcare, Helsinki, Finland) at around 18 to 20 cmH_2O PEEP.

During the study period patients were ventilated with an Engström Carestation ventilator (GE Healthcare, Madison, USA). EELV measurements were carried out with the COVX module (GE Healthcare, Helsinki, Finland) integrated within the ventilator. This module was described in detail previously (9). At baseline, patients were switched to the Engström ventilator and ventilated according to their original settings before any measurements were performed. PEEP was increased to 15 cm H_2O and the inspiratory pressure was adjusted to maintain tidal volume and without changing other ventilator settings. After a steady state had been achieved for at least 20 minutes, EELV was measured twice (wash-out and wash-in). This was repeated after a steady state lasting 10 minutes at both PEEP 10 cm H_2O and PEEP 5 cm H_2O. In all patients the same sequence of PEEP steps was used. Before each EELV measurement, hemodynamic and ventilatory parameters were recorded and arterial blood gas analysis performed (ABL 700; Radiometer, Copenhagen, Denmark) in order to calculate the arterial oxygen tension PaO_2/FiO_2 ratio. Arterial blood samples were taken 10 minutes after the PEEP change and just before the EELV measurement to avoid any influence of the

step change in FiO_2 required for the nitrogen wash-out/washin test. At the time of the EELV measurement, no muscle relaxation was used in the patients evaluated.

In all patients, EELV values were indexed according to predicted body weight (PBW) using the ARDSnet formula (10), which was calculated for men as 50 + 0.91 × (height (cm) – 152.4), and for women as 45.5 + 0.91 × (height (cm) – 152.4). In order to compare EELV values, reference EELV was calculated for each patient. Predicted sitting EELV was calculated for men as 2.34 × height (m) + 0.009 × age (years) – 1.09, and for women as 2.24 × height (m) + 0.001 × age (years) – 1.00 (11).

Statistical analysis

Statistical analysis was performed with SPSS version 14.0 (SPSS Inc., Chicago, IL, USA). Data are expressed as mean ± standard deviation. Comparisons between the three groups were performed using one-way analysis of variance. When appropriate, post hoc analyses were performed with Bonferroni's test. To test whether and how EELV and PaO_2/FiO_2 ratio decreased with lower PEEP levels, we used analysis of variance for repeated measurements. Again, Bonferroni's test was used for post hoc analyses if appropriate. Correlation between EELV and the PaO_2/FiO_2 ratio or dynamic compliance was analyzed using Pearson's correlation. For all comparisons $p < 0.05$ was considered significant.

Results

We examined 45 mechanically ventilated patients, retrospectively divided into three groups. Group N (n = 19) consisted of patients with traumatic brain injury (seven), cerebrovascular accident (seven), postoperative condition after neurosurgery (three), Fournier gangrene without evidence for pulmonary complications (one), and diagnostic laparotomy, without evidence for intra-abdominal hypertension (one). Group P (n = 16) consisted of patients with pneumonia (12), aspiration pneumonia (three) and major atelectasis (one). In group S (n = 10) all patients had abdominal sepsis. In the latter group, three out of the 10 patients had an open abdomen after decompression for intra-abdominal hypertension; the remainder of the patients with abdominal sepsis had an intra-abdominal pressure ranging from 10 to 15 cmH_2O. Patient's baseline data were comparable between the three groups, except for Lung Injury Score and baseline PEEP. Baseline PaO_2/FiO_2 ratio

and baseline dynamic compliance were lower in the two groups with lung disorders (groups P and S; Table 1).

Table 1. Data on the study patients by subgroup.

	Normal lung function (N)	Primary lung disorder (P)	Secondary lung disorder (S)
N	19	16	10
Gender, female (%)	36.8	31.3	30.0
Age (yrs)	49 (16)	52 (17)	52 (18)
Height (cm)	176 (9)	177 (10)	169 (6)
Weight (kg)	73.6 (11.6)	76.4 (15.0)	78.7 (27.3)
PBW (kg)	69.8 (10.6)	71.0 (10.8)	64.4 (7.2)
Lung Injury score	0.9 (0.5)	2.4 (0.8)	2.1 (0.3)
Tint (hrs)	20.2 (16.6)	28.9 (46.9)	30.1 (26.2)
Survival	16/19 (84%)	13/16 (81%)	4/10 (40%)
Baseline PEEP	6.2 (2.1)	11.3 (4.1)**	11.1 (2.6)**
Baseline PaO_2/FiO_2 ratio (kPa)	49.7 (11.9)	26.1 (11.2)**	32.7 (13.1)*
Baseline compliance dynamic (ml/cm H_2O)	50.3 (13.0)	35.6 (12.1)*	38.8 (12.2)*
Predicted sitting EELV (L)	3.3 (0.4)	3.4 (0.4)	3.2 (0.2)
Ventilation mode			
- Pressure control	7	8	4
- Pressure support	5	6	6
- Volume control	1	0	0
- Pressure controlled - Volume guaranteed	6	2	0

Unless otherwise stated, values are presented as mean ± standard deviation. The LIS (Murray) is based on dynamic compliance. *P = 0.05, **P =0.001, versus group N. Tint, time between intubation and inclusion.

Measured EELV is presented in Figure 1. In group N, measured EELV at 5 cmH_2O PEEP was 66% of the predicted sitting FRC (Fig. 2). In both groups with lung disorders (groups P and S), EELV was significantly ($p < 0.001$) reduced to 42%, and 35% of the predicted sitting FRC, respectively. Mean EELV values at 15, 10, and 5 cmH_2O PEEP were 40.9, 37.1, and 31.3 ml/kg PBW, respectively, in group N; 26.0, 23.6, and 20.2 ml/kg PBW in group P; and 23.4, 20.6, and 17.2 ml/kg PBW in group S.

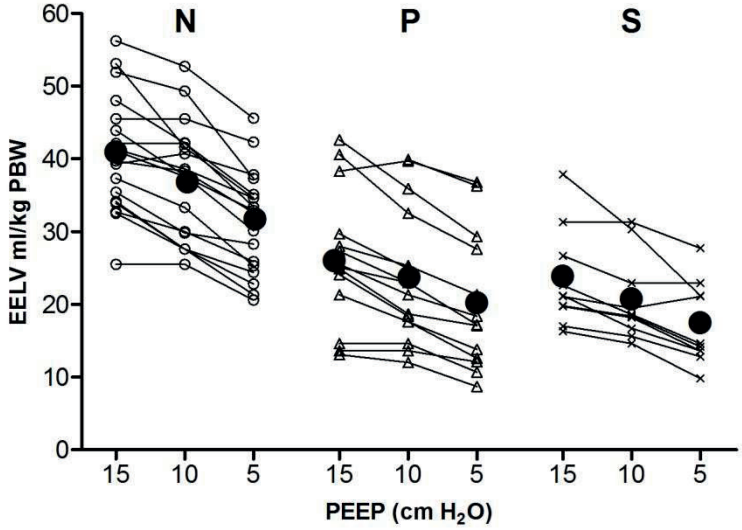

Figure 1: Progression of EELV (ml/kg PBW) in the individual patients over three stepwise reductions in PEEP. Mean EELV at each PEEP level is presented as black dots. Patients are divided according to the type of lung condition. Group N = normal lungs, group P = primary lung disorder, group S = secondary lung disorder.

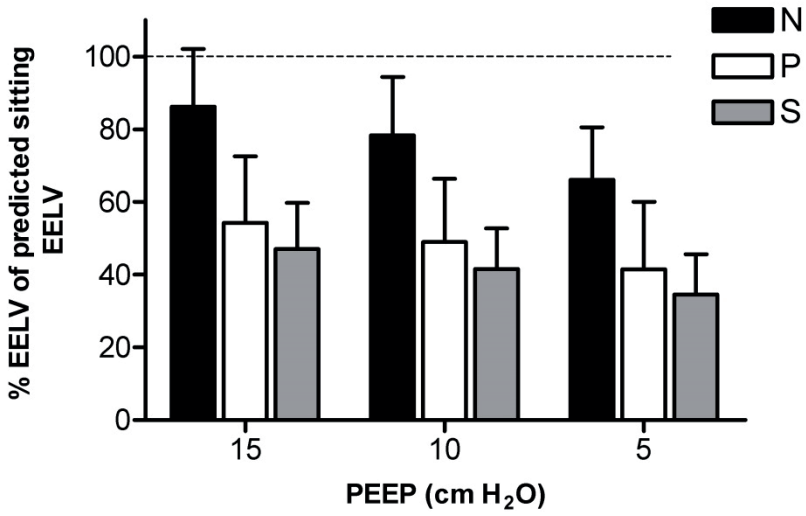

Figure 2: Measured EELV as percentage of predicted sitting EELV at three PEEP levels. The black dotted line represent predicted sitting EELV (100%). Patients in group N had normal lungs, those in group P had a primary lung disorder, and those in group S had a secondary lung disorder. Values are expressed as mean ± standard deviation.

The effect of the stepwise reduction in PEEP on the change in EELV in each patient in the three study groups is shown in Figure 1. Irrespective of group, EELV decreased linearly with reductions in PEEP; only in some patients was an increase or decrease in the slope observed after stepwise reduction in PEEP level. In all three groups, EELV decreased significantly ($p < 0.001$) while decreasing PEEP from 15 to 5 cm H_2O, whereas the PaO_2/FiO_2 ratio did not change (Figures 1 and 3). Patients in group S had lower EELV, but higher PaO_2/FiO_2 ratio, compared with group P (Figures 1 and 3). EELV was correlated with the PaO_2/FiO_2 ratio in group P ($R_2 = 0.40$; $p = 0.02$), but not in groups N and S. Correlation between change in EELV and change in compliance was significant in group S ($p < 0.001$; $R_2 = 0.52$), but not in groups N (P = 0.51) and P (P = 0.94; Figure 4).

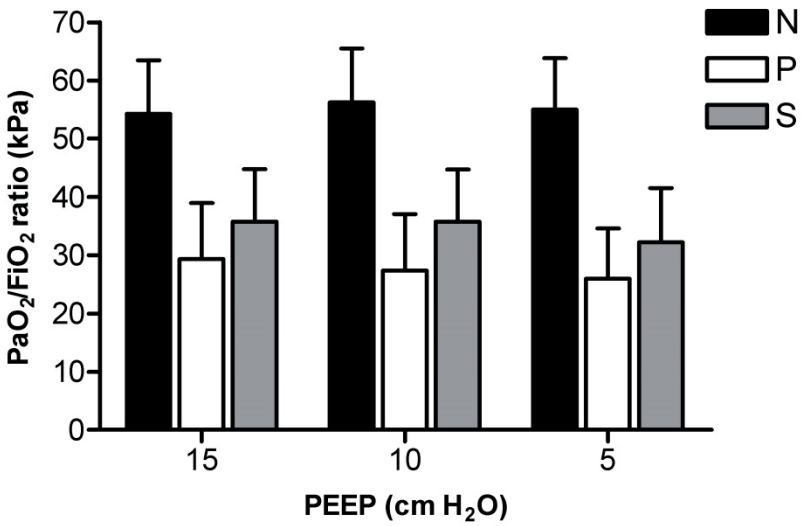

Figure 3: PaO_2/FiO_2 ratio in different types of lung conditions at three PEEP levels. Patients in group N had normal lungs, those in group P had a primary lung disorder, and those in group S had a secondary lung disorder. Values are expressed as mean ± standard deviation.

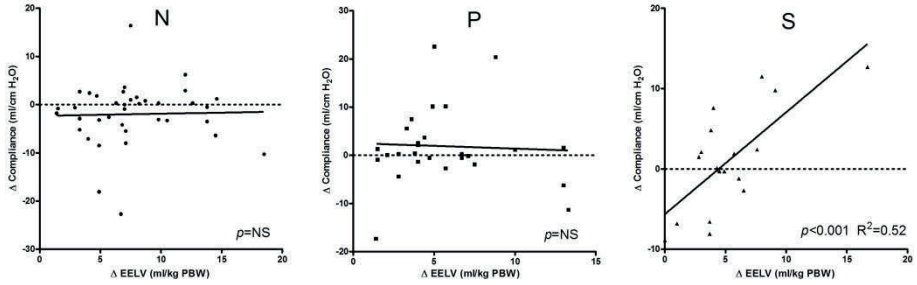

Figure 4: Correlation between change in EELV and change in dynamic compliance. Data are presented as the difference between the lowest PEEP level (5 cmH_2O) and 10 or 15 cmH_2O PEEP. Patients in group N had normal lungs, those in group P had a primary lung disorder, and those in group S had a secondary lung disorder.

Discussion

In mechanically ventilated patients with and without acute respiratory failure, measured EELV was markedly reduced in comparison with the predicted sitting FRC. Only in patients with secondary lung disorders were EELV changes accompanied by compliance changes, indicating derecruitment after reducing the PEEP. In addition, we did not identify a good correlation between measured EELV and the PaO_2/FiO_2 ratio in any of the three study groups.

Blood gases are frequently used to monitor the patient's lung function during mechanical ventilation. One should note that determining lung collapse by PaO_2/FiO_2 ratio assumes minimal extrapulmonary shunt. Cressoni and coworkers (12) have shown that variation in gas exchange cannot be used with sufficient confidence to assess anatomical lung recruitment in patients with acute lung injury (ALI)/acute respiratory distress syndrome (ARDS). It therefore seems reasonable to monitor lung volume changes caused by alveolar recruitment or alveolar collapse by repeated measurements of FRC instead of arterial oxygenation. FRC is defined as the relaxed equilibrium volume of the lungs when there is no muscle activity and no pressure difference between alveoli and the atmosphere (13). FRC is determined in spontaneously breathing, resting normal individuals at the end of a normal expiration, and therefore EELV is used to denote 'FRC' during mechanical ventilation.

Most studies addressing EELV in the ICU describe new techniques with good accuracy and good repeatability, but without presenting their data on the

measured EELV values for the individual ICU patient (5-7,14,15). Olegard and colleagues (8) measured EELV in a mixed ICU population and found EELV volumes ranging from 1,153 to 5,468 ml, but they did not report on the PEEP levels used. Only Neumann and coworkers (16) presented the measured mean EELV data for postoperative patients, and patients with ALI and chronic obstructive pulmonary disease at different PEEP levels (0, 5, and 10 cmH_2O). In their study, at a PEEP of 5 cmH_2O the measured EELV values were 2.5 l and 1.5 l in the postoperative and ALI groups, respectively. We found comparable EELV data for the similarly defined groups of patients (groups N and P) at comparable PEEP levels.

Normally, FRC reference values are obtained from spontaneously breathing patients in the standing or sitting position (11), but no reference values are available for supine mechanically ventilated patients. Ibanez and colleagues (9) showed that FRC decreased by 25% after changing the patient's position from sitting to supine during spontaneous breathing in healthy volunteers. If one assumes that ventilation of a 'healthy' lung at a PEEP of 5 cmH_2O occurs approximately at FRC level, then we found a reduction of 34% in group N (measured EELV compared with predicted sitting FRC). This extra reduction in EELV (34% versus 25%) is probably due to loss of muscle tension attributed to the use of sedation in our ICU patients. Furthermore, we opted not to use the regression equations of Ibanez and colleagues (9) to calculate predicted supine FRC for our patients, because their study population consisted of relatively short (mean 1.65 m) and young people (mean 35 years), and age was not included in their regression equations, whereas our ICU population consisted mainly of tall, elderly people. Instead, we decided to use the predicted sitting FRCs (11) and to reduce these based on the reduction observed in patients without lung disorders at 5 cmH_2O PEEP (34%) to estimate the predicted supine FRC. In groups P and S, measured EELV values were 63% and 53%, respectively, of the predicted supine FRC at a PEEP of 5 cmH_2O.

EELV measurements alone cannot be used to define optimal ventilator settings, because EELV can be increased without recruitment (already open alveoli are further inflated). Therefore, increases in both EELV and dynamic compliance should be used to identify successful recruitment. In our study, we did not perform a recruitment maneuver but applied 15 cmH_2O PEEP in all patients. In group N (without lung disorders), the PaO_2/FiO_2 ratio at 5 cmH_2O PEEP was already 49.7 kPa (373 Torr), indicating that the lung was almost entirely open at this PEEP level and therefore application of higher PEEP levels would only further inflate the already open alveoli. Gatinnoni and coworkers (17) showed that ARDS from

extrapulmonary origin had an abnormally increased chest wall elastance and a major response to the application of 15 cmH_2O PEEP, whereas ARDS from primary pulmonary origin showed a lack of recruitment and an increase in total respiratory elastance with the application of PEEP. The group with primary lung disorders could be compared to ARDS from pulmonary origin with consolidation, whereas group S could be compared to ARDS from extrapulmonary origin with prevalent edema and lung collapse. In our study we found a significant correlation between EELV and compliance in group S, but not in groups N and P (Figure 4). This change in lung volume accompanied by compliance indicates recruitment or derecruitment. In this study, patients with secondary lung disorders benefitted from higher PEEP, whereas patients with primary or without lung disorders did not, and application of higher PEEP in this setting would lead to overdistention.

Surprisingly, patients with secondary lung disorders due to abdominal sepsis had the lowest EELV values at the PEEP levels we used (Figure 1). From obese patients, we have learned that increased intra-abdominal pressure leads to decreased chest wall compliance and a cranial shift of the diaphragm, with consequent reduction in lung volume and atelectasis formation, especially in the basal parts of the lung. In group P (patients with pneumonia), EELV was also decreased but this was due to consolidation in a part of the lung.

For our measurements we used the NMBW method with a step change of 0.2 in FiO_2 to measure EELV. With this method, the alveolar EELV is calculated without the anatomical dead space (8). We were able to perform stable measurements in both controlled and partial support ventilatory modes, and we found no significant difference in EELV between the two modes. Using this NMBW method, it is assumed that there is no transfer of nitrogen from alveoli to blood during the EELV measurement, but this can be eliminated by an EELV measurement during wash-out and one during wash-in.

Conclusion

We conclude that in mechanically ventilated and sedated patients, EELV is markedly reduced compared with predicted sitting FRC values. In addition, it has become clear that PEEP induced changes in EELV not only represent recruitment or derecruitment, but they can also be the result of inflation or deflation of already ventilated lungs. Therefore, EELV alone is not the 'magic' bullet, but in combination with compliance it can provide additional information to optimize the ventilator settings.

Key messages

• EELV is markedly reduced in critically ill patients.
• EELV in ICU patients without lung disorders ventilated at 5 cm H_2O PEEP is reduced with 34% compared with FRC reference values in sitting position.
• Compliance and EELV are correlated only in patients with respiratory failure because of secondary lung disorders, indicating successful recruitment.
• During mechanical ventilation, EELV in combination with compliance can provide additional information that can help in optimizing ventilator settings.

References

1. Hedenstierna G. The recording of FRC--is it of importance and can it be made simple? *Intensive Care Med* 1993; 19: 365-6.
2. Drummond GB. Computed tomography and pulmonary measurements. *Br J Anaesth* 1998; 80: 665-71.
3. Gattinoni L, Caironi P, Pelosi P, Goodman LR. What has computed tomography taught us about the acute respiratory distress syndrome? *Am J Respir Crit Care Med* 2001; 164: 1701-11.
4. East TD, Wortelboer PJ, van Ark E, Bloem FH, Peng L, Pace NL, et al. Automated sulfur hexafluoride washout functional residual capacity measurement system for any mode of mechanical ventilation as well as spontaneous respiration. *Crit Care Med* 1990; 18: 84-91.
5. Di Marco F, Rota SL, Milan B, Stucchi R, Centanni S, Brochard L, et al. Measurement of functional residual capacity by helium dilution during partial support ventilation: in vitro accuracy and in vivo precision of the method. *Intensive Care Med* 2007; 33: 2109-15.
6. Fretschner R, Deusch H, Weitnauer A, Brunner JX. A simple method to estimate functional residual capacity in mechanically ventilated patients. *Intensive Care Med* 1993; 19: 372-6.

7. Patroniti N, Bellani G, Manfio A, Maggioni E, Giuffrida A, Foti G, et al. Lung volume in mechanically ventilated patients: measurement by simplified helium dilution compared to quantitative CT scan. *Intensive Care Med* 2004; 30: 282-9.
8. Olegard C, Sondergaard S, Houltz E, Lundin S, Stenqvist O. Estimation of functional residual capacity at the bedside using standard monitoring equipment: a modified nitrogen washout/washin technique requiring a small change of the inspired oxygen fraction. *Anesth Analg* 2005; 101: 206-12, table.
9. Ibanez J, Raurich JM. Normal values of functional residual capacity in the sitting and supine positions. *Intensive Care Med* 1982; 8: 173-7.
10. Knoben JE, Anderson PO. Handbook of clinical drug data. 7th ed. Hamilton, Ill.: Drug Intelligence; 1993.
11. Quanjer PH, Tammeling GJ, Cotes JE, Pedersen OF, Peslin R, Yernault JC. Lung volumes and forced ventilatory flows. Report Working Party Standardization of Lung Function Tests, European Community for Steel and Coal. Official Statement of the European Respiratory Society. *Eur Respir J Suppl* 1993; 16: 5-40.
12. Cressoni M, Caironi P, Polli F, Carlesso E, Chiumello D, Cadringher P, et al. Anatomical and functional intrapulmonary shunt in acute respiratory distress syndrome*. *Crit Care Med* 2007; 36: 669-75.
13. Lumb AB. Nunn's Applied Respiratory Physiology. fifth edition ed. Elsevier; 2006.
14. Eichler W, Schumacher J, Roth-Isigkeit A, Braun J, Kuppe H, Klotz KF. Automated evaluation of functional residual capacity by oxygen washout. *J Clin Monit Comput* 2002; 17: 195-201.
15. Zinserling J, Wrigge H, Varelmann D, Hering R, Putensen C. Measurement of functional residual capacity by nitrogen washout during partial ventilatory support. *Intensive Care Med* 2003; 29: 720-6.
16. Neumann P, Zinserling J, Haase C, Sydow M, Burchardi H. Evaluation of respiratory inductive plethysmography in controlled ventilation: measurement of tidal volume and PEEP-induced changes of end-expiratory lung volume. *Chest* 1998; 113: 443-51.
17. Gattinoni L, Pelosi P, Suter PM, Pedoto A, Vercesi P, Lissoni A. Acute respiratory distress syndrome caused by pulmonary and extrapulmonary disease. Different syndromes? *Am J Respir Crit Care Med* 1998; 158: 3-11.

Chapter 3

Measurement of end-expiratory lung volume in intubated children without interruption of mechanical ventilation

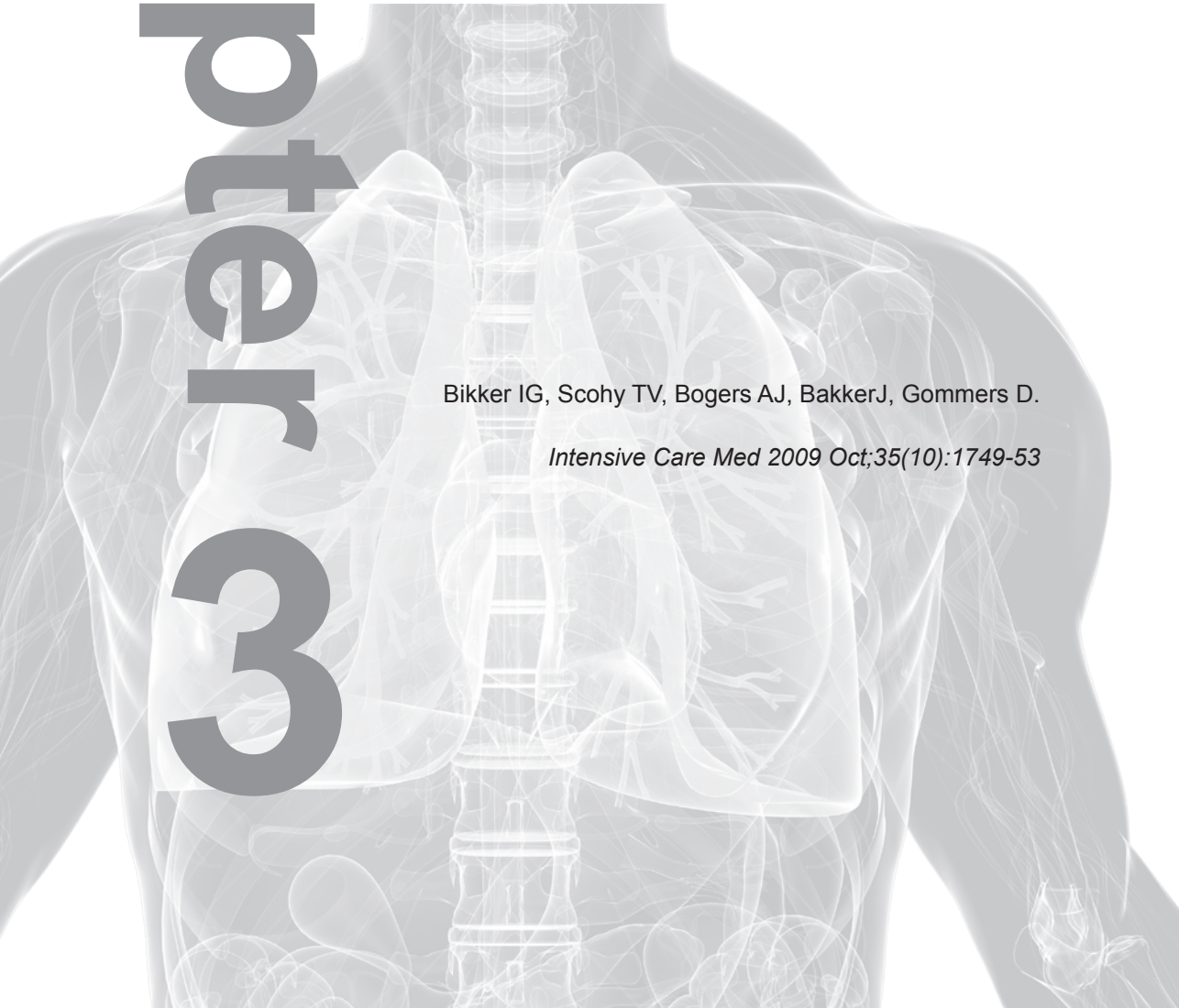

Bikker IG, Scohy TV, Bogers AJ, BakkerJ, Gommers D.

Intensive Care Med 2009 Oct;35(10):1749-53

Abstract

Purpose

Monitoring end-expiratory lung volume (EELV) is a valuable tool to optimize respiratory settings that could be of particular importance in mechanically ventilated pediatric patients. We evaluated the feasibility and precision of an intensive care unit (ICU) ventilator with an in-built nitrogen washout/washin technique in mechanically ventilated pediatric patients.

Methods

Duplicate EELV measurements were performed in 30 patients between 5 and 43 kg after cardiac surgery (age, median + range: 26, 3-141 months). All measurements were taken during pressure-controlled ventilation at 0 cm H_2O of positive end-expiratory pressure (PEEP).

Results

Linear regression between duplicate measurements was excellent (R_2 = 0.99). Also, there was good agreement between duplicate measurements, bias ± SD: -0.3% (-1.5 mL) ± 5.9% (19.2 mL). Mean EELV ± SD was 19.6±5.1 mL/kg at 0 cm H_2O PEEP. EELV correlated with age (p<0.001, r 0.92, R_2 0.78), body weight (p<0.001, r 0.91, R_2 0.82) and height (p<0.001, r 0.94, R_2 0.75).

Conclusion

This ICU ventilator with an in-built nitrogen washout/washin EELV technique can measure EELV with precision, and can easily be used for mechanically ventilated pediatric patients.

Introduction

Monitoring end-expiratory lung volume (EELV) might be a valuable tool to optimize respiratory settings in anesthetized ventilated patients (1). General anesthesia is known to promote lung volume reduction, which promotes atelectasis, lung compliance, and arterial oxygenation (2). In children, decreased lung volume is of special importance due to the lower elastic retraction forces and a lower relaxation volume, which makes them more prone to airway collapse (3;4). Furthermore, EELV has been described as one of the variables to be known to adequately assess mechanical characteristics of the ventilated lung (5).

However, determining EELV in ventilated patients is not without difficulty. EELV can be measured with computer tomography (6;7), but this technique is not available for routine measurements. Traditionally, EELV measurement techniques are based on dilution of tracer gases, like sulfur hexafluoride washout (8;9), closed circuit helium dilution (10), or open-circuit multibreath nitrogen washout (11-13). All these techniques require expensive and/or complex instrumentation, and are generally not suitable for routine EELV measurements during surgery and in the intensive care unit (ICU). An alternative is the simplified helium dilution method, using a re-breathing bag with a helium mixture. However, an important disadvantage of this latter technique is the interruption of mechanical ventilation for a short period of time (14).

Recently, Stenqvist et al. (15) introduced a novel method to measure EELV without interruption of mechanical ventilation, based on a simplified and modified Nitrogen Multiple Breath Washout (NMBW) technique, which is integrated within a mechanical ventilator. This method requires a step change in the inspired oxygen fraction (FiO_2), without the need for supplementary tracer gases or specialized additional monitoring equipment (15). Although this method has been successfully applied in adult ventilated patients at the ICU and whilst undergoing surgery (15-17), no data regarding feasibility and precision exist for mechanically ventilated pediatric patients.

Therefore, we evaluated the feasibility and precision of this NMBW device to measure EELV during mechanical ventilation of pediatric patients after cardiac surgery.

Methods

After approval of the local institutional human investigations committee, 30 mechanically ventilated children were enrolled in the study. All patients underwent cardiac surgery for congenital heart repair, and received postoperative mechanical ventilatory support in the ICU. Exclusion criteria were: severe cardiovascular instability, thoracic deformations, and residual intracardiac shunt postoperatively evaluated by transesophageal echocardiography (TEE).

EELV measurements were carried out with the COVX module (GE Healthcare, Helsinki, Finland) integrated within the ventilator. This module has been described in detail earlier (15). Briefly, O_2 and CO_2 are measured with standard clinical sensors and the residual N_2 as remaining ventilator air is calculated. A step change in the N_2 concentration is induced by changing the FiO_2. The N_2 volume change and N_2 fraction change is measured with the COVX module integrated in the Engström Carestation ventilator and EELV is calculated.

Patients were nasotracheally intubated with a cuffed Hi-Contour pediatric endotracheal tube (Mallinckrodt) and anesthesia was maintained with midazolam 0.1 mg/kg/h and sufentanil 1 mcg/kg/h. During the operation, patients were ventilated in pressure-controlled mode at the following settings: tidal volume of 6-8 mL/kg, frequency adjusted to maintain a $PaCO_2$ level between 4.5 and 5.5 kPa, positive end-expiratory pressure (PEEP) of 8 cm H_2O, I/E ratio of 1:1 and FiO_2 of 0.5. After weaning from cardiopulmonary bypass (CPB), the lungs were routinely re-expanded by a recruitment maneuver (RCM) and mechanical ventilation was continued with the same settings as before CPB. Once admitted to the ICU, mechanical ventilation was continued with the same settings as before transportation except for the FiO_2, which was set at 0.40 or 0.45. FiO_2 was decreased because the measurement requires a FiO_2 step change and becomes less precise at a FiO_2 above 0.65, according to manufacturer's specifications. Patients were sedated by midazolam intravenously (0.1 mg/kg/h) and morphine (10 mcg/kg/h).

After stabilization at the ICU, EELV was measured twice (washout and washin) with the COVX module by nitrogen washout/washin with first an incremental and second a decremental FiO_2 step of 0.2 at a PEEP of 0 cm H_2O. This measurement was repeated after 10 min. Before measurements, hemodynamic and ventilatory parameters were recorded and arterial blood gas analysis was performed.

Statistical analysis

Statistical analysis was performed with Graphpad software package (version 5.0, Graphpad Software Inc., San Diego, USA). Results are expressed as mean + SD for normally distributed data and median and interquartile range (IQR) for not normally distributed data. The Shapiro-Wilk normality test was used to evaluate the distribution of all data. Agreement between duplicate measurements was analyzed using Spearman correlation and Bland-Altman's analysis (18). For all comparisons, $p < 0.05$ was considered significant.

Results

In the present study, 30 mechanically ventilated patients were examined; Table 1 presents demographic data and main physiologic characteristics. All patients were studied after congenital cardiothoracic surgery and tolerated the procedure well. Repairs included closure of ventricular septal defect (7), closure of atrial septal defect (8), correction of tetralogy of Fallot (3), repair of subpulmonary stenosis (3) and subaortal stenosis (2), pacemaker implantation (1) and total cavopulmonary connection (6). The hemodynamic and ventilatory parameters before the measurements at 0 cm H_2O PEEP are provided in table 2.

Table 1: Characteristics of the patient population

N	30
Gender, female/male	9/21
Age in months, (range)	26 (3-141)
Weight, kg	10.9 (8.5)
Height, m	0.87 (0.35)

Data are presented as median with interquartile range unless stated otherwise

Table 2: Hemodynamic and ventilatory parameters before EELV measurement

Heart rate, bpm	124 (22)
Mean arterial pressure, mmHg	65 (11)
FiO_2, %	41 (2)
Tidal volume, mL/kg	7.7 (1.0)
pH	7.41 (0.05)
PaO_2, kPa	20.7 (7.3)
$PaCO_2$, kPa	4.38 (0.46)
SaO_2, %	98.4 (2.4)

Data are presented as mean with standard deviation unless stated otherwise

Linear regression between duplicate EELV measurements (as average of washin/washout) measured with the nitrogen washin/washout technique was performed. Duplicate measurements were highly correlated (p<0.001, r = 0.99, R_2 = 0.99). To assess the difference between the duplicate measurements a Bland-Altmann analysis was performed (Fig. 1). Bias ± SD was -0.3% (-1.5 mL) ± 5.9% (19.2 mL).

Mean EELV ± SD was 19.6±5.1 mL/kg at a PEEP level of 0 cm H_2O. Figure 2 shows the relation between EELV and patient characteristics. EELV was highly correlated with age (p<0.001, r 0.92, R_2 = 0.78), body weight (p<0.001, r = 0.91, R_2 = 0.82) and height (p<0.001, r = 0.94, R_2 = 0.75).

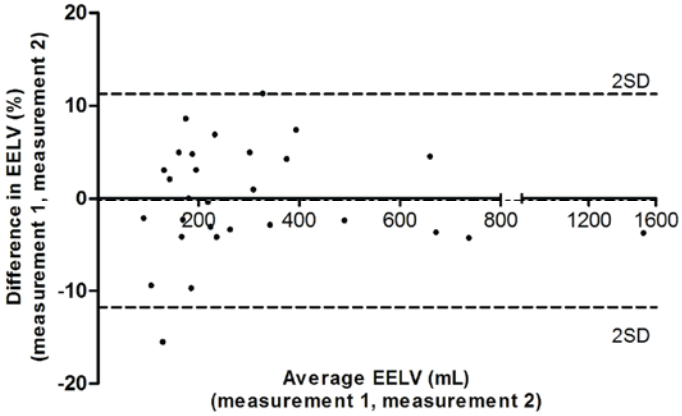

Figure 1: Bland-Altman analysis. Comparison of duplicate end-expiratory lung volume (EELV) measurements with the multibreath nitrogen washout technique. Measurements were performed in the supine position at 0 cm H_2O positive end-expiratory pressure (PEEP) in mechanically ventilated pediatric patients after cardiac surgery.

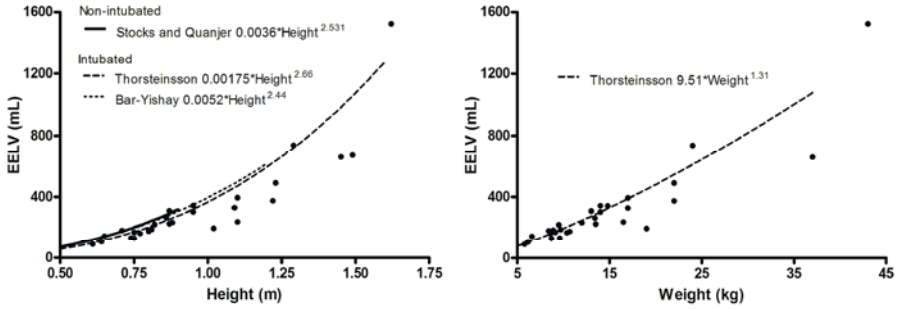

Figure 2: Relation between EELV (average of duplicates) and height or body weight. Measurements were performed in the supine position at 0 cm H_2O PEEP in mechanically ventilated pediatric patients after cardiac surgery. The lines represent non-linear regression equations from non-intubated children, Stocks and Quanjer (1) and intubated children at 0 cm H_2O PEEP, Thorsteinsson et al. (2) and Bar-Yishay et al. (3).

Discussion

The present study shows that, in sedated mechanically ventilated pediatric patients, this non-invasive multiple breath nitrogen washout technique can easily measure EELV with good precision. We confirmed that EELV is highly correlated with the patient's height and body weight (Fig. 2).

Precise and easily performable measurements of EELV are essential in order to use this parameter to optimize respiratory settings. Although accurate and precise methods to measure EELV are available for ventilated pediatric patients, these older methods require complex equipment or tracer gases that limit their use in clinical practice (8;19). In this study, we used an ICU ventilator with an in-built multiple breath nitrogen washout technique to measure EELV during mechanical ventilation; a good agreement was found between duplicate measurements with this device. Chiumello et al. (20) recently compared this technique with computed tomography and helium dilution in adult ICU patients and described high reproducibility between duplicate measurements (bias ± SD: 48 ±165 mL). In our pediatric patients an even better level of precision was found: bias ± SD 1.0 % (-1.7 mL) ± 5.7% (15.5 mL).

Although accuracy was not evaluated in the present study, measured EELV was comparable to that reported in other studies (21-24). Ungern-Sternberg et al. (24) described the effect of cardiopulmonary bypass and aortic clamping on EELV in children during mechanical ventilation with 3 cm H_2O PEEP; in their study EELV increased from 22±5 to 27±6 mL/kg after opening of the chest and decreased markedly to 16±5 mL/kg after closing the chest and was still reduced to 18±5 mL/kg during the following 90 min. These values are comparable with our measured EELV (mean ± SD) of 19.6±5.1 mL/kg. Moreover, our values are similar to those of pediatric patients during nitrous-oxide-halothane anesthesia, in which an EELV (mean ± SD) of 19±6 mL/kg was found during mechanical ventilation and 22±7 mL/kg during spontaneous breathing (22).

Schibler et al. (25) investigated the effect of different levels of PEEP on EELV in 22 mechanically ventilated children. At 0 cm H_2O PEEP, EELV was 20±7 mL/kg, which is comparable to our results. At a PEEP of 5 and 10 EELV increased to 24±8 and 28±6 mL/kg, respectively. In the present study, we did not use PEEP during the measurements to allow comparison to studies in which EELV was measured without PEEP (21;23;26). The application of PEEP is known to increase EELV and to prevent the formation of atelectasis. If higher PEEP levels were used, the EELV could be restored to above the normal values displayed in figure 2.

Among our patients, characteristics such as age, height, and body weight were highly correlated with measured EELV (Fig. 2). Our data are comparable with data from two previous studies (21;23) in which children were ventilated without the application of PEEP. Below 1 m of height or below 15 kg body weight, the agreement was excellent, but above 1 m of height most of our values were slightly below their regression equations. The reason for this is unknown. Thorsteinsson et al. (23), measured EELV directly after induction of anesthesia in healthy children and in children with cardiac anomalies, whereas we measured EELV after cardiac surgery with CPB. It is known that cardiac surgery and CBP may lower EELV (24;27). Bar-Yishay et al. (21), measured EELV in awake children in the supine position or during ketamine anesthesia. Ketamine anesthesia is known to preserve lung function (28).

A potential limitation of the present study is that accuracy was not evaluated. However, measured values with this technique were close to those of previous studies. Another potential limitation of the used technique is the measurement of EELV in patients requiring a FiO_2 > 65%. It has been suggested in the manufacturer's specifications that the accuracy error increases from 10% to 15% at a FiO_2 > 0.65 in adult patients. However, in the present study we only measured at a FiO_2 < 65. An important advantage of this method is that no tracer gases and no expensive or specialized equipment are required, bringing this parameter closer to clinical practice.

Therefore, we conclude that this nitrogen washout EELV technique can measure EELV with good precision. Especially below a height of 1 m or 15 kg body weight, our data are in good agreement with earlier comparable studies. Furthermore, this device can easily be used in mechanically ventilated pediatric patients without a tracer gas and without interruption of mechanical ventilation.

Reference List

1. Hedenstierna G. The recording of FRC--is it of importance and can it be made simple? *Intensive Care Med* 1993; 19: 365-6.
2. Hedenstierna G, Edmark L. The effects of anesthesia and muscle paralysis on the respiratory system. *Intensive Care Med* 2005; 31: 1327-35.
3. Lumb AB. Nunn's Applied Respiratory Physiology. 6th ed. Philadelphia: Elsevier; 2005.
4. Mansell A, Bryan C, Levison H. Airway closure in children. *J Appl Physiol* 1972; 33: 711-4.
5. Schibler A, Frey U. Role of lung function testing in the management of mechanically ventilated infants. *Arch Dis Child Fetal Neonatal Ed* 2002; 87: F7-F10.
6. Drummond GB. Computed tomography and pulmonary measurements. *Br J Anaesth* 1998; 80: 665-71.
7. Gattinoni L, Caironi P, Pelosi P, Goodman LR. What has computed tomography taught us about the acute respiratory distress syndrome? *Am J Respir Crit Care Med* 2001; 164: 1701-11.
8. Fuchs SI, Buess C, Lum S, Kozlowska W, Stocks J, Gappa M. Multiple breath washout with a sidestream ultrasonic flow sensor and mass spectrometry: a comparative study. *Pediatr Pulmonol* 2006; 41: 1218-25.
9. Ungern-Sternberg BS, Hammer J, Frei FJ, Jordi Ritz EM, Schibler A, Erb TO. Prone equals prone? Impact of positioning techniques on respiratory function in anesthetized and paralyzed healthy children. *Intensive Care Med* 2007; 33: 1771-7.
10. Di Marco F, Rota SL, Milan B, Stucchi R, Centanni S, Brochard L, et al. Measurement of functional residual capacity by helium dilution during partial support ventilation: in vitro accuracy and in vivo precision of the method. *Intensive Care Med* 2007; 33: 2109-15.
11. Fretschner R, Deusch H, Weitnauer A, Brunner JX. A simple method to estimate functional residual capacity in mechanically ventilated patients. *Intensive Care Med* 1993; 19: 372-6.
12. Hammer J, Numa A, Newth CJ. Total lung capacity by N2 washout from high and low lung volumes in ventilated infants and children. *Am J Respir Crit Care Med* 1998; 158: 526-31.
13. Sivan Y, Deakers TW, Newth CJ. An automated bedside method for measuring functional residual capacity by N2 washout in mechanically ventilated children. *Pediatr Res* 1990; 28: 446-50.
14. Patroniti N, Bellani G, Manfio A, Maggioni E, Giuffrida A, Foti G, et al. Lung volume in mechanically ventilated patients: measurement by simplified helium dilution compared to quantitative CT scan. *Intensive Care Med* 2004; 30: 282-9.
15. Olegard C, Sondergaard S, Houltz E, Lundin S, Stenqvist O. Estimation of functional residual capacity at the bedside using standard monitoring equipment: a modified nitrogen washout/washin technique requiring a small change of the inspired oxygen fraction. *Anesth Analg* 2005; 101: 206-12.
16. Bikker IG, van Bommel J, Dos Reis MD, Bakker J, Gommers D. End-expiratory lung volume during mechanical ventilation: a comparison to reference values and the effect of PEEP in ICU patients with different lung conditions. *Crit Care* 2008; 12: R145.
17. Erlandsson K, Odenstedt H, Lundin S, Stenqvist O. Positive end-expiratory pressure optimization using electric impedance tomography in morbidly obese patients during laparoscopic gastric bypass surgery. *Acta Anaesthesiol Scand* 2006; 50: 833-9.
18. Bland JM, Altman DG. Statistical methods for assessing agreement between two methods of clinical measurement. *Lancet* 1986; 1: 307-10.

19. Ungern-Sternberg BS, Regli A, Frei FJ, Hammer J, Jordi Ritz EM, Erb TO. Decrease in functional residual capacity and ventilation homogeneity after neuromuscular blockade in anesthetized preschool children in the lateral position. *Paediatr Anaesth* 2007; 17: 841-5.

20. Chiumello D, Cressoni M, Chierichetti M, Tallarini F, Botticelli M, Berto V, et al. Nitrogen washout/washin, helium dilution and computed tomography in the assessment of End Expiratory Lung Volume. *Crit Care* 2008; 12: R150.

21. Bar-Yishay E, Shulman DL, Beardsmore CS, Godfrey S. Functional residual capacity in healthy preschool children lying supine. *Am Rev Respir Dis* 1987; 135: 954-6.

22. Larsson A, Jonmarker C, Lindahl SG, Werner O. Lung function in the supine and lateral decubitus positions in anaesthetized infants and children. *Br J Anaesth* 1989; 62: 378-84.

23. Thorsteinsson A, Jonmarker C, Larsson A, Vilstrup C, Werner O. Functional residual capacity in anesthetized children: normal values and values in children with cardiac anomalies. *Anesthesiology* 1990; 73: 876-81.

24. Ungern-Sternberg BS, Petak F, Saudan S, Pellegrini M, Erb TO, Habre W. Effect of cardiopulmonary bypass and aortic clamping on functional residual capacity and ventilation distribution in children. *J Thorac Cardiovasc Surg* 2007; 134: 1193-8.

25. Schibler A, Henning R. Positive end-expiratory pressure and ventilation inhomogeneity in mechanically ventilated children. *Pediatr Crit Care Med* 2002; 3: 124-8.

26. Stocks J, Quanjer PH. Reference values for residual volume, functional residual capacity and total lung capacity. ATS Workshop on Lung Volume Measurements. Official Statement of The European Respiratory Society. *Eur Respir J* 1995; 8: 492-506.

27. Gilliland HE, Armstrong MA, McMurray TJ. The inflammatory response to pediatric cardiac surgery: correlation of granulocyte adhesion molecule expression with postoperative oxygenation. *Anesth Analg* 1999; 89: 1188-91.

28. Ungern-Sternberg BS, Regli A, Frei FJ, Ritz EM, Hammer J, Schibler A, et al. A deeper level of ketamine anesthesia does not affect functional residual capacity and ventilation distribution in healthy preschool children. *Paediatr Anaesth* 2007; 17: 1150-5.

Chapter 4

Chapter 4

Alveolar recruitment strategy and PEEP improve oxygenation, dynamic compliance of respiratory system and end-expiratory lung volume in pediatric patients undergoing cardiac surgery for congenital heart disease

Scohy TV, Bikker IG, Hofland J, de Jong PL, Bogers AJ, Gommers D.

Paediatr Anaesth 2009 Oct 23.

Abstract

Objective:
Optimizing alveolar recruitment by alveolar recruitment strategy (ARS) and maintaining lung volume with adequate positive end-expiratory pressure (PEEP) allow preventing ventilator-induced lung injury (VILI). Knowing that PEEP has its most beneficial effects when dynamic compliance of respiratory system (Crs) is maximized, we hypothesize that the use of 8 cm H_2O PEEP with ARS results in an increase in Crs and end-expiratory lung volume (EELV) compared to 8 cm H_2O PEEP without ARS and to zero PEEP in pediatric patients undergoing cardiac surgery for congenital heart disease.

Methods:
Twenty consecutive children were studied. Three different ventilation strategies were applied to each patient in the following order: 0 cm H_2O PEEP, 8 cm H_2O PEEP without an ARS, and 8 cm H_2O PEEP with a standardized ARS. At the end of each ventilation strategy, Crs, EELV, and arterial blood gases were measured.

Results:
EELV, Crs, and PaO_2/FiO_2 ratio changed significantly ($p < 0.001$) with the application of 8 cm H_2O + ARS. Mean $PaCO_2$ – $PetCO_2$ difference between 0 PEEP and 8 cm H_2O PEEP + ARS was also significant ($p < 0.05$).

Conclusion:
An alveolar recruitment strategy with relative high PEEP significantly improves Crs, oxygenation, PaCO2 – PetCO2 difference, and EELV in pediatric patients undergoing cardiac surgery for congenital heart disease.

Introduction

General anesthesia is known to promote atelectasis, which leads to reductions in lung volume, lung compliance, and arterial oxygenation (1). The goal of mechanical ventilation is to establish an acceptable level of gas exchange, while preventing ventilator induced lung injury (VILI). VILI is prevented by preventing repetitive re-opening of atelectatic lung areas and thus by decreasing alveolar stress (2). Optimizing alveolar recruitment by alveolar recruitment strategy (ARS) and maintaining lung volume with adequate positive end-expiratory pressure (PEEP) allow to prevent lung injury by decreasing alveolar stress (3–5).

In infants and children, we found only two studies reporting on ARS on normal lungs (4,6). Tusman et al. (4) used ARS to open up the lung and used PEEP of 5 cm H_2O to keep the lung open showing less atelectasis on magnetic resonance imaging. Marcus et al. (6) used only ARS (no PEEP) and showed an increase in compliance for 7 min. In their animal (adult New Zealand rabbits) study (lung lavage model), Rimensberger et al. (7,8) showed that ventilation after ARS of 30 cm H_2O boosted ventilatory cycle onto the deflation limb of the pressure / volume (PV) curve, when a PEEP of 8 cm H_2O was used. This ARS resulted in a significant increase in end-expiratory lung volume (EELV), oxygenation, and dynamic compliance despite equal PEEP levels used before and after ARS.

Knowing that PEEP has its most beneficial effects when dynamic compliance is maximized (9), we hypothesize that the use of 8 cm H_2O PEEP with ARS would result in an increase in Crs, EELV, and oxygenation compared to 8 cm H_2O PEEP without ARS and to zero cm H_2O PEEP (ZEEP), in pediatric patients undergoing cardiac surgery for congenital heart disease.

Methods

After obtaining approval from the local ethics committee and obtaining parental informed consent, 20 consecutive children scheduled for cardiac surgery for congenital heart disease were included. We included infants after cardiac surgery for congenital heart disease, infants without any residual intracardiac shunt, and who needed postoperative mechanical ventilatory support at the ICU. The exclusion criteria included (I) residual intracardiac shunting evaluated by transesophageal echocardiography (TEE), (II) hemodynamic instability defined by

>5mcg/kg/min dobutamine, (III) rhythm other than sinus rhythm, (IV) valve regurgitation evaluated by TEE, and (V) respiratory failure defined by a FiO_2 > 0.8.

Before induction of anesthesia, all patients were monitored with a five-lead, two-channel electrocardiogram, non-invasive blood pressure measurement, and pulse oximetry. After the insertion of a peripheral venous line, general anesthesia was induced using midazolam 0.2 mg/kg, sufentanil 2 mcg/kg, and pancuronium 0.15 mg/kg. Patients were nasotracheally intubated with a cuffed Hi-Contour pediatric endotracheal tube (Mallinckrodt, Athlone, Ireland) and pressure controlled ventilated (PCV) using a Engstrom Carestation ventilator (GE Healthcare, Helsinki, Finland). Anesthesia was maintained using midazolam 0.1 mg/kg/h and sufentanil 1 mcg/kg/h. Invasive monitoring via 20G arterial line in the femoral artery, an internal jugular central venous catheter, a Foley bladder catheter, a rectal temperature probe, and the Oldelft MicroMultiplane TEE probe (Oldelft, Delft, The Netherlands) connected to a iE33 (Philips, Andover, MA, USA) were routinely inserted (10). Mechanical ventilation was performed at the following settings (tidal volume of 8 ml/kg, frequency adjusted to maintain a $PaCO_2$ level between 4.5 and 5.5 kPa, PEEP of 8 cm H_2O, and I:E ratio 1:1). No additional catheters were inserted. During cardiopulmonary bypass (CPB), continuous positive airway pressure was applied at a level of 8 cm H_2O. After weaning from CPB, the lungs were re-expanded by an ARS: peak airway pressure of 40 cm H_2O, PEEP of 8 cm H_2O for five consecutive mechanical breaths with I:E ratio 1:1, which was sufficient to recruit all of the visible atelectasis before closure of the thorax. Mechanical ventilation was continued with the same settings as before cardiopulmonary bypass. The existence of any residual intra-cardiac shunt was ruled out by TEE (10). At the end of the operation, the patients were disconnected from the ventilator and ventilated by hand bagging during transport to the ICU. Once admitted at the ICU, an ARS as used intraoperatively was performed, and mechanical ventilation was continued with the same settings as before transportation. Patients were sedated by midazolam intravenously (0.1 mg/kg/h) and morphine (10 mcg/kg/h).

After arrival at the ICU, three different ventilation strategies were applied to each patient in the following order: 0 cm H_2O PEEP, 8 cm H_2O PEEP without an ARS, and 8 cm H_2O PEEP with a standardized ARS. The ARS was performed as intraoperatively (4). Each ventilation strategy commenced after disconnection from the ventilator for 15 s, which has been shown to result in immediate lung collapse (4) and was applied for 20 min. At the end of each ventilation strategy, Crs (ml/kg/cm H_2O), EELV as determined with a COVX module integrated in the ventilator (GE Healthcare, Helsinki, Finland), and arterial blood gases were

measured. Measurements of EELV were obtained by multiple breath nitrogen washout technique. This equipment has been described in detail earlier (11).

Fluid management during the study was guided clinically in the beginning of each ventilation strategy, if right atrial pressure (RAP) and blood pressure (BP) raise while compressing the liver manually, the patients were considered hypovolemic. Hypovolemia was treated with gelofusine bolus 5 ml/kg. This action was repeated until BP stayed stable, and only RAP raised during manual liver compression.

After each ventilator setting, we specially looked for air leakage in the thoracic drainage systems.

Statistical analysis

Statistical analysis was performed using GRAPHPAD 5.0 software package (Graphpad software Inc. San Diego, CA, USA). Results are expressed as mean ±SD for normal distributed data and median + interquartile range (IQR) for not normally distributed data. The Shapiro–Wilk normality test was used to evaluate the distribution of all data. To compare EELV, compliance, and PaO_2/FiO_2 ratio, values were normalized to 0 cm H_2O PEEP. Repeated measures ANOVA with Bonferroni's posthoc analysis was used to test whether the normalized EELV, compliance, and PaO_2/FiO_2 ratio were different at the used PEEP levels. A $p<0.05$ was considered to represent a significant difference.

Results

Twenty consecutive mechanically ventilated pediatric patients after cardiac surgery were studied. None of the patients met any exclusion criteria. The main demographic data are reported in Table 1. Surgery included the correction of ASD (5), VSD (4), subvalvular PS after TOF (3), TOF (2), SVD (2), subvalvular AS (1), aortic coarctation (1), DCRV (1), and PM implantation (1). In all patients, EELV, Crs, and blood gases were collected. None of the patients were excluded.

Descriptive statistics of EELV/kg (Fig. 1), Crs (Fig. 2), and PaO_2/FiO_2 ratio (Fig. 3) are shown for the three measured PEEP levels: 0 cm H_2O (0), 8 cmH_2O (8), and 8 cm H_2O + ARS (8 + ARS). Data are normalized to values at 0 cm H_2O PEEP (0 PEEP = 100%).

Tabel 1: Patient demographics

N	20
Gender, female/male	6/14
Age, months (median +range)	34 (3 - 132)
Weight, kg (median + range)	10.1 (8.8 – 15.5)
Length, m (median + range)	0.85 (0.75 – 1.07)

Table 2:

	0 cm H_2O	**8 cm H_2O**	**ARS + 8 cm H_2O**
EELV (ml/kg)	18.65	28.55*	34.95*
Crs (ml/kg/cm H_2O)	0.67	0.78*	0.91*
PaO_2/FiO_2 ratio (kPa)	53.4	56.8	65.8*
$PaCO_2$ - $PetCO_2$	0.24	0.22	0.12*

* = Significant compared to 0 cm H_2O

Median EELV/kg increased from 18.65 ml (IQR 15.95–21.45) to 28.55 ml (IQR 23.40–31.45) while increasing PEEP from 0 to 8 cm H_2O, and with the application of an ARS, median EELV/kg increased to 34.95 ml (IQR 28.60 – 39.85). The changes from 0 to 8 ($p < 0.001$; 99% CI 12.11 to 6.86), from 8 to 8 + ARS ($p < 0.001$; 99% CI 8.04 to 2.79), and from 0 to 8 + ARS ($p < 0.001$; 99 % CI 17.53 to 12.22) were significant (Table 2).

We also found a significant increase in median Crs that increased from 0.67 ml/kg/cm H_2O (IQR 0.59–0.75) to 0.78 ml/kg/cm H_2O (IQR 0.65–0.87) while increasing PEEP from 0 to 8 cm H_2O ($p < 0.01$; 95% CI 22.48 to 2.92), and with the application of an ARS, median Crs increased to 0.91 ml/kg/cm H_2O (IQR 0.77–1.06), between 8 and 8 + ARS: ($p < 0.001$; 95% CI 31.43 to 11.87). Between 0 and 8 + ARS, $p < 0.001$ (95% CI 44.13 to 24.57) (Table 2).

Median PaO_2/FiO_2 ratio increased from 53.4 kPa (IQR 46.5–61.3) to 56.8 kPa (IQR 46.5–63.3) while increasing PEEP from 0 to 8 cm H_2O (p = NS), and with the application of an ARS, median PaO_2/FiO_2 ratio increased to 65.8 kPa (IQR 50.5–71.70),($p < 0.01$, 95% CI 26.73 to 5.96). Between 0 and 8 + ARS, $p < 0.001$ (95% CI 31.58 to 10.82) (Table 2).

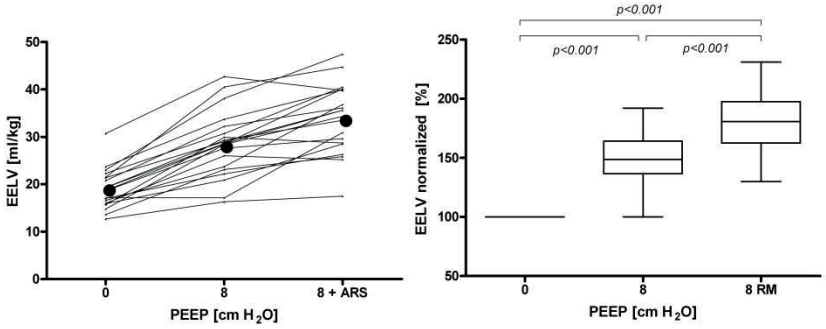

Figure 1: End-expiratory lung volume(EELV)

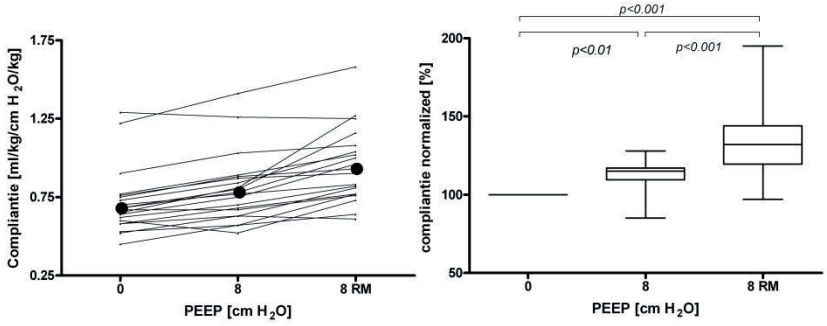

Figure 2: Compliance

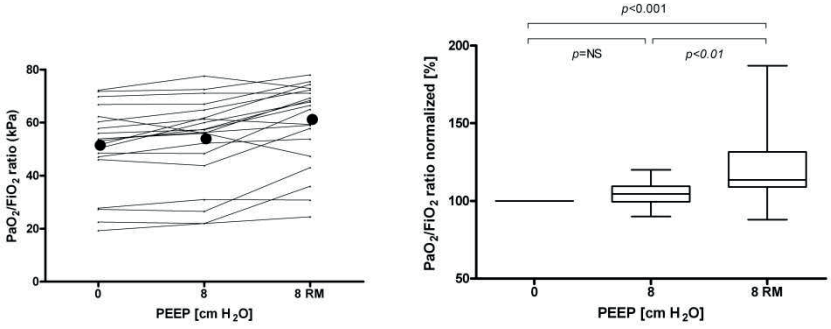

Figure 3: PaO_2/FiO_2 ratio

Mean $PaCO_2$ – $PetCO_2$ differences (Fig. 4) decrease from 0.24 kPa (SD 0.29) to 0.22 kPa (SD 0.37) while increasing PEEP from 0 to 8 cm H_2O (*p* = NS) and to 0.12 kPa (SD 0.26) with an ARS (*p* = NS) (Fig. 4), the difference between 0 and 8 + ARS was significant (*P* = 0.014; 95% CI 0.026 to 0.213) (Table 2).

We found no significant differences in heart rate (HR), mean arterial pressure (MAP), and right atrial pressure (RAP) between the three strategies. Mean HR, RAP, and MAP in the 0 cm H_2O group were 123 b/min (SD 21.2), 9.64 mmHg (SD 4.16), and 64.3 mmHg (SD 10.3). In the 8 cm H_2O group, mean HR, RAP, and MAP were respectively 123 b/min (SD 21.5), 11.1 mmHg (SD 4.2), and 66.5 mmHg (SD 9.6). In the 8 + ARS group, mean HR, RAP, and MAP were respectively 123 b/min (SD 22.8), 10.8 mmHg (SD 4.2), and 69.2 mmHg (SD 13.3). Eleven patients received one fluid bolus, and nine patients received two fluid boluses when applying 8 cm H_2O. After ARS + 8 cm H_2O, eight patients received one fluid bolus.

None of the patients had air leakage on any moment.

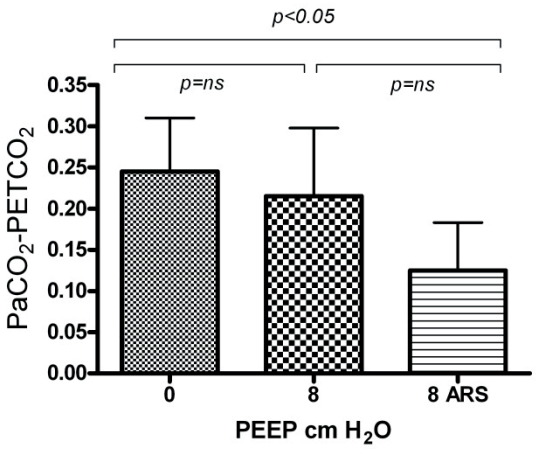

Figure 4: $PaCO_2$–$PetCO_2$.

Discussion

We applied ARS and 8 cm H_2O PEEP in 20 infants without apparent lung disease after cardiac surgery for congenital heart disease and obtained significantly improved dynamic compliance of respiratory system (Crs), EELV, and oxygenation compared to 8 cm H_2O PEEP without ARS and compared to zero PEEP. There were no statistical significant changes in any of the other hemodynamic measurements.

The principal objective of the ventilatory management of acute lung injury is to maintain an acceptable gas exchange without inflicting additional lung damage (8). The key elements of such a lung protective approach are to limit lung over-distention and to maintain sufficient EELV to prevent alveolar collapse (8). The significant simultaneous increase in EELV and Crs observed during ARS + PEEP compared to PEEP alone is because of the extra recruitment of collapsed alveoli. If ARS + PEEP would preferentially over-distend aerated alveolar units before expanding collapsed areas, it would cause only an increase in EELV, and Crs would remain unchanged or even decrease. An increase in EELV after enhancing the total airway pressure is to be expected and carries the risk of hyperinflating the lungs, but an increase in both, Crs and EELV, indicates that there is no over-distention. The significant ($p < 0.05$) decrease in $PaCO_2$–$PETCO_2$ difference (Figure 4) and the significant increase in PaO_2/FiO_2 ratio ($p < 0.001$), although clinically not relevant, indicates that there is less ventilation perfusion mismatch, shunting or both, in the 8 cm H_2O PEEP + ARS group compared to 0 cm H_2O PEEP group. Less ventilation perfusion mismatch means less atelectasis.

We optimized alveolar recruitment by ARS and maintained lung volume with adequate PEEP, hereby decreasing low volume trauma by decreasing shear stress of repetitive closing and reopening of small airways and thus preventing for VILI (3–5). We also showed that Crs and EELV improved after 8 cm H_2O PEEP + ARS indicating that there is no alveolar stress or over-distention which would cause large volume trauma. Because mechanical ventilation should maximize oxygenation and minimize VILI while having the least detrimental effect on hemodynamics (9), further investigation is needed to clarify the optimal PEEP level with an ARS in children without apparent lung disease under general anesthesia, because it is possible that a lower or higher PEEP might result in an even bigger efficacy.

Conclusion

Our study provides strong evidence to conclude that ARS + PEEP of 8 cm H_2O significantly decreases ventilation perfusion mismatch, shunting or both and improves dynamic compliance of the respiratory system (Crs), oxygenation, and EELV. Such changes likely reduce alveolar stress and may thereby reduce the potential risk for VILI in children recovering from heart surgery.

References

1. Rusca M, Proietti S, Schnyder P, Frascarolo P, Hedenstierna G, Spahn DR, et al. Prevention of atelectasis formation during induction of general anesthesia. Anesth Analg 2003; 97: 1835-9.
2. Pinhu L, Whitehead T, Evans T, Griffiths M. Ventilator-associated lung injury. Lancet 2003; 361: 332-40.
3. Kaditis AG, Motoyama EK, Zin W, Maekawa N, Nishio I, Imai T, et al. The effect of lung expansion and positive end-expiratory pressure on respiratory mechanics in anesthetized children. Anesth Analg 2008; 106: 775-85, table.
4. Tusman G, Bohm SH, Tempra A, Melkun F, Garcia E, Turchetto E, et al. Effects of recruitment maneuver on atelectasis in anesthetized children. Anesthesiology 2003; 98: 14-22.
5. Amato MB, Barbas CS, Medeiros DM, Magaldi RB, Schettino GP, Lorenzi-Filho G, et al. Effect of a protective-ventilation strategy on mortality in the acute respiratory distress syndrome. N Engl J Med 1998; 338: 347-54.
6. Marcus RJ, van der Walt JH, Pettifer RJ. Pulmonary volume recruitment restores pulmonary compliance and resistance in anaesthetized young children. Paediatr Anaesth 2002; 12: 579-84.
7. Rimensberger PC, Cox PN, Frndova H, Bryan AC. The open lung during small tidal volume ventilation: concepts of recruitment and "optimal" positive end-expiratory pressure. Crit Care Med 1999; 27: 1946-52.
8. Rimensberger PC, Pristine G, Mullen BM, Cox PN, Slutsky AS. Lung recruitment during small tidal volume ventilation allows minimal positive end-expiratory pressure without augmenting lung injury. Crit Care Med 1999; 27: 1940-5.
9. Ward NS, Lin DY, Nelson DL, Houtchens J, Schwartz WA, Klinger JR, et al. Successful determination of lower inflection point and maximal compliance in a population of patients with acute respiratory distress syndrome. Crit Care Med 2002; 30: 963-8.
10. Scohy TV, Gommers D, Jan ten Harkel AD, Deryck Y, McGhie J, Bogers AJ. Intraoperative evaluation of micromultiplane transesophageal echocardiographic probe in surgery for congenital heart disease. Eur J Echocardiogr 2007; 8: 241-6.
11. Olegard C, Sondergaard S, Houltz E, Lundin S, Stenqvist O. Estimation of functional residual capacity at the bedside using standard monitoring equipment: a modified nitrogen washout/washin technique requiring a small change of the inspired oxygen fraction. Anesth Analg 2005; 101: 206-12.

Chapter 5

Assessment of ventilation inhomogeneity during mechanical ventilation using a rapid-response oxygen sensor-based oxygen washout method

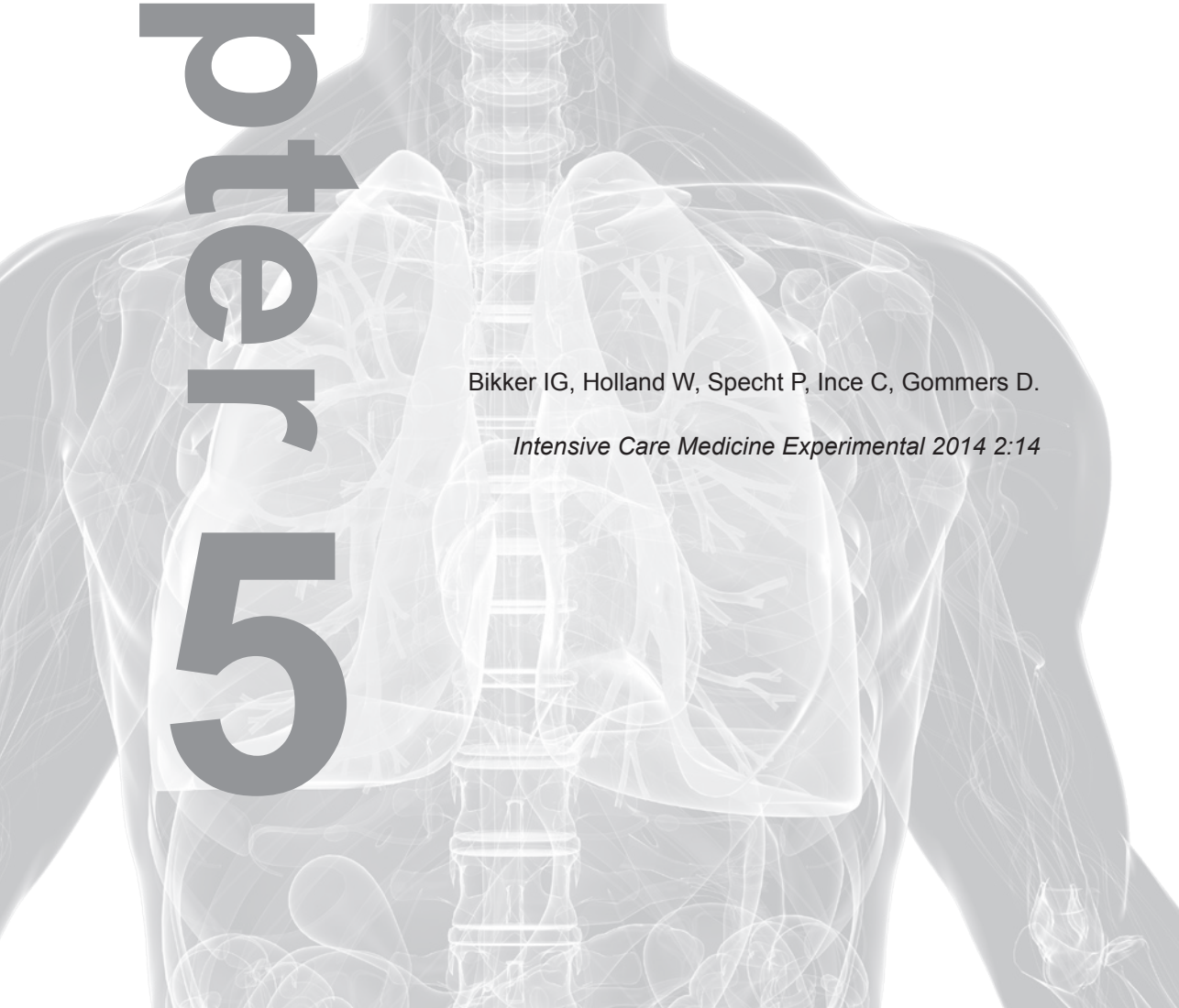

Bikker IG, Holland W, Specht P, Ince C, Gommers D.

Intensive Care Medicine Experimental 2014 2:14

Abstract

Purpose:
Ventilatory inhomogeneity indexes in critically ill mechanically ventilated patients could be of importance to optimize ventilator settings in order to reduce additional lung injury. The present study compared six inhomogeneity indexes calculated from the oxygen washout curves provided by the rapid oxygen sensor of the LUFU end-expiratory lung volume measurement system.

Methods:
Inhomogeneity was tested in a porcine model before and after induction of acute lung injury (ALI) at four different levels of positive end-expiratory pressure (PEEP; 15, 10, 5 and 0 cm H_2O). The following indexes were assessed: lung clearance index (LCI), mixing ratio, Becklake index, multiple breath alveolar mixing inefficiency, moment ratio and pulmonary clearance delay.

Results:
LCI, mixing ratio, Becklake index and moment ratio were comparable with previous reported values and showed acceptable variation coefficients at baseline with and without ALI. Moment ratio had the highest precision, as calculated by the variation coefficients. LCI, Becklake index and moment ratio showed comparable increases in inhomogeneity during decremental PEEP steps before and after ALI.

Conclusions:
The advantage of the method we introduce is the combined measurement of end-expiratory lung volume (EELV) and inhomogeneity of lung ventilation with the LUFU fast-response medical-grade oxygen sensor, without the need for external tracer gases. This can be combined with conventional breathing systems. The moment ratio and LCI index appeared to be the most favourable for integration with oxygen washout curves as judged by high precision and agreement with previous reported findings. Studies are under way to evaluate the indexes in critically ill patients.

Background

Although mechanical ventilation is critical for the survival of most patients with respiratory failure, it can also induce lung damage and may even be the primary factor in lung injury (1).

In 1970, Mead et al. estimated that forces acting on lung tissue might be 4.5 times higher when lungs are inhomogeneously ventilated (2). This was confirmed in an experimental work using tomographic microscopy, which generates detailed three-dimensional alveolar geometries (3). This inhomogeneity raises stress and increases the risk to develop ventilator-induced lung injury (VILI). Therefore, the use of an inhomogeneity index as a target for ventilation strategies would be very beneficial in this context.

Although inhomogeneity indexes are often used in pulmonary function labs and improve after application of positive end-expiratory pressure (PEEP) in paediatric anaesthesia, use in the intensive care unit (ICU) is limited by the need of specialized equipment and tracer gases (4,5). Huygen et al. (6,7) and Gültuna et al. (8) worked on the development of inhomogeneity indexes and indicator gas injectors based on SF6 for critically ill patients, but implementation remained difficult due to the need of specialized equipment and gas containers at the bedside (6,7). The availability of a routine method to quantify inhomogeneous alveolar ventilation at the bedside is expected to help to optimize ventilator settings in individual patients to achieve optimal gas exchange. Recently, methods were introduced to measure end-expiratory lung volume (EELV) with an ICU ventilator based on an oxygen washout curve (9,10). In the LUFU system developed by Weismann et al., oxygen concentration is measured with a diverting oxygen analyser with response time < 200 ms. This method offered the possibility to develop an index of ventilatory inhomogeneity which we believe will be of great potential use in combination with EELV measurement to optimize ventilatory settings at the bedside.

The aim of this study was to develop a bedside-available computer program to compare six well-established indexes of ventilatory inhomogeneity calculated from the oxygen washout/washin curve of the LUFU system (11). The system was evaluated for reproducibility and agreement with historical reference values in a porcine model before and after induction of acute lung injury (ALI), at four different levels of PEEP.

Methods

The study was approved by the local animal experimental committee and was in accordance with the National Guidelines for Animal Care and Handling (permit number 142-08-01).

Description of the indexes of ventilatory inhomogeneity

Ventilatory inhomogeneity is calculated from an oxygen washout procedure performed with the LUFU system (Dräger Medical, Lubeck, Germany). This system was developed to measure EELV based on oxygen washout and has been described earlier (12). Briefly, O2 is measured with a side stream sensor, and airway flow is retrieved from the EVITA XL ventilator (Dräger Medical, Lubeck, Germany). A step change in the O2 concentration is induced by changing the FiO_2. Oxygen concentration and flow are integrated in the LUFU system, and the EELV is calculated from the washout or washin procedure.

The indexes were calculated as described in the article by Larsson et al. (11) and are shown in Figure 1. All indexes were calculated with a computer model programmed in MATLAB (MathWorks, Natick, MA, USA). Apparatus dead space was always subtracted from the tidal volume measurement when cumulative ventilation was calculated. 'Volume turnover' (TO) is defined as the cumulative expired volume divided by EELV. Some indexes are designed to be less dependent on tidal volume, dead space and lung volumes by comparing the measured inhomogeneity to inhomogeneity in an ideal lung. Ideal number of breaths and ideal volume turnovers refer to the washout in the simulated lung, which has the same EELV, dead space and tidal volume as the patient, but with uniform alveolar gas.

Lung clearance index (LCI) equals the number of observed volume turnovers required to reach the final end-tidal oxygen concentration within a 1/40th part of the total oxygen shift (difference between final and initial concentration levels; see Fig. 1a). In Figure 1, the vertical dashed line is drawn through the intersection point of the horizontal crossing level line with the washin curve. Its upper x-axis coordinate value determines the needed number as TO_actual_(1/40) (13).

Mixing ratio is the ratio between the observed and the ideal number of breaths required to reach the final end-tidal oxygen concentration within a 1/40th part of the total oxygen concentration shift (see Fig. 1a,b). The vertical dashed

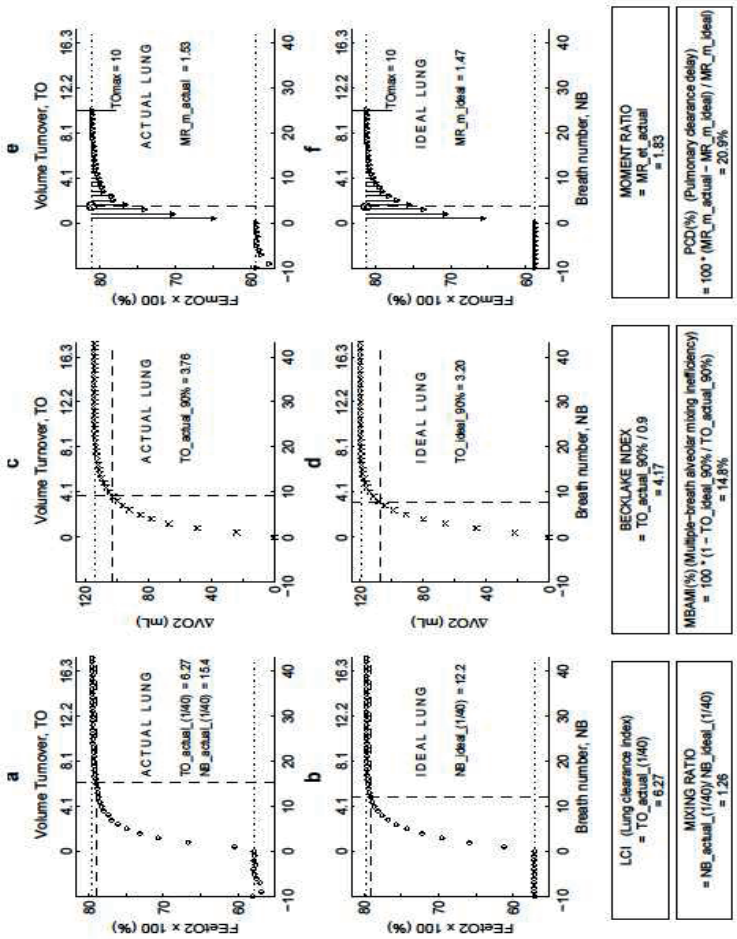

Figure 1 Washin curves and calculations of the six indexes for one studied animal at 5 cm H_2O PEEP. Graphs (a, c, e) show curves as observed from the actual lung. Graphs (b, d, f) show curves as calculated from an ideal lung (well-mixed one-compartment model) that has the same FRC, VD and tidal volume as the actual lung. Text boxes below the graphs contain the expressions to calculate these indexes. Horizontal axes display breath number (lower) and volume turnovers (upper). Vertical axes display expired end-tidal oxygen concentration (a, b), change in oxygen volume content in the lung (mL) (c, d) and mean expired oxygen concentration (e, f). Dotted horizontal lines represent the initial and final levels of expired end-tidal or mean concentrations (a, b, e, f) and of oxygen volume change in the lung (c, d). Dashed horizontal lines represent crossing reference lines. Dashed vertical lines determine the specific numbers of volume turnovers or number of breaths, used in the expressions to calculate the indexes.

lines determine these numbers as NB_actual_(1/40) and NB_ideal_(1/40), respectively (14).

Becklake index is the number of volume turnovers required to wash 90% of the ultimate total increase of oxygen content in the lung, divided by 0.9 (see Fig. 1c). The vertical dashed line is drawn through the interception point of the horizontal crossing level line with the washin curve. Its upper x-axis coordinate value determines the needed number as TO_actual_90% (15).

Multiple-breath alveolar mixing inefficiency (MBAMI) is defined as 100 × (1 – Volume turnover ideal/Volume turnover actual), where the number of volume turnovers refers to how many turnovers are required to wash 90% of functional residual capacity (FRC) free of tracer gas (Fig. 1c,d) (16).

Moment ratio is designed to summarize the whole washout curve using moment analysis; it equals the mean residence time. It is the ratio between the first (μ1) and zeroth (μ0) moments of the washout curve (17):

$$\mu 0 = \sum_{k=1}^{N} Y(k)(\eta_k - \eta_{k-1})$$

And

$$\mu 1 = \sum_{k=1}^{N} \eta_k Y(k)(\eta_k - \eta_{k-1})$$

where k is the number of breaths, η is the number of volume turnovers at breath k, N is the number of the washout breaths at which ηk exceeds a preselected value (10, as mostly used), and Y(k) is the end-tidal tracer gas concentration at breath k minus by the concentration at the end of washin. We used the same calculation as Larsson et al. who started the summations with the first washout breath (k = 1). The calculated value of MR_et_actual is shown in Figure 1 upper right text box (11). A mechanical analogon may help to understand the concept of moment ratio. Consider a mechanical balance on which a weightless beam is attached a series of weights proportional to the length of

the line pieces and positioned along the beam as suggested in Figure 1e,f. The horizontal position of the pivotal point (encircled cross mark) where the beam balances determines the moment ratio.

Pulmonary clearance delay (PCD; %) is calculated as the alternative method proposed by Larsson et al., based on moment ratio: PCD (%) = 100 × (Actual moment ratio – Ideal moment ratio)/Ideal moment ratio (11). This way of expressing PCD has the advantage of being easily adapted to automatic calculation. Contrary to Larsson et al., we truncated the summation process at TO=

10 (see Fig. 1e,f). The values involved in the summation are shown as vertical solid line pieces. The involved moment ratio's named MR_m_actual and MR_m_ideal for the actual and the ideal lung, respectively, are indicated by the drawn dashed lines.

The indexes were evaluated for integration with oxygen-based washout and automated calculation; precision was calculated as the variation coefficient. Also, values were compared with previously reported findings, also used by Larsson et al. (11).

LUFU system

The LUFU system to measure EELV was developed and described in great detailby Weismann et al. (12). Briefly, this system measures only oxygen with a small diverting oxygen analyser (response time < 200 ms). Currently, this system has to be connected to a Dräger ICU ventilator; in the current study, we used an Evita XL ventilator. Measurements are started by manually changing the inspired oxygen fraction with a change of at least 10%. The LUFU system then calculates the EELV from the washout/in curve, without the need for external tracer gases. Because only suitable side stream sensors are available, the resulting problem of corrupted synchronicity between flow and gas concentration measurement was solved by the use of an ingenious physical/mathematical model of the pneumatical circuit of the analyser (12,18). Also, the washout curve has to be meticulously corrected for oxygen consumption; the oxygen consumption is always calculated during the ten breaths before each measurement. As described by Weismann et al., measurements should be performed during steady state, with a stable cardiac output.

Animal preparation

Seven healthy female cross-bred Yorkshire/Landrace pigs (28 to 31 ± 1.2 kg) were studied. After induction, the pigs were placed in the supine position on a thermo-controlled operation table. Anaesthesia and analgesia were maintained with an intravenous infusion with a combination of midazolam (1 to 1.7 mg/kg/h) and sufentanil (0.01 to 0.02 mg/kg/h, Sufenta Forte 0.05 mg/mL, Janssen-Cilag BV, Tilburg, the Netherlands). Muscle relaxation was obtained with an infusion of pancuronium bromide (0.17 to 0.33 mg/kg/h, Pavulon 2 mg/mL, NV Organon, Oss, the Netherlands). After tracheotomy, the pigs were connected to an EVITA XL ventilator.

In addition, an arterial catheter was inserted through the right carotid artery and a pulmonary artery thermodilution catheter (7.5 Fr, Edwards Life Sciences,

Irvine, CA, USA) through the right jugular vein in the pulmonary artery. A catheter was also placed in the urinary bladder to avoid urine retention. Ventilatory data and volume-based capnography were sampled continuously during the experiment (NICO, Novametrix, Wallingford, CT, USA). Mechanical ventilation and washin and washout procedures to obtain the oxygen curves for lung volume and inhomogeneity index calculations were performed with the EVITA XL ventilator in a volume-controlled mode. Tidal volume was set at 8 mL/kg, respiratory rate was adjusted to a $PaCO_2$ of 4.5 to 6.0 kPa, the inspiratory to expiratory ratio was 1:2 and PEEP was 5 cm H_2O.

Experimental protocol

After a stabilization period of 30 min, baseline values were recorded, and the pre-lung injury measurements were performed. Lung volume was measured with the LUFU system and was performed in quadruplicate (four washin and four washout) by changing the FiO_2 from 0.8 to 0.6 and from 0.6 to 0.8. Washin and washout procedures were started immediately after the end of the previous procedure. After the repeatability measurements at baseline (5 cm H_2O PEEP), inhomogeneity was measured at four decremental PEEP levels (15, 10, 5 and 0 cm H_2O PEEP). Single measurements (one washin and one washout) were performed after a steady state of 15 min at the end of each PEEP step.

Severe ALI was induced by injection of oleic acid (0.13 ± 0.04 mL/kg, C18H34O2, Boom BV, Meppel, the Netherlands) into the right atrium with the PEEP set at 2 cm H_2O. Each animal received a bolus of 0.1 mL/kg injected over 20 min to obtain a PaO_2 below 10 kPa; if necessary, additional injections were given to reach this target (19). After a steady state of at least 1.5 h after the induction of ALI, PEEP was increased to 5 cm H_2O, and baseline measurements were repeated. Thereafter, the same PEEP trial was performed as described above.

Statistical analysis

Statistical analysis was performed with the GraphPad software package (GraphPad Software Inc., San Diego, CA, USA). Results are expressed as mean ± standard deviation (SD) for normally distributed data and median ± interquartile range (IQR) for abnormally distributed data. The Shapiro-Wilk normality test was used to evaluate the distribution of all data. Changes in the inhomogeneity indexes, and hemodynamic and ventilatory parameters before and after induction of ALI, were evaluated with the Wilcoxon matched-pairs test. The Wilcoxon matched pairs-test was also used to evaluate change in the inhomogeneity indexes between PEEP steps during the decremental PEEP trial.

Results

Oleic acid infusion significantly decreased EELV, arterial oxygenation and respiratory compliance (Table 1). Venous admixture and the ratio of alveolar dead space volume divided by alveolar tidal volume (VDalv/VTalv) were both increased by the induction of ALI, indicating an increased ventilation-perfusion mismatch (Table 1). Effects of the different PEEP steps on EELV, PaO_2/FiO_2 (PF) ratio and dynamic compliance are shown in Table 2 and Figure 2.

Table 1: Data on hemodynamic and ventilatory parameters before and after induction of lung injury during baseline.

	Before acute lung injury (n=7)	After acute lung injury (n=7)
Heart rate (bpm)	84 (15)	126 (29)*
MAP (mmHg)	87 (8)	88 (10)
PaCO2 (kPa)	4.7 (0.5)	6.4 (0.5)*
PaO2 (kPa)	54.2 (4.0)	8.0(4.3)*
Shunt (%)	10 (3)	52 (19)*
VD alveolar/VT alveolar (%)	28 (5)	44 (7)*
Compliance (mL/cm H_2O)	22 (4)	10 (2)*
EELV (L)	0.65 (0.12)	0.21 (0.02)*
Lactate (mmol/L)	0.9 (0.4)	0.9 (0.3)

Data are means ± SD. * indicates p <0.05

The calculated six ventilation inhomogeneity indexes during baseline are shown in Table 3. The mean variation coefficients, as a measure of repeatability, are also presented (Table 3). LCI, mixing ratio, Becklake index and moment ratio were comparable with historical reference values and showed acceptable mean variation coefficients (Table 3). MBAMI and PCD were not comparable with historical reference values and showed very low repeatability (mean variation coefficient 33.5 and 29.3, respectively). PCD showed no correlation between washout and corresponding washin measurements. After induction of ALI, LCI, Becklake index, MBAMI and moment ratio significantly increased (Table 3). The slope of phase 3 of the volume-based capnogram was also significantly increased after induction of ALI (Table 3).

Table 2: EELV and Inhomogeneity indices parameters before and after induction of lung injury during baseline.

	Before acute lung injury (n=7)	After acute lung injury (n=7)	Mean variation coefficient %	N2 washout in normal subjects (ref.11)
EELV (L)	537 (127)	159 (55)**	5.2	
Lung clearance index	6.7 (0.6)	12.7 (4.3)**	10.4	7.1 (1.3)
Mixing ratio	1.2 (0.1)	1.3 (0.1)	7.8	1.57 (0.22)
Becklake	4.6 (0.5)	11.2 (4.5)**	11.3	3.7 (0.8)
MBAMI (%)	14.6 (6.0)	35.8 (19.4)*	33.5	25 (10)
Moment ratio	1.8 (0.1)	3.0 (0.5)*	5.6	2.02 (0.14)
Pulmonary clearance delay mean (%)	11.0 (4.2)	13.7 (7.8)	29.3	31 (25)
Slope phase 3 capnogram (kPa/L)	2.1(1.2)	7.0 (3.7)*		

All measurements were performed at 5 cm H_2O of PEEP. Capnogram values are averaged over 100 successive breaths and increased significantly after induction of ALI. Values are expressed as mean (SD), **p<0.01, *p<0.05,(Wilcoxon matched-pairs test).

Table 3: EELV and Inhomogeneity indices parameters during different levels of PEEP before and after ALI

	Before acute lung injury				After acute lung injury			
PEEP (cm H_2O)	**15**	**10**	**5**	**0**	**15**	**10**	**5**	**0 *α***
EELV (L)	1458	1064*	720*	400*	848*	446*	238*	182*
LCI	6.1	6.3	6.4*	7.3*	7.2	9.8*	12.9*	19.7
Mixing ratio	1.2	1.2	1.2	1.1	1.2	1.3	1.5*	1.4
Becklake	4.2	4.2	4.5	5.6*	4.9	6.7*	11.7*	19.3
MBAMI (%)	13.6	12.9	14.8	20.6	15.6	25.8*	45.2*	39.5
Moment ratio	1.6	1.7	1.7*	2.0*	2.0	2.4*	2.9*	3.9
Pulmonary clearance delay *(%)*	14.7	13.0	10.6	10.0*	15.9	17.4	20.2	10.3

Values are expressed as means. *Significance compared to PEEP 15 (Wilcoxon matched-pairs test, p<0.05), α; n=6 (unable to perform measurements in 2 piglets).

The inhomogeneity indexes at the different PEEP levels are shown in Table 2. Before ALI, LCI and moment ratio significantly increased after lowering PEEP from 10 to5 cm H_2O and from 5 to 0 (Table 2). Becklake index and PCD significantly increased after lowering PEEP from 5 to 0 before ALI (Table 2). The mixing ratio showed no response to PEEP changes before the induction of ALI. After induction of ALI, almost all indexes (except mixing ratio) increased significantly after lowering PEEP from 15 to 10 cm H_2O, and all indexes increased significantly after lowering PEEP from 10 to 5 cm H_2O (Table 2). At ZEEP, no significant differences were found due to a lower sample size as we were not able to measure reliably with the extensive lung injury caused by the oleic acid. MBAMI and PCD values may not be reliable due to the low repeatability as shown in the baseline measurements.

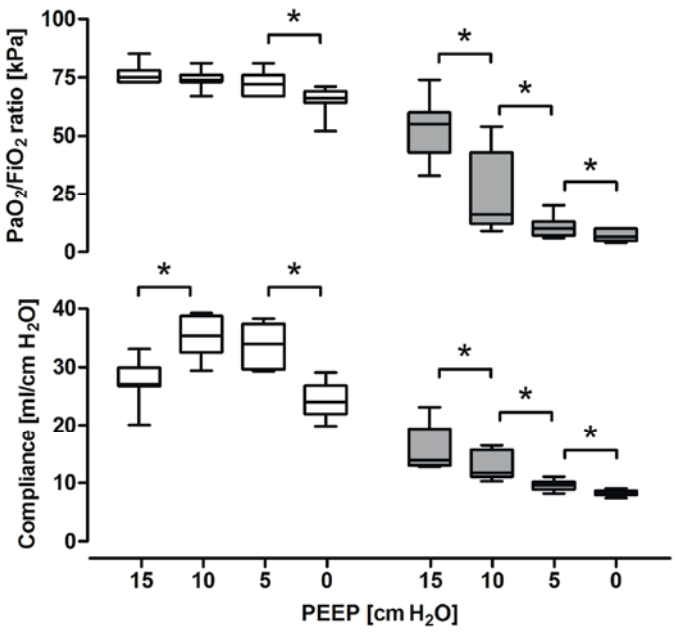

Figure 2: PaO_2/FiO_2 ratio and dynamic compliance at the four decremental steps in PEEP levels, before (open bars) and after (grey bars) the induction of acute lung injury in a porcine model. The TV index at these levels is presented in figure 2. Data are presented as box-and-whisker plot (5-25-median-75-95%). Asterisks indicate a significant difference between the PEEP levels (p<0.05).

Discussion

This paper describes the assessment and integration of a ventilatory inhomogeneity index based on a rapid oxygen sensor incorporated into LUFU equipment without the need for external tracer gases. The moment ratio and LCI index appeared to be the most favourable for integration with oxygen washout curves. To our knowledge, this is the first study to describe indexes of alveolar inhomogeneity measured by medical grade oxygen sensors and conventional breathing systems and applicable during mechanical ventilation.

Technical considerations

Although numerous indexes have been proposed, all require specialized equipment (e.g. mass spectrometer) and/or tracer gases (e.g. SF6, helium) (20). To date, unfortunately, no ventilatory inhomogeneity index has been implemented for routine use in adult critically ill patients. Inhomogeneity can be determined based on single-breath or multiple-breath washout (21). Single-breath washout is clinically available with exhaled volumetric capnography. The upslope of the third phase of this capnogram can be used as a measure of ventilatory inhomogeneity. However, a breath from vital capacity to residual volume should be used to analyse the accessible lung; during normal tidal breathing, only inhomogeneity of this ventilated volume is shown. Also, the contribution of peripheral airways is unknown. The advantage of a multiple-breath washout technique includes the evaluation of both convention- and diffusion-dependent inhomogeneity and the possibility of application during normal tidal breathing without patient cooperation. To obtain a multiple-breath washout index without the use of an insoluble external tracer gas, nitrogen and oxygen can be used as naturally available gases. Most indexes use nitrogen but requires a mass spectrometer for a precise washout curve (11,20,22). Oxygen washout without advanced equipment is limited by slow medical-grade oxygen sensors and the oxygen consumption correction (23). The present study uses an improved oxygen sensor integrated in the LUFU system, originally developed and validated for EELV measurements(9,12). Importantly, the LUFU equipment corrects for the changing inspired oxygen fraction, which influences the gas viscosity and thereby flow through the side stream sampling system (12).

Oxygen consumption is a major factor, complicating the use of oxygen as a tracer gas. Weismann et al. developed the LUFU method for EELV measurement-based oxygen washout and previously described the calculations and basic conditions (12). In short, oxygen transport through the lung membrane is regarded

as constant throughout the washin/washout cycle. It is calculated as the oxygen consumption and tissue oxygen. During measurements, patients must be stable, with stable lung perfusion and oxygenation. Absorption is measured during stable conditions at the end of each washin or washout. This constant consumption is subtracted from each breath during washin/washout. Under these conditions, oxygen consumption does not influence these conditions. We also implemented an automated correction for small artefacts of the washout curve in our program. The use of the fast LUFU oxygen sensor can easily lead to small disturbances caused by environmental factors (e.g. vibrations). We observed short negative disturbances in two to three successive breaths. An automated detection was implemented and correction was performed with interpolated values.

Observed effects in the inhomogeneity indexes

We were able to calculate several inhomogeneity indexes based on oxygen washout with acceptable repeatability. At baseline, LCI, mixing ratio, Becklake index and moment ratio were comparable with historical reference values and showed acceptable variation coefficients. Moment ratio had the lowest variation coefficient, which nearly approached the EELV measurement itself. We were not able to measure inhomogeneity reliably and consistently with the PCD and MBAMI indexes. In the automatically calculated PCD, further analysis even showed no correlation between washin and washout. A possible explanation could be an attempt to compensate indexes for tidal volume, dead space and EELV by comparing the actual measured effects to the ideal effects simulated in an ideal lung (PCD, MBAMI and mixing ratio). This could exaggerate the influence of small artefacts on the calculations. The good reproducibility of the moment ratio may be explained by the underlying principle. It is not dependent on a piece of the washout curve, but rather takes the whole washout curve into account, resulting in a mean number of volume turnovers. LCI and mixing ratio are depending on the point at which the concentration is reduced to 1/40th of the initial concentration. Becklake index and MBAMI are dependent on the point where 90% of the tracer gas has been washed out and thus are heavily dependent on the tail of the washout curve. The tail of the washout curve may be especially vulnerable to artefacts when using oxygen as a soluble tracer gas.

Induction ventilatory inhomogeneity by oleic acid increases all indexes, with a significant increase in the LCI, Becklake index, MBAMI and moment ratio. This is in agreement with Tsang et al. (24). In their study, ALI was induced with oleic acid in eight mongrel dogs, and the multiple-breath helium washout technique was used to analyse the development of ventilatory inhomogeneity. Inhomogeneity

increased mainly due to an increase in the heterogeneity of tissue compliance in the peripheral airways, airway closure and a decrease in ventilation through collateral channels (24). We also observed a significant increase in inhomogeneity using the volumetric capnogram over 100 successive breaths at baseline which evaluates breath inhomogeneity (25). As the heterogeneity in mixing of alveolar units with different time constants increases, the slope of phase 3 of the capnogram will increase.

The LCI, Becklake index and moment ratio showed comparable increases in inhomogeneity during decremental PEEP steps before and after ALI. As shown in Figure 2, the decremental PEEP steps resulted in major reductions in PF ratio and compliance, which suggests an increased ventilation/perfusion mismatch due to inhomogeneous ventilation. The dilution factor (ratio alveolar tidal volume/EELV) could influence these results. If changed by increasing PEEP and thereby EELV, this could delay washout and increase the measured inhomogeneity. In our study, we did not find increased inhomogeneity at higher PEEP. If inhomogeneity indexes were to be used for evaluating the optimal PEEP setting, one would not only be interesting during lower PEEP steps where an increased shunt fraction can be expected. Higher PEEP may lead to lung overdistension, resulting in uneven ventilation. In our study, no increase in inhomogeneity was seen in any of the indexes. Whether these indexes are insensitive to overdistention or the used PEEP steps to low is currently unknown.

Which index based on oxygen washout to use in critically ill patients?

In our study, LCI, mixing ratio, Becklake index and moment ratio showed acceptable precision. Inhomogeneity expressed by moment ratio analysis showed the highest reproducibility, and this index was able to detect the oleic acid-induced inhomogeneity and may be able to detect PEEP-induced changes. With its relatively low dependence on a specific part of the washout curve and thereby relatively insensitive to small artefacts, it may be favourable for oxygen washout. LCI had a slightly higher variation coefficient, but it is currently the most described inhomogeneity index in pulmonary function labs, has even been suggested as the end point for clinical trials (13) and is easy to understand. Comparing the measured values with the ideal values for an ideal lung (as used by MBAMI, PCD and mixing ratio) could theoretically improve results and reliability. In our study, this could not be confirmed; PCD and MBAMI showed low precision.

Limitations

In the current study, we used a 20% step change in the inspired oxygen fraction, which should be feasible in most critically ill patients. Only the most seriously ill patients would require the lower step change of 10%. Also, we did not study the impact of body position; in future human studies, this might influence these measurements because off airway closure and airway secretions. Furthermore, we did use PEEP steps in a nonrandomized order which could influence results; if future PEEP titration studies would be performed, this should be a consideration.

Conclusions

Our study has shown that ventilatory inhomogeneity can be assessed with precision, using oxygen washout curves measured with the LUFU equipment without the need for external tracer gases. The moment ratio and LCI index appeared to be the most reproducible for integration with oxygen washout curves. Studies are under way to evaluate the indexes in critically ill patients.

References

1. Ricard JD, Dreyfuss D, Saumon G. Ventilator-induced lung injury. *Curr Opin Crit Care* 2002; 8: 12-20.
2. Mead J, Takishima T, Leith D. Stress distribution in lungs: a model of pulmonary elasticity. *J Appl Physiol* 1970; 28: 596-608.
3. Rausch SM, Haberthur D, Stampanoni M, Schittny JC, Wall WA. Local strain distribution in real three-dimensional alveolar geometries. *Ann Biomed Eng* 2011; 39: 2835-43.
4. Riedel T, Kyburz M, Latzin P, Thamrin C, Frey U. Regional and overall ventilation inhomogeneities in preterm and term-born infants. *Intensive Care Med* 2009; 35: 144-51.
5. Schibler A, Henning R. Positive end-expiratory pressure and ventilation inhomogeneity in mechanically ventilated children. *Pediatr Crit Care Med* 2002; 3: 124-8.
6. Huygen PE, Feenstra BW, Holland WP, Ince C, Stam H, Bruining HA. Design and validation of an indicator gas injector for multiple gas washout tests in mechanically ventilated patients. *Crit Care Med* 1990; 18: 754-9.
7. Huygen PE, Gultuna I, Ince C, Zwart A, Bogaard JM, Feenstra BW, et al. A new ventilation inhomogeneity index from multiple breath indicator gas washout tests in mechanically ventilated patients. *Crit Care Med* 1993; 21: 1149-58.
8. Gultuna I, Huygen PE, Jabaaij C, Holland WP, Ince C, Bruining HA. A simple device to inject indicator gas for wash-out tests during mechanical ventilation. *Intensive Care Med* 1992; 18: 304-8.

9. Maisch S, Boehm SH, Weismann D, Reissmann H, Beckmann M, Fuellekrug B, et al. Determination of functional residual capacity by oxygen washin-washout: a validation study. *Intensive Care Med* 2007; 33: 912-6.

10. Bikker IG, van Bommel J, Dos Reis MD, Bakker J, Gommers D. End-expiratory lung volume during mechanical ventilation: a comparison to reference values and the effect of PEEP in ICU patients with different lung conditions. *Crit Care* 2008; 12: R145.

11. Larsson A, Jonmarker C, Werner O. Ventilation inhomogeneity during controlled ventilation. Which index should be used? *J Appl Physiol* 1988; 65: 2030-9.

12. Weismann D, Reissmann H, Maisch S, Fullekrug B, Schulte J. Monitoring of functional residual capacity by an oxygen washin/washout; technical description and evaluation. *J Clin Monit Comput* 2006; 20: 251-60.

13. Horsley A. Lung clearance index in the assessment of airways disease. *Respir Med* 2009; 103: 793-9.

14. Edelman NH, Mittman C, Norris AH, Shock NW. Effects of respiratory pattern on age differences in ventilation uniformity. *J Appl Physiol* 1968; 24: 49-53.

15. Becklake MR. A new index of the intrapulmonary mixture of inspired air. *Thorax* 1952; 7: 111-6.

16. Cumming G, Guyatt AR. Alveolar gas mixing efficiency in the human lung. *Clin Sci (Lond)* 1982; 62: 541-7.

17. Saidel GM, Salmon RB, Chester EH. Moment analysis of multibreath lung washout. *J Appl Physiol* 1975; 38: 328-34.

18. Patroniti N, Saini M, Zanella A, Weismann D, Isgro S, Bellani G, et al. Measurement of end-expiratory lung volume by oxygen washin-washout in controlled and assisted mechanically ventilated patients. *Intensive Care Med* 2008; 34: 2235-40.

19. Grotjohan HP, van der Heijde RM, Jansen JR, Wagenvoort CA, Versprille A. A stable model of respiratory distress by small injections of oleic acid in pigs. *Intensive Care Med* 1996; 22: 336-44.

20. Wauer HJ, Lorenz BA, Kox WJ. FRC measurement in intensive care patients. A definition of standards. *Anaesthesist* 1998; 47: 844-55.

21. Robinson PD, Latzin P, Verbanck S, Hall GL, Horsley A, Gappa M, et al. Consensus statement for inert gas washout measurement using multiple- and single- breath tests. *Eur Respir J* 2013; 41: 507-22.

22. Saidel GM, Saniie J, Chester EH. Lung washout during spontaneous breathing: parameter estimation with a time-varying model. *Comput Biomed Res* 1980; 13: 446-57.

23. Mitchell RR, Wilson RM, Sierra D. ICU monitoring of ventilation distribution. *Int J Clin Monit Comput* 1986; 2: 199-206.

24. Tsang JY, Emery MJ, Hlastala MP. Ventilation inhomogeneity in oleic acid-induced pulmonary edema. *J Appl Physiol* 1997; 82: 1040-5.

25. Lumb AB. Nunn's Applied Respiratory Physiology. 6th ed. Philadelphia: Elsevier; 2005.

Chapter 9

Lung volume calculated from electrical impedance tomography in ICU patients at different PEEP levels

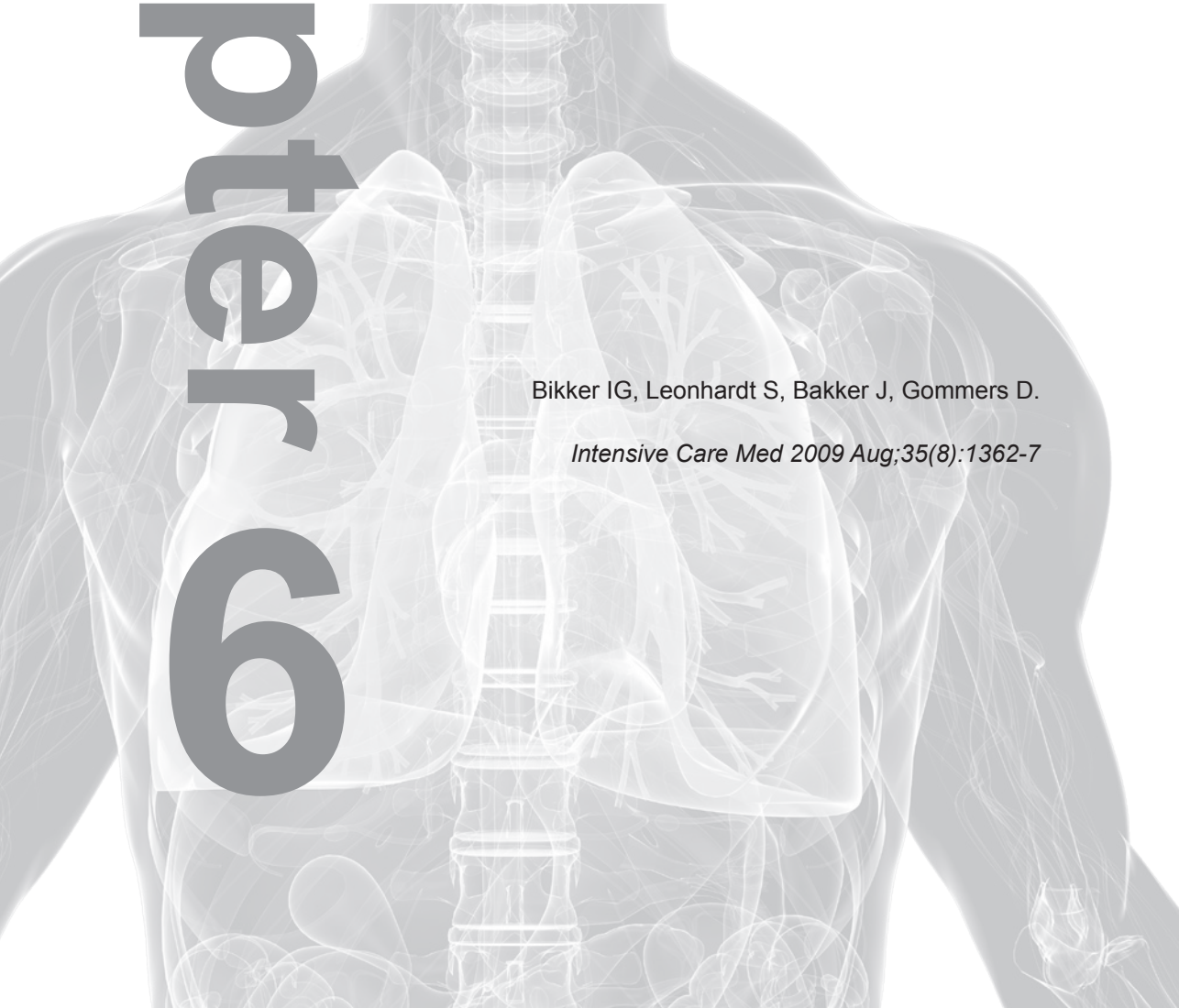

Bikker IG, Leonhardt S, Bakker J, Gommers D.

Intensive Care Med 2009 Aug;35(8):1362-7

Abstract

Purpose:
To study and compare the relationship between end-expiratory lung volume (EELV) and changes in end-expiratory lung impedance (EELI) measured with electrical impedance tomography (EIT) at the basal part of the lung at different PEEP levels in a mixed ICU population.

Methods:
End-expiratory lung volume, EELI and tidal impedance variation were determined at four PEEP levels (15–10–5–0 cm H_2O) in 25 ventilated ICU patients. The tidal impedance variation and tidal volume at 5 cm H_2O PEEP were used to calculate change in impedance per ml; this ratio was then used to calculate change in lung volume from change in EELI. To evaluate repeatability, EELV was measured in quadruplicate in five additional patients.

Results:
There was a significant but relatively low correlation ($r = 0.79$; $R_2 = 0.62$) and moderate agreement (bias 194 ml, SD 323 ml) between ΔEELV and change in lung volume calculated from the ΔEELI. The ratio of tidal impedance variation and tidal volume differed between patients and also varied at different PEEP levels. Good agreement was found between repeated EELV measurements and washin/washout of a simulated nitrogen washout technique.

Conclusion:
During a PEEP trial, the assumption of a linear relationship between change in global tidal impedance and tidal volume cannot be used to calculate EELV when impedance is measured at only one thoracic level just above the diaphragm.

Introduction

Electrical impedance tomography (EIT) may be a promising new tool for bedside monitoring of regional lung ventilation and changes in end-expiratory lung volume (EELV) (1, 2). EIT is a technique based on the injection of small currents and voltage measurements using electrodes on the skin surface generating cross-sectional images representing impedance change in a slice of the thorax. It is a radiation free, non-invasive and portable lung imaging technique.

When there is a linear relationship between Δimpedance and Δvolume, EIT can be used to calculate dynamic EELV changes based on impedance changes. Adler et al. (3) demonstrated a linear increase in impedance in dogs when the lung was inflated with a calibrated syringe. Also, EELV measured by an open-circuit nitrogen washout maneuver increased nearly linearly with impedance change (n = 10, R_2 = 0.95) (4). This principle was used during various procedures with rapidly changing lung volumes to calculate a dynamic EELV in the whole lung, calibrated with impedance change and tidal volumes at one thoracic level (5–7). However, it remains unclear whether this principle is only valid for an open lung state and perhaps not for a diseased lung with recruitment/derecruitment as a result of PEEP changes at the site of the EIT measurement. In ventilated critically ill patients, ventilation is not divided homogenously (8), and, besides change in air volume, other factors (e.g., cardiac oscillations and volume of the pulmonary vascular bed) may contribute to impedance change. During a PEEP trial, inter-electrode distance and chest geometry (EIT assumes a round chest) will be affected. Furthermore, EIT measures an eclipse with a central diameter of approximately 5–10 cm. During an incremental PEEP trial, with increased lung volume, the lung regions move in the cranio-caudal axis, and the individual pixel of the EIT map may no longer be representative for the same lung region (9). Because the electrical current flows on three-dimensional trajectories, it remains unclear how movements of inhomogenous lung tissue in the cranio-caudal axis affect the diagnostic value of EIT measurements in the supine patient.

Therefore, this study aimed to evaluate the relationship between measured EELV and changes in volume calculated from ΔEELI measured at the basal part of the lung during a PEEP trial in a mixed ICU population.

Materials and methods

The study population consisted of a convenient sample of 30 mechanically ventilated patients. The study data were obtained during PEEP trials integrated in standard practice, with the approval and need for informed consent waived for routinely collected data by the local human investigations committee. For all patients, chest X-rays and CT scans (if available) were retrospectively evaluated and related to clinical history and data to divide the patients into four groups: (1) patients without acute respiratory failure (non-ARF; group N), (2) with respiratory failure due to primary lung disorders (group P), (3) patients with respiratory failure due to secondary lung disorders (group S) and (4) patients admitted to the ICU after major surgery (group MS). All patients were adequately sedated and had a regular breathing pattern. Patients with an air leak due to pneumothorax, severe airflow obstruction due to COPD (defined as forced expired volume in 1 s or vital capacity below predicted value minus 2 SD) and severe cardiovascular instability were excluded from the study.

In 25 patients impedance measurements were performed during 2 min with a silicone belt with 16 integrated electrocardiographic electrodes placed around the thoracic cage at the fifth or sixth intercostal space, connected with an EIT device (EIT evaluation kit 2, Dräger, Lubeck, Germany). EIT data were generated by application of a small alternating electrical current of 5 mA and 50 kHz. During the study period, patients were ventilated with an Engström Carestation ventilator (GE Healthcare, Madison, WI). EELV measurements were performed with the COVX module (GE Healthcare, Helsinki, Finland) integrated within the ventilator. Lung volumes were calculated based on a multibreath simulated nitrogen washout by measurement of oxygen and carbon dioxide. This COVX module has been extensively described by Olegard et al. (10) and recently validated in ICU patients by Chiumello et al. (11). At baseline, patients were switched to the Engström ventilator and ventilated according to their original settings before any measurements were made. After a steady state of at least 20 min, PEEP was increased to 15 cm H_2O without changing the other ventilator settings. After a steady state, EELV was measured twice (washout and washin). This was repeated at a PEEP of 10, 5 and (if clinically acceptable) 0 cm H_2O. Before each EIT and EELV measurement, hemodynamic and ventilatory parameters were recorded, and arterial blood gas analysis was performed (ABL 700, Radiometer, Copenhagen, Denmark) in order to calculate the PaO_2/FiO_2 ratio. Dynamic compliance was calculated by dividing expiratory tidal volume by the driving pressure.

In five additional patients quadruplicate EELV measurements were made at three PEEP levels (15, 10 and 5 cm H_2O) to evaluate the repeatability of the simulated nitrogen washout technique. PEEP was increased from the original settings to 15 cm H_2O, and after a steady state of 20 min the EELV was measured in quadruplicate (4 washins and 4 washouts). This was repeated after a steady state of 15 min at 10 and 5 cm H_2O.

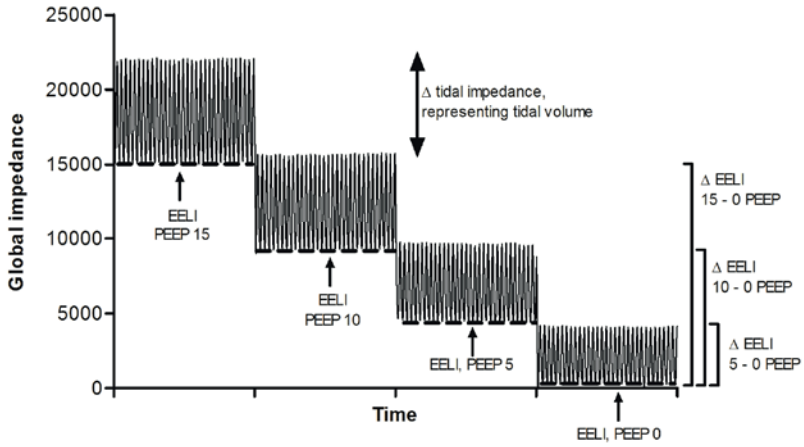

Figure 1: Electrical impedance tomography (EIT) recording in a patient at different PEEP levels. ΔEnd-expiratory lung impedance (EELI) was calculated as the difference between EELI at each PEEP level and the lowest used PEEP level

EIT analysis

EIT data were stored and analyzed offline on a personal computer (Dell, P4, 2.4 GHz). Figure 1 presents a diagram of a representative patient. At each designated PEEP level, mean tidal impedance variation and mean EELI were calculated. The ratio between tidal impedance variation and tidal volume at 5 cm H_2O PEEP was used to calculate Δvolume from the EELI between the different PEEP levels. ΔMean EELI between PEEP levels was divided by this ratio to calculate a Δlung volume. ΔLung volume was calculated between each PEEP level and the lowest used PEEP level (0 or 5 cm H_2O). Distribution of tidal ventilation was expressed with the center of gravity index (12). Change in global tidal impedance was divided into two equal regions of interest, dorsal and ventral, each accounting for 50% of the EIT image. The center of gravity was calculated by dividing the dorsal tidal impedance variation by the total tidal impedance variation.

Statistical analysis

Statistical analysis was performed with Graphpad software package (Graphpad software Inc. San Diego, CA). Results are expressed as mean ± SD for normal distributed data and median + interquartile range (IQR) for not normally distributed data. The Shapiro–Wilk normality test was used to evaluate the distribution of all data. Changes in EELV measured with the nitrogen washout/in method and changes in EELV calculated from EELI were analyzed with linear regression, Spearman's correlation and a Bland–Altman analysis. Wilcoxon's matched-pairs test was used to analyze the tidal impedance variation and the tidal volume ratio.

The repeatability of the quadruplicate EELV measurements in five patients was evaluated with the variation coefficient (SD divided by the average). Bland–Altman analysis was used to analyze the agreement between washin/washout measurements in these five patients.

Results

This study examined the relation between EELV and EELI in 25 mechanically ventilated patients. Table 1 presents physiologic and demographic data on the study population. Patients were retrospectively divided into four groups: group N (n = 9) consisted of two patients with traumatic brain injury, five with cerebral vascular accidents and two with a postoperative condition after neurosurgery; group P (n = 6) consisted solely of patients with pneumonia; group S (n = 4) consisted of patients with abdominal sepsis; in group MS (n = 6) two patients were admitted to the ICU after liver transplantation, one after kidney transplantation, two after trans-thoracic esophagectomy and one patient after coronary bypass surgery.

Of the 25 patients, 20 were ventilated with pressure or volume-controlled ventilation and 5 patients with pressure support ventilation; all had a stable breathing pattern and stable EELI. Mean time after intubation was 17.2h. In total, 13 patients were measured at a PEEP of 15, 10 and 5 cm H_2O and 12 patients at

Table 1: Data on patient characteristics

	EELI-EELV relationship	EELV repeatability
n	25	5
Gender, female/total	8/25	4/5
Age (years)	51 (15)	59 (21)
Height (cm)	177 (9)	172 (11)
Weight (kg)	76 (12)	74 (26)
Time after intubation (hours)	17.2 (11.0)	28.4 (17.2)
Baseline PEEP (cm H_2O)	7.3 (2.7)	8.6 (2.2)
Baseline PaO_2/FiO_2 ratio (mmHg) (range)	344 (533-123)	245 (360-145)
Ventilation mode		
- Pressure control	15	4
- Pressure support	5	1
- Volume control	1	
- Pressure controlled-volume guaranteed	4	

Data are presented as mean (SD), unless stated otherwise. PEEP, positive end-expiratory pressure; EELI, end-expiratory lung impedance; EELV, end-expiratory lung volume.

a PEEP of 15, 10, 5 and 0 cm H_2O. In five additional ICU patients we evaluated the repeatability of the simulated nitrogen washout technique; all patients tolerated this procedure well. Table 1 also presents data on the characteristics of this group.

The correlation between Δlung volume measured with a multibreath simulated nitrogen washout technique and Δlung volume calculated from EELI is shown in Figure A; although significant, the correlation was moderate (r = 0.79, R_2 = 0.62). To assess the difference between the two methods, a Bland–Altmann analysis was performed (Fig. 2). Calculating Δlung volume from EELI resulted in an overestimation compared with the multiple breath washout technique (bias 194 ml). Large differences in Δlung volume were found between the two methods (SD 323 ml). To calculate Δlung volume from EIT, the ratio or slope between tidal impedance variation and tidal volume at 5 cm H_2O was used. This ratio is shown in Figure 3 for each group of patients at the PEEP levels applied. During the decremental PEEP trial, overall the decrease in the slope was significant (15 vs. 5: p<0.001; 10 vs. 5: p <0.001; 0 vs. 5 cm H_2O: p = 0.001). In all individual patient categories this ratio was different at 15 versus 5 cm H_2O PEEP; between patients the slopes also differed.

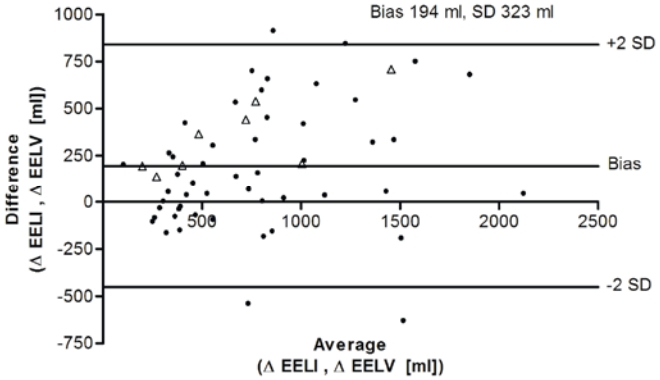

Figure 2: Bland–Altman analysis. Comparison of Δend-expiratory lung volume (ΔEELV) measured with a multibreath nitrogen washout technique and Δlung volume obtained from changes in end-expiratory lung impedance (EELI) calculated with the slope between tidal impedance variation and tidal volume at 5 cm H_2O PEEP. Open triangles represent patients on assisted spontaneous breathing, and black dots represent patients on controlled ventilation.

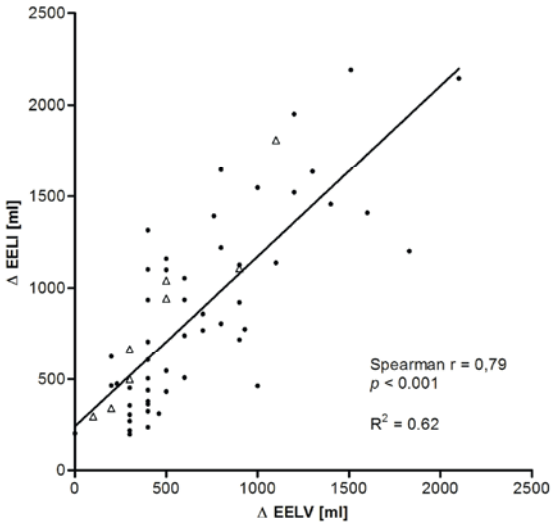

Figure A (supplemental): Linear correlation between Δend-expiratory lung volume (ΔEELV) measured with a multibreath nitrogen washout technique and Δlung volume obtained from changes in end-expiratory lung impedance (EELI) calculated with the slope between tidal impedance variation and tidal volume at 5 cm H_2O PEEP. Changes in EELV and EELI were calculated from the lowest measured PEEP level (0 or 5 cm H_2O). Open triangles represent patients on assisted spontaneous breathing and black dots represent patients on controlled ventilation.

The right panel of Figure 3 shows the dorsal to ventral center of gravity index of the tidal impedance variation for each patient group. In group N and group MS there was a significantly higher center of gravity at 15 and 10 compared to 5 cm H_2O PEEP, indicating increased tidal ventilation distribution in the dorsal, dependent lung areas.

Figure 4 shows arterial oxygenation and dynamic compliance for each patient group. No significant differences were found between the groups; however, this may be due to the small numbers of patients per group.

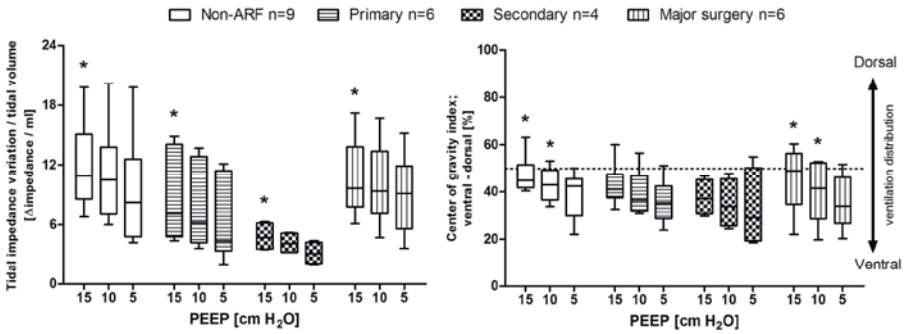

Figure 3 Tidal impedance variation at the studied PEEP levels. Left panel shows the ratio of tidal impedance variation divided by tidal volume (impedance/ml). Right panel shows the center of gravity index. Patients are divided into groups according to the type of lung condition. Data are presented as box-and-whisker plot (min.-25–50–75%-max.), asterisks indicate significance compared to 5 cm H_2O PEEP within each group, p <0.05

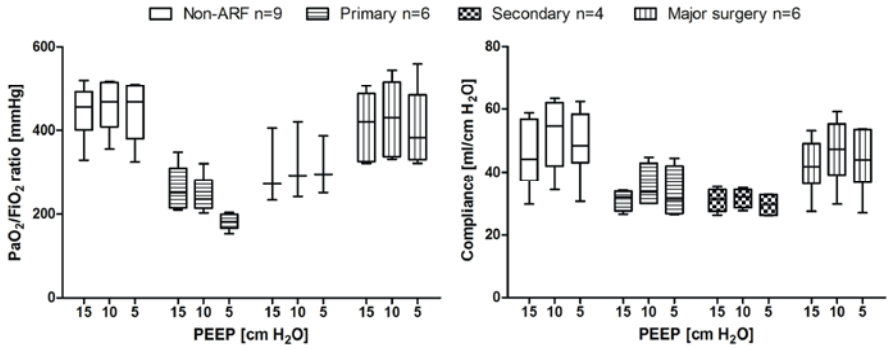

Figure 4: PaO_2/FiO_2 ratio (left) and dynamic compliance (right) at the PEEP levels examined in the four patient groups. Patients are divided into groups according to the type of lung condition. Data are presented as box-and-whisker plot (min.-25–50–75%-max.)

In the five patients with quadruplicate EELV measurements (used to evaluate repeatability of the simulated nitrogen washout technique), mean EELV was 2,232 (SD 1,468), 1,992 (SD 1,304) and 1,565 (SD 1,042) ml at 15, 10 and 5 cm H_2O PEEP, respectively. There was good agreement between the measurements with variation coefficients of 0.018 (range 0.012–0.027), 0.032 (0.018–0.050) and 0.039 (0.005–0.101), and within subjects the SDs were 34 (range 11–52), 29 (10–48) and 23 (7–38) ml at 15, 10 and 5 cm H_2O PEEP, respectively. Also, there was good agreement between the washin and washout measurements, bias -0.76 ± 3.22%.

Discussion

This study assessed the relationship between Δlung volume measured with a simulated nitrogen washout technique and Δlung volume calculated from EIT in critically ill patients. Compared to the nitrogen washout technique, EIT overestimated Δlung volume, and large overestimations or underestimations occurred in the individual patient. The ratio between tidal impedance variation and tidal volume decreased at lower PEEP levels, indicating a change in ventilation distribution at lower PEEP.

This study has some methodological considerations that need to be addressed. First, both techniques (EIT and the simulated nitrogen washout technique integrated into the Engström Carestation ventilator) are novel techniques with ongoing development. Second, Olegard et al. (10) investigated the precision of the simulated nitrogen washout technique and found a bias of -9 ml and limits of agreement of 356 ml when performing repeated measurements with an FiO_2 step of 0.1 and 0.3; this could in part explain the moderate correlation found in the present study. However, the simulated nitrogen washout method did correlate well in a recent comparison with helium dilution and CT scanning (11). Also, we evaluated the repeatability of the simulated nitrogen washout technique at 15, 10 and 5 cm H_2O PEEP and found good agreement between the repeated measurements. Therefore, and based on the significantly lower ratios between tidal impedance variation and tidal volume during the decremental PEEP trial, we believe that the results also reflect lung physiology.

The results of the present study do not support the assumption of a purely linear relationship between Δvolume and Δimpedance in critically ill patients, especially as impedance was measured at only one thoracic level. Although we

found a significant correlation, the level of agreement was poor. A linear relationship has been reported in different settings. For example, Erlandsson et al. (5) described good agreement between impedance tidal variation and tidal volume (R_2 = 0.95) in morbidly obese patients undergoing surgery. The results of our study do not contradict these findings, because tidal volume is less likely to affect recruitment or derecruitment compared to PEEP change in the whole lung. In animal studies, good agreement was found between impedance and volume when inflating the lung with a calibrated syringe (3, 13). Hinz et al. (4) measured impedance and lung volume with an open circuit nitrogen washout technique in ten critically ill patients with acute respiratory failure. In their study, the patients were a heterogeneous group with different causes of respiratory failure, and the measured EELV ranged from 815 to 2,002 ml at 0 cm H_2O PEEP. Agreement between change in EELV and change in EELI was good (R_2 = 0.95). Surprisingly, the slope between Δvolume and Δimpedance was very similar for all their patients (4). In our study, however, we found different slopes between tidal impedance variation and tidal volume for each patient (Fig. 3). This slope is dependent on the electrical conductivity of the measured tissue and may be influenced by edema and other lung pathology (14, 15). In the present study, the different slopes explain the moderate correlation, because they indicate a change in the distribution of ventilation at different PEEP levels. With EIT, PEEP has been shown to shift ventilation in the frontal to dorsal direction (8). This phenomenon was also present in the present study, indicated by the center of gravity index (Fig. 3). At higher PEEP levels, tidal ventilation distribution made a significant shift in groups N and MS to the dorsal parts of the lung, indicating decreased atelectasis. Also, with atelectasis in the dependent regions near the diaphragm, PEEP is likely to shift ventilation and air content in the cranial-to-caudal direction. Consequently, Δvolume calculated from Δimpedance measured at one thoracic level would not be representative for Δvolume in the entire lung. This explanation is supported by the difference in time between measurement and intubation, because lung recruitment with increased airway pressures is more effective at the start of mechanical ventilation. In the study of Hinz et al., patients were intubated on average 7 ± 3 days, whereas in the present study patients were ventilated only 17.2 ± 11.0 h before measurement.

While the results of this study indicate that EIT measured at one basal thoracic level cannot predict lung volume changes in the entire lung, EIT has been shown to reliably assess ventilation distribution as compared with CT scanning. Victorino et al. (16) compared EIT with the same CT slice and showed good agreement between EIT images and dynamic CT scanning, good agreement in

detection of right–left ventilation imbalance and relative ventilation distribution in layers of the thoracic section. Furthermore, in anesthetized pigs a good correlation was shown between the changes in lung air content determined by EIT and electron beam CT (17). An experimental ALI study by Meier et al. (18) explored global and regional lung recruitment and lung collapse, and compared EIT with corresponding CT slices during an incremental and decremental PEEP trial; here, a strong correlation between regional volume changes was established. However, even in this latter study the intra-individual relationship between tidal volume and tidal impedance was much stronger than the overall correlation between all studied animals (n = 8). Thus, EIT has been shown to be very precise and reproducible, especially when looking at regional ventilation and not at overall lung volume (18).

In conclusion, the assumption of a strictly linear relationship between global tidal impedance variation and tidal volume cannot be used to calculate EELV based on DEELI during a PEEP trial when impedance is measured only at one thoracic level just above the diaphragm. This is particularly so when there is considerable change in the geometry of the electrical current conduction pathways such as, for example, in the case of recruitment and derecruitment. In this case, the relationship may become nonlinear. Thus, there might be a different slope between tidal impedance variation and tidal volume in different patients. Nevertheless, this intra-individual slope can be used to monitor regional ventilation distribution to assess the effect of ventilator settings.

References

1. Brunow dC, Fonseca MC, Johnston C. Electric impedance tomography, the final frontier is close: the bedside reality. *Crit Care Med* 2007; 35: 1996-7.
2. Putensen C, Wrigge H, Zinserling J. Electrical impedance tomography guided ventilation therapy. *Curr Opin Crit Care* 2007; 13: 344-50.
3. Adler A, Amyot R, Guardo R, Bates JH, Berthiaume Y. Monitoring changes in lung air and liquid volumes with electrical impedance tomography. *J Appl Physiol* 1997; 83: 1762-7.
4. Hinz J, Hahn G, Neumann P, Sydow M, Mohrenweiser P, Hellige G, et al. End-expiratory lung impedance change enables bedside monitoring of end-expiratory lung volume change. *Intensive Care Med* 2003; 29: 37-43.
5. Erlandsson K, Odenstedt H, Lundin S, Stenqvist O. Positive end-expiratory pressure optimization using electric impedance tomography in morbidly obese patients during laparoscopic gastric bypass surgery. *Acta Anaesthesiol Scand* 2006; 50: 833-9.
6. Lindgren S, Odenstedt H, Erlandsson K, Grivans C, Lundin S, Stenqvist O. Bronchoscopic suctioning may cause lung collapse: a lung model and clinical evaluation. *Acta Anaesthesiol Scand* 2008; 52: 209-18.

7. Odenstedt H, Lindgren S, Olegard C, Erlandsson K, Lethvall S, Aneman A, et al. Slow moderate pressure recruitment maneuver minimizes negative circulatory and lung mechanic side effects: evaluation of recruitment maneuvers using electric impedance tomography. *Intensive Care Med* 2005; 31: 1706-14.

8. Kunst PW, de Vries PM, Postmus PE, Bakker J. Evaluation of electrical impedance tomography in the measurement of PEEP-induced changes in lung volume. *Chest* 1999; 115: 1102-6.

9. Schibler A, Calzia E. Electrical impedance tomography: a future item on the "Christmas Wish List" of the intensivist? *Intensive Care Med* 2008; 34: 400-1.

10. Olegard C, Sondergaard S, Houltz E, Lundin S, Stenqvist O. Estimation of functional residual capacity at the bedside using standard monitoring equipment: a modified nitrogen washout/washin technique requiring a small change of the inspired oxygen fraction. *Anesth Analg* 2005; 101: 206-12.

11. Chiumello D, Cressoni M, Chierichetti M, Tallarini F, Botticelli M, Berto V, et al. Nitrogen washout/washin, helium dilution and computed tomography in the assessment of End Expiratory Lung Volume. *Crit Care* 2008; 12: R150.

12. Luepschen H, Meier T, Grossherr M, Leibecke T, Karsten J, Leonhardt S. Protective ventilation using electrical impedance tomography. *Physiol Meas* 2007; 28: S247-S260.

13. Lindgren S, Odenstedt H, Olegard C, Sondergaard S, Lundin S, Stenqvist O. Regional lung derecruitment after endotracheal suction during volume- or pressure-controlled ventilation: a study using electric impedance tomography. *Intensive Care Med* 2007; 33: 172-80.

14. Pasquali E. Problems in impedance pneumography: electrical characteristics of skin and lung tissue. *Med Biol Eng* 1967; 5: 249-58.

15. Zhang J, Patterson RP. EIT images of ventilation: what contributes to the resistivity changes? *Physiol Meas* 2005; 26: S81-S92.

16. Victorino JA, Borges JB, Okamoto VN, Matos GF, Tucci MR, Caramez MP, et al. Imbalances in regional lung ventilation: a validation study on electrical impedance tomography. *Am J Respir Crit Care Med* 2004; 169: 791-800.

17. Frerichs I, Hinz J, Herrmann P, Weisser G, Hahn G, Dudykevych T, et al. Detection of local lung air content by electrical impedance tomography compared with electron beam CT. *J Appl Physiol* 2002; 93: 660-6.

18. Meier T, Luepschen H, Karsten J, Leibecke T, Grossherr M, Gehring H, et al. Assessment of regional lung recruitment and derecruitment during a PEEP trial based on electrical impedance tomography. *Intensive Care Med* 2008; 34: 543-50.

Chapter 7

Bedside measurement of changes in lung impedance to monitor alveolar ventilation in dependent and non-dependent parts by electrical impedance tomography during a positive end-expiratory pressure trial in mechanically ventilated intensive care unit patients

Bikker IG, Leonhardt S, Reis Miranda D, Bakker J, Gommers D.

Crit Care 2010;14(3):R100.

Abstract

Introduction

As it becomes clear that mechanical ventilation can exaggerate lung injury, individual titration of ventilator settings is of special interest. Electrical impedance tomography (EIT) has been proposed as a bedside, regional monitoring tool to guide these settings. In the present study we evaluate the use of ventilation distribution change maps (ΔfEIT maps) in intensive care unit (ICU) patients with or without lung disorders during a standardized decremental positive end-expiratory pressure (PEEP) trial.

Methods:

Functional EIT (fEIT) images and PaO_2/FiO_2 ratios were obtained at four PEEP levels (15 to 10 to 5 to 0 cm H_2O) in 14 ICU patients with or without lung disorders. Patients were pressure-controlled ventilated with constant driving pressure. fEIT images made before each reduction in PEEP were subtracted from those recorded after each PEEP step to evaluate regional increase/decrease in tidal impedance in each EIT pixel (ΔfEIT maps).

Results:

The response of regional tidal impedance to PEEP showed a significant difference from 15 to 10 (p = 0.002) and from 10 to 5 (p = 0.001) between patients with and without lung disorders. Tidal impedance increased only in the non-dependent parts in patients without lung disorders after decreasing PEEP from 15 to 10 cm H_2O, whereas it decreased at the other PEEP steps in both groups.

Conclusions:

During a decremental PEEP trial in ICU patients, EIT measurements performed just above the diaphragm clearly visualize improvement and loss of ventilation in dependent and non-dependent parts, at the bedside in the individual patient.

In response: editorial in Crit Care 2010;14(4):192. Safer ventilation of the injured lung: one step closer. Marini JJ.

Introduction

Mechanical ventilation is critical for the survival of most patients with respiratory failure admitted to the ICU, but it has become clear that it can exaggerate lung damage and may even be the primary factor in lung injury (1). Protective ventilatory strategies to minimize this lung injury include reduction of tidal volume and prevention or minimization of lung collapse and overdistension by adequate setting of the positive end expiratory pressure (PEEP) (2). Currently, PEEP setting is often guided by global lung parameters such as arterial oxygenation or global compliance, which are not specific for regional lung collapse or overdistension (3). If a regional monitoring tool for lung collapse and overdistension would be available at the bedside, this would aid optimization of ventilator settings in individual patients.

Electrical impedance tomography (EIT) is a non-invasive, real-time imaging method that provides a crosssectional ventilation image of the lung (4-6). It is based on the measurement of lung tissue impedance by injection of small currents and voltage measurements, using electrodes on the skin surface. Recently, different studies described ventilation distribution change maps to evaluate lung collapse or overdistension (7-9). Costa et al. described the use of these ventilation distribution change maps in two ICU patients (7). They introduced an algorithm in which ventilation at a PEEP level is expressed as a percentage from maximal ventilation as seen after a lung recruitment maneuver. In lung-lavaged pigs, Meier et al. composed functional EIT images or ventilation distribution maps by subtracting the EIT images from two PEEP levels to show improvement or loss of regional ventilation between these two PEEP levels (9). As the clinically set PEEP is often guided by decremental PEEP trials, it would be of interest to evaluate the ventilation distribution change maps during this procedure.

In the present study we evaluate the use of ventilation distribution change maps in ICU patients with two distinct types of lung conditions: with or without lung disorders during a standardized decremental PEEP trial. Furthermore we investigated if the EIT measurements at the bedside may visualize alveolar recruitment and derecruitment in the dependent and non-dependent lung regions.

Materials and methods

Following approval by the local institutional human investigations committee, patients were enrolled after providing informed consent from their legal representatives. The study population consisted of 14 mechanically ventilated patients on a mixed ICU. In eight of these patients, end-expiratory lung volume was also measured and these data have recently been published (10). For all 14 patients, chest x-rays and, if available, CT-scans were retrospectively evaluated and related to clinical history and data to divide these patients into two groups; without lung disorders (Group N) and with lung disorders (Group D). Patients were regarded to be without lung disorders when no clinical signs of respiratory failure, pneumonia or significant atelectasis were present. The group with lung disorders was defined as PaO_2/FiO_2 ratio <300 mmHg and proven pneumonia or abdominal sepsis. All patients were well sedated and ventilated in pressure-controlled mode, without spontaneous breathing activity. All patients were ventilated with constant driving pressures throughout the procedure, mean applied driving pressure was 12 cm H_2O (range 9 to 18) in Group N and 16 cm H_2O (range 12 to 21) in Group D. Exclusion criteria for participation in the study were: pneumothorax, severe airflow obstruction due to Chronic Obstructive Pulmonary Disease (COPD) (defined as forced expired volume in 1 s or vital capacity below predicted value minus 2SD), lung transplantation, thoracic deformations and severe cardiovascular instability.

In all patients, impedance measurements were performed during two minutes with a silicone belt with 16 integrated electrocardiographic electrodes placed around the thoracic cage at the fifth or sixth intercostal space (Fig. 1), connected with an EIT device (EIT evaluation kit 2, Dräger, Lübeck, Germany). EIT data were generated by application of a small alternating electrical current of 5 mA at 50 kHz. After baseline measurements at the clinical set ventilator settings (Table 1), PEEP was increased to 15 cm H_2O. After a steady state of 15 minutes PEEP was decreased stepwise each 10 minutes to 10, then to 5 and, if clinically acceptable, to 0 cm H_2O. The stability of each steady state was evaluated by a stable end-expiratory EIT signal and a stable arterial saturation. Before the end of each PEEP level, EIT was measured during two minutes and hemodynamic and ventilatory parameters were recorded. Dynamic compliance was calculated by dividing expiratory tidal volume by the constant driving pressure set for each patient. In addition, arterial blood gas analysis was performed (ABL 700, Radiometer, Copenhagen, Denmark) in order to calculate the PaO_2/FiO_2 ratio.

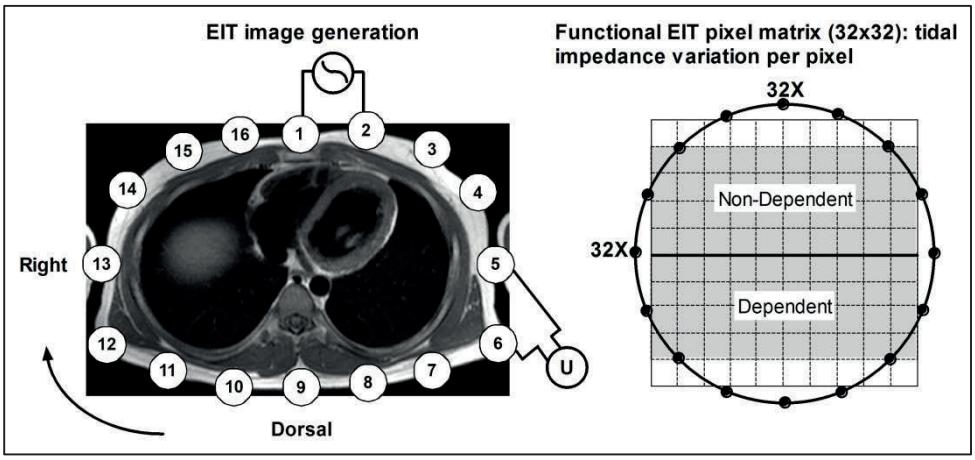

Figure 1 Principle of electrical impedance tomography (EIT) and the functional EIT image (fEIT). Electrical excitation currents are applied between pairs of adjacent surface electrodes (1 to 16); the resulting voltages are measured between the other electrodes (U). In the fEIT image, impedance variation induced by the tidal volume is divided into a 32×32 matrix. Each pixel contains the individual tidal impedance variation, creating an image of ventilation distribution. The ventral to dorsal oriented ROIs are marked in gray in the right panel.

EIT data were stored and analyzed offline on a personal computer (Dell, P4, 2.4 GHz, Round Rock, Texas, USA). The EIT scans consist of images of impedance with a 32 × 32 color-coded matrix relative to the lowest impedance during the PEEP trial (rel. ΔZ). The difference between rel. ΔZ at the end of inspiration and expiration is defined as tidal impedance variation (TIV). This tidal impedance variation is visualized in the functional EIT (fEIT) image, which contains tidal impedance variation per pixel (32×32 matrix) averaged over one minute (Fig. 1). For analysis of the regional distribution of ventilation, the EIT images were subdivided into two symmetrical non-overlapping ventral to dorsal oriented layers defined as dependent and non-dependent regions of interest (ROI). fEIT images before each PEEP step were subtracted from fEIT images at the end of the next PEEP step to obtain ventilation change maps or ΔfEIT images. This ΔfEIT image represents the change in tidal impedance per pixel. With pressure-controlled ventilation with constant driving pressure, the change in tidal impedance per pixel represents the change in tidalvolume per pixel or pixel compliance (7). A weighted pixel count was used to evaluate total increase and decrease in TIV between PEEP steps in the ΔfEIT images and expressed as the percentage positive of total impedance change by equation 1. In this equation a value of 50% represents a balance between gain and loss of TIV at a given PEEP step.

$$\%\text{positive of total } \Delta TIV = \frac{\sum \text{positive } \Delta TIV}{\sum \text{positive } \Delta TIV + \sum \text{negative } \Delta TIV}$$

Equation 1

Statistical analysis

Statistical analysis was performed with Graphpad software package (version 5.0, Graphpad Software Inc., San Diego, CA, USA). Due to the small number of patients, results are expressed as median and interquartile range. Regional compliance changes between each PEEP step were evaluated with the Wilcoxon matched pair test. EELV, PaO_2/FiO_2 ratio and dynamic compliance wasevaluated using ANOVA for repeated measurements. The percentage positive of the total tidal impedance change during each PEEP step between both groups was evaluated with the Mann-Whitney U test. For all comparisons p <0.05 was considered significant.

Results

Table 1 presents data on the 14 mechanically ventilated patients. Group N (n = 6) consisted of postoperative patients (two transhiatal esophagectomy, one liver transplantation and one kidney transplantation) without evidenceof pulmonary complications (n = 4), and patients requiring ventilatory support after traumatic brain injury (n = 2). Group D (n = 8) consisted of patients with pneumonia (n = 5) and respiratory failure associated with abdominal sepsis (n = 3). Eight patients were measured at a PEEP of 15, 10 and 5 cm H_2O and six patients at a PEEP of 15, 10, 5 and 0 cm H_2O. Respiratory data during the PEEP steps are presented in Table 2. One patient in the group without lung disorders had a transient drop in blood pressure at PEEP 15 cm H_2O and measurements were continued at 10 PEEP cm H_2O. All other patients tolerated the PEEP trial well.

Table 1: Data on patient characteristics

	Without lung disorders (group N)	With lung disorders (group D)	p-value
Number of patients	6	8	
Gender, female/male	3/6	3/8	ns
Age (years)	57 (6)	56 (15)	ns
BMI	22.4 (1.8)	24.3 (5.5)	ns
Time of mechanical ventilation (hours)	18.0 (12.5)	8.0 (16.3)	ns
Baseline PEEP (cm H_2O)	5.0 (0.0)	10.0 (1.0)	0.001
Baseline EELV (L)	1.65 (0.55)	1.2 (1.2)	ns
Baseline PaO_2/FiO_2 ratio (kPa)	59.8 (8.4)	33.5 (6.7)	< 0.01
Baseline FiO_2	35.0 (3.8)	50.0 (10.0)	< 0.01
Baseline dynamic compliance (ml/cm H_2O)	40.1 (12.3)	34.7 (15.6)	ns
Reasons for mechanical ventilation	-Postoperative(n=4) -Neurological (n=2)	-Pneumonia (n=5) -Abdominal sepsis (n=3)	

Data are presented as median and (where appropriate) interquartile range; ns, nonsignificant

Table 2: Respiratory parameters during the decremental PEEP steps

PEEP (cm H2O)		15	10	5	0	Sig. between groups
EELV	**N**	2.3 (0.3)	2.2 (0.2)	1.8 (0.2)*	1.5 (0.2)	
(L)	**D**	1.9 (1.0)	1.6 (1.0)*	1.3 (0.8)*	1.2 (0.6)	*p*=NS
PaO_2/FiO_2 ratio	**N**	62.3 (1.9)	63.7 (9.4)*	58.3 (13.9)	50.3 (13.8)	
(kPa)	**D**	37.9 (10.5)	39.0 (8.6)	33.5 (15.2)	26.8 (5.1)	*p*<0.01
Cdyn	**N**	38.6 (7.4)	45.0 (4.5)	45.0 (4.6)	41.0 (1.2)	
(ml/cm H_2O)	**D**	34.1 (11.0)	37.0(12.6)*	35.0(13.3)*	29.0 (7.1)	*p*=NS

Data are presented as median and (where appropriate) interquartile range. N without lung disorders, D with lung disorders. Asterisk represents significance within groups vs. 15 cm H_2O PEEP: * p<0.05

Figure 2 exemplarily shows the effect of PEEP on regional ventilation in a patient with lung disorder and in a patient without lung disorder. The ventilation distribution is presented as ventilation distribution maps (fEIT) at each PEEP level and ventilation distribution change maps (ΔfEIT) between PEEP levels. A clear difference can be seen in response to the change in PEEP in the non-dependent and dependent lung regions between these two patients (Figure 2).

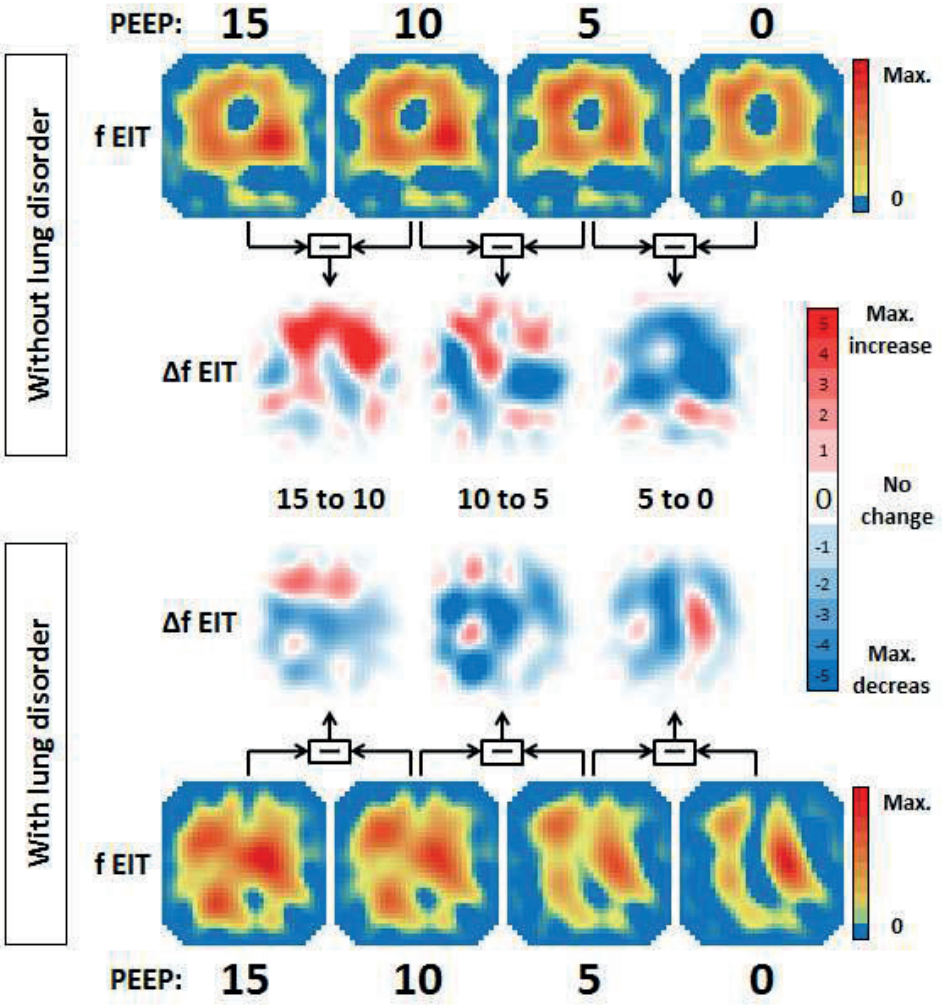

Figure 2 The effect of a decremental PEEP trial on regional ventilation shown in two representative patients. The functional EIT (fEIT) image at the different PEEP levels (15 to 10 to 5 to 0 cm H_2O) shows the ventilation distribution in a colour-coded matrix in a patient without lung disorders and a patient with lung disorders. The ΔfEIT images are created by subtracting fEIT before the PEEP step from fEIT after each PEEP step. The increase or decrease in regional ventilation between PEEP (ΔfEIT) steps is displayed in a color-coded matrix. Each EIT image represents a thoracic slice with the ventral lung regions at the top and dorsal lung regions at the bottom.

In Figure 3, the tidal impedance per cm H_2O driving pressure is presented for two ventral to dorsal ROIs at all PEEP levels. In both groups, tidal impedance decreased towards 0 cm H_2O PEEP. However, this was different for the individual ROIs. In Group N, tidal impedance increased in the non-dependent ROI after decreasing PEEP from 15 to 10 cmH_2O, whereas decreased in the dependent ROI during each PEEP step. In Group D, tidal impedance variation was significantly lower compared to Group N in both regions. Further, tidal impedance did not change in the non-dependent region between PEEP steps 15 to 10 and 5 to 0 and in the dependent region between PEEP step 5 to 0. Tidal impedance decreased significantly during the other PEEP changes.

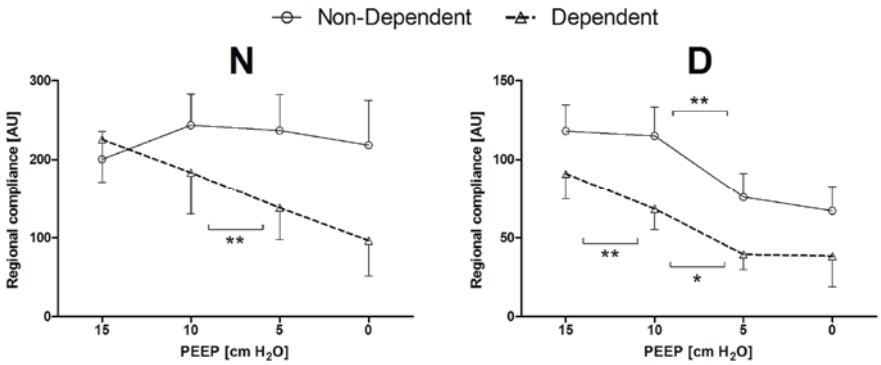

Figure 3 Changes in regional compliance in patients without (left) and patients with (right) lung disorders. During pressure-controlled ventilation with constant driving pressure, the tidal impedance change per pixel can be regarded as regional compliance change per pixel. The open triangle represents the dependent lung region and the open circle represents the non-dependent lung region at the different used PEEP levels. Data are presented as mean and SEM. Significance: * p <0.05; ** p <0.01.

The ΔfEIT images between PEEP steps for the individual patient are shown in Figure 4. In this figure, also the change in PaO_2/FiO_2 ratio and change in dynamic compliance during each PEEP step is presented.

In Figure 5 the total impedance change is shown for each PEEP step. Only during the PEEP step from 15 to 10 the increase was higher than the decrease whereas in all other step the decrease was more than the increase. In all patients, the response of regional tidal impedance to PEEP showed a significant difference from 15 to 10 cm H_2O (p = 0.002) and from 10 to 5 cm H_2O (p = 0.001) between patients with and without lung disorders (Fig. 5).

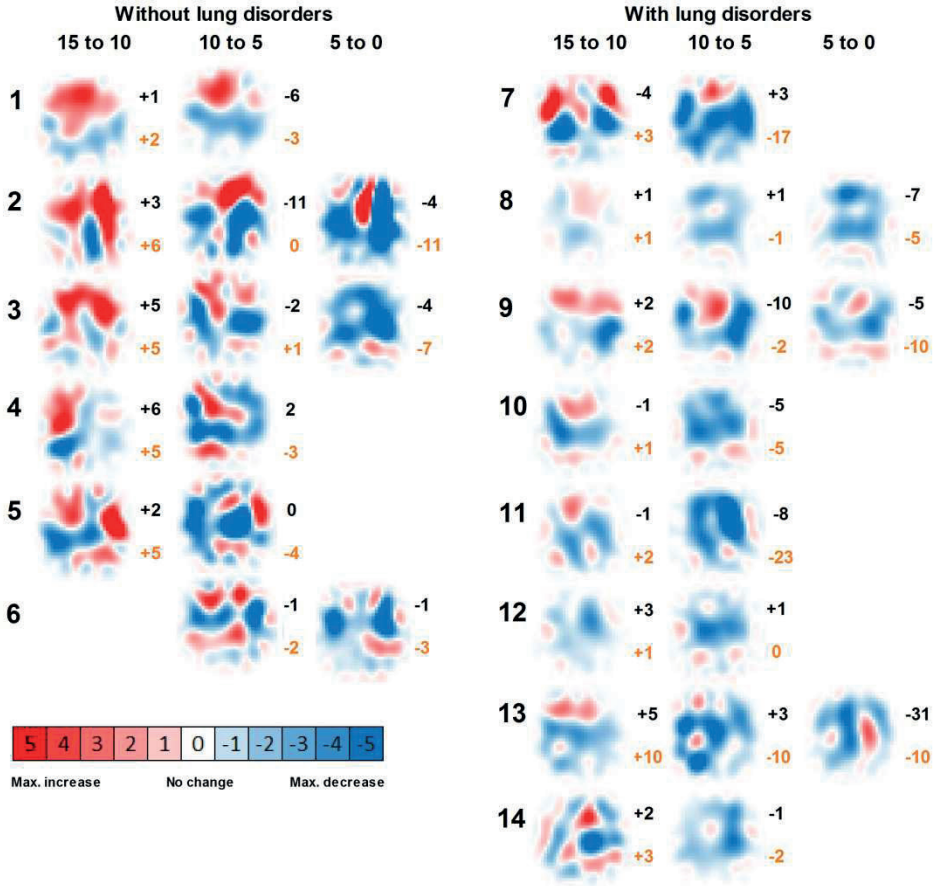

Figure 4 ΔfEIT images in patients without (1 to 6) and with (8 to 14) lung disorders between the PEEP steps used. PaO_2/FiO_2 ratio change (black) and compliance change (red) are presented next to each ΔfEIT image. Images containing a colour-coded 32 × 32 matrix, are generated by subtracting fEIT before the PEEP step from fEIT after each PEEP step. PEEP is decreased stepwise from 15 to 0 cm H_2O. Each EIT image represents a thoracic slice with the ventral lung regions at the top and dorsal lung regions at the bottom.

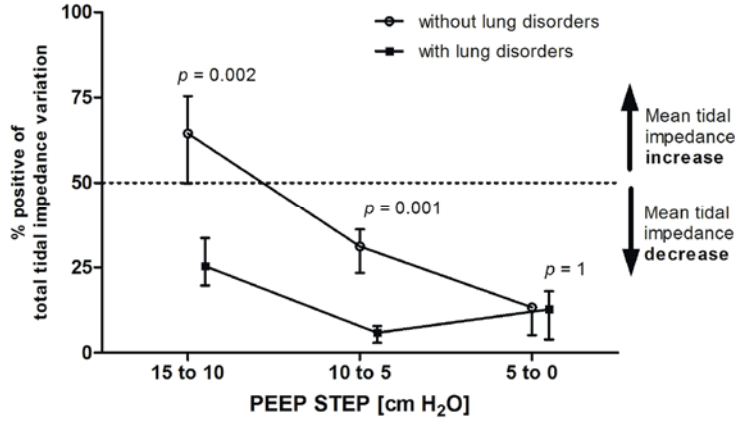

Figure 5: Response to decremental PEEP steps on tidal impedance change in patients with or without lung disorders. During pressurecontrolled ventilation with constant driving pressure, the tidal impedance change per pixel can be regarded as regional compliance change per pixel. The percentage positive of the total Δtidal impedance is calculated from the total increase and total decrease in each Δfunctional EIT image. Data are presented as median and interquartile range.

Discussion

This trial shows that EIT is suitable for bedside monitoring of tidal impedance or regional compliance during decremental PEEP steps and can differentiate between dependent and non-dependent lung regions. There was a significant difference in response to a stepwise decrease in PEEP between patients with and without lung disorders, indicating a different PEEP dependency between these two groups.

Using EIT, increase or decrease of tidal impedance variation becomes visible in ΔfEIT maps (Fig. 4). During a decremental PEEP trial, as used in the present study, improvement in tidal impedance variation can be caused by recruitment of non-ventilated collapsed alveoli or increased ventilation in previously overdistended alveoli. To obtain an equal balance between derecruitment and overdistension, a value of 50% increase of the total tidal impedance change per ΔfEIT map could be used during decremental PEEP steps. If this value is above 50%, more reduction in overdistention compared to increase in derecruitment is present, whereas below 50%, derecruitment is predominant in the measured EIT slice. In the group without lung disorders, total tidal impedance increased after reducing the PEEP from 15 and from 10 cm H_2O; this was due to increased tidal impedance variation in the ventral lung regions, with less loss in the dorsal lung

regions (Fig. 3 and 5). This indicates that during 15 cm H_2O of PEEP alveoli in the ventral part were inflated throughout the ventilatory cycle or overdistended and after lowering the PEEP to 10 cm H_2O ventilation increased in the non-dependent part. In this group, after further lowering the PEEP from 10 to 5 cm H_2O, tidal impedance increase in the ventral part was exceeded by loss of the tidal impedance in the dorsal part; total impedance change was below 50% during this latter PEEP step (Fig. 5). In the group with lung disorders, for each PEEP step there was less increase of tidal impedance in the ventral lung regions and more decrease in tidal impedance in the dorsal regions; total positive impedance change was below 50% for each PEEP step (Fig. 5). Therefore, in order to prevent alveolar collapse in the dorsal part in this caudal thoracic EIT level, a higher PEEP level should be used in these patients with lung disorders compared to the group without lung disorders (Fig. 3 and 5).

EIT is able to show the effect of PEEP on tidal impedance change in each pixel of the functional image matrix. If one accepts the proposed linear relationship between impedance and tidal volume (11-13), the Δimpedance per pixel reflects Δtidal volume in the individual pixel. During pressure-controlled ventilation, the volume change with constant driving pressure or by diving impedance by the driving pressure can be regarded as regional compliance change in each pixel (7).

In the present study, each patient showed an individual response in tidal impedance change during each stepwise decrease in PEEP, and the response differs between dependent and non-dependent lung regions (Fig. 4). This is in accordance with the common understanding of gravity-dependent tidal volume distributions in acute lung injury and acute respiratory disease syndrome (14,15). While the PEEP setting is often guided by global compliance measurements (16-18) or pressure-volume curve analysis (19,20), these global indicators cannot discriminate between the dependent and non-dependent lung regions. EIT is capable of monitoring regional ventilation distribution at the bedside (21-23). Setting PEEP by the use of tidal impedance or regional compliance requires a definition of the ‘optimal’ PEEP with regard to the balance between decreased alveolar surface stress and increased alveolar collapse during stepwise decrease in PEEP. In order to minimize ventilator-induced lung injury (24), it is proposed that the lung should be opened by a recruitment maneuver and thereafter a relatively adequate PEEP should be used to keep the lung open, with the lowest inspiratory airway pressure to prevent alveolar overdistention (25). In the present study, we did not use a recruitment maneuver; however, we have shown that a compromise must be found between lowering alveolar overdistention in the non-dependent part and prevention of alveolar collapse in the dependent part. If optimal PEEP is

defined as an equal balance between increase and decrease in tidal impedance, at this thoracic EIT level optimal PEEP would be in the studied patients around 10 cm H_2O in patients without lung disorders, and at least 15 cm H_2O in patients with lung disorders (Figure 5). Because EIT is now able to adequately visualize regional change in ventilation, a definition is needed if this method is used to set the optimal PEEP. In the future, three-dimensional EIT could help to monitor the entire lung.

A potential limitation of the present study is that EIT measures an eclipse with a central diameter of 5 to 10 cm. The individual pixel in the EIT matrix contains a vast number of alveoli; during tidal ventilation and/or stepwise change in PEEP, different alveoli might be included in the EIT pixel. However, because the individual pixel contains alveoli from the same lung region, it is unlikely to influence the results of this study. In the present study, we didn't compare our findings to another imaging technique like CT scanning. However, Meier et al. used the same method in an experimental animal study and showed good agreement between CT and regional ventilation (9). In addition, for future studies smaller decremental PEEP steps should be chosen in order to establish the optimum PEEP setting for each individual patient.

Conclusions

We conclude that during a decremental PEEP trial in ICU patients, EIT measurements performed just above the diaphragm clearly visualize improvement or loss of ventilation in dependent and non-dependent parts, at the bedside in the individual patient. There was a significant difference in response to a stepwise decrease in PEEP between patients with and without lung disorders, indicating a different PEEP dependency between these two groups. However, the individual response to the decrease of PEEP within the groups was also different indicating that optimal PEEP should be titrated individually and can not be generalized for a group of patients. In addition, the response to the decrease of PEEP was different between dependent and non-dependent lung regions within a patient, suggesting that optimal PEEP may be defined as an equal balance between increase and decrease in tidal impedance. This definition of the optimal PEEP in order to minimize VILI needs further research to prove its benefit.

Key messages

• EIT is suitable for bedside monitoring of tidal impedance or regional compliance during decremental PEEP steps and can differentiate between dependent and non-dependent lung regions.
• During a decremental PEEP trial in ICU patients, EIT measurements performed just above the diaphragm clearly visualize improvement and loss of ventilation in dependent and non-dependent parts, at the bedside in the individual patient.
• Differences in response to decremental PEEP steps were found not only between patient groups, but also within groups indicating that the optimal PEEP should be titrated individually and can not be generalized for a group of patients.
• A definition of the optimal EIT PEEP is needed if this technique is going to be used in the clinical setting.

References

1. Ricard JD, Dreyfuss D, Saumon G. Ventilator-induced lung injury. *Curr Opin Crit Care* 2002; 8: 12-20.
2. ARDSnet. Ventilation with lower tidal volumes as compared with traditional tidal volumes for acute lung injury and the acute respiratory distress syndrome. The Acute Respiratory Distress Syndrome Network. *N Engl J Med* 2000; 342: 1301-8.
3. Cressoni M, Caironi P, Polli F, Carlesso E, Chiumello D, Cadringher P, et al. Anatomical and functional intrapulmonary shunt in acute respiratory distress syndrome*. *Crit Care Med* 2007; 36: 669-75.
4. Frerichs I, Dargaville PA, Dudykevych T, Rimensberger PC. Electrical impedance tomography: a method for monitoring regional lung aeration and tidal volume distribution? *Intensive Care Med* 2003; 29: 2312-6.
5. Hedenstierna G. Using electric impedance tomography to assess regional ventilation at the bedside. *Am J Respir Crit Care Med* 2004; 169: 777-8.
6. Putensen C, Wrigge H, Zinserling J. Electrical impedance tomography guided ventilation therapy. *Curr Opin Crit Care* 2007; 13: 344-50.
7. Costa EL, Borges JB, Melo A, Suarez-Sipmann F, Toufen C, Jr., Bohm SH, et al. Bedside estimation of recruitable alveolar collapse and hyperdistension by electrical impedance tomography. *Intensive Care Med* 2009; 35: 1132-7.
8. Frerichs I, Hinz J, Herrmann P, Weisser G, Hahn G, Dudykevych T, et al. Detection of local lung air content by electrical impedance tomography compared with electron beam CT. *J Appl Physiol* 2002; 93: 660-6.
9. Meier T, Luepschen H, Karsten J, Leibecke T, Grossherr M, Gehring H, et al. Assessment of regional lung recruitment and derecruitment during a PEEP trial based on electrical impedance tomography. *Intensive Care Med* 2008; 34: 543-50.

10. Bikker IG, van Bommel J, Dos Reis MD, Bakker J, Gommers D. End-expiratory lung volume during mechanical ventilation: a comparison to reference values and the effect of PEEP in ICU patients with different lung conditions. *Crit Care* 2008; 12: R145.

11. Adler A, Amyot R, Guardo R, Bates JH, Berthiaume Y. Monitoring changes in lung air and liquid volumes with electrical impedance tomography. *J Appl Physiol* 1997; 83: 1762-7.

12. Erlandsson K, Odenstedt H, Lundin S, Stenqvist O. Positive end-expiratory pressure optimization using electric impedance tomography in morbidly obese patients during laparoscopic gastric bypass surgery. *Acta Anaesthesiol Scand* 2006; 50: 833-9.

13. Lindgren S, Odenstedt H, Olegard C, Sondergaard S, Lundin S, Stenqvist O. Regional lung derecruitment after endotracheal suction during volume- or pressure-controlled ventilation: a study using electric impedance tomography. *Intensive Care Med* 2007; 33: 172-80.

14. Gattinoni L, Pelosi P, Crotti S, Valenza F. Effects of positive end-expiratory pressure on regional distribution of tidal volume and recruitment in adult respiratory distress syndrome. *Am J Respir Crit Care Med* 1995; 151: 1807-14.

15. Luecke T, Meinhardt JP, Herrmann P, Weiss A, Quintel M, Pelosi P. Oleic acid vs saline solution lung lavage-induced acute lung injury: effects on lung morphology, pressure-volume relationships, and response to positive end-expiratory pressure. *Chest* 2006; 130: 392-401.

16. Maisch S, Reissmann H, Fuellekrug B, Weismann D, Rutkowski T, Tusman G, et al. Compliance and dead space fraction indicate an optimal level of positive end-expiratory pressure after recruitment in anesthetized patients. *Anesth Analg* 2008; 106: 175-81.

17. Suarez-Sipmann F, Bohm SH, Tusman G, Pesch T, Thamm O, Reissmann H, et al. Use of dynamic compliance for open lung positive end-expiratory pressure titration in an experimental study. *Crit Care Med* 2007; 35: 214-21.

18. Suter PM, Fairley B, Isenberg MD. Optimum end-expiratory airway pressure in patients with acute pulmonary failure. *N Engl J Med* 1975; 292: 284-9.

19. Amato MB, Barbas CS, Medeiros DM, Magaldi RB, Schettino GP, Lorenzi-Filho G, et al. Effect of a protective-ventilation strategy on mortality in the acute respiratory distress syndrome. *N Engl J Med* 1998; 338: 347-54.

20. Maggiore SM, Richard JC, Brochard L. What has been learnt from P/V curves in patients with acute lung injury/acute respiratory distress syndrome. *Eur Respir J Suppl* 2003; 42: 22s-6s.

21. Frerichs I, Schmitz G, Pulletz S, Schadler D, Zick G, Scholz J, et al. Reproducibility of regional lung ventilation distribution determined by electrical impedance tomography during mechanical ventilation. *Physiol Meas* 2007; 28: S261-S267.

22. Frerichs I, Dargaville PA, van Genderingen H, Morel DR, Rimensberger PC. Lung volume recruitment after surfactant administration modifies spatial distribution of ventilation. *Am J Respir Crit Care Med* 2006; 174: 772-9.

23. Victorino JA, Borges JB, Okamoto VN, Matos GF, Tucci MR, Caramez MP, et al. Imbalances in regional lung ventilation: a validation study on electrical impedance tomography. *Am J Respir Crit Care Med* 2004; 169: 791-800.

24. Pinhu L, Whitehead T, Evans T, Griffiths M. Ventilator-associated lung injury. *Lancet* 2003; 361: 332-40.

25. Lachmann B. Open up the lung and keep the lung open. *Intensive Care Med* 1992; 18: 319-21.

Chapter 8

Electrical impedance tomography measured at two thoracic levels can visualize the ventilation distribution changes at the bedside during a decremental positive end-expiratory lung pressure trial

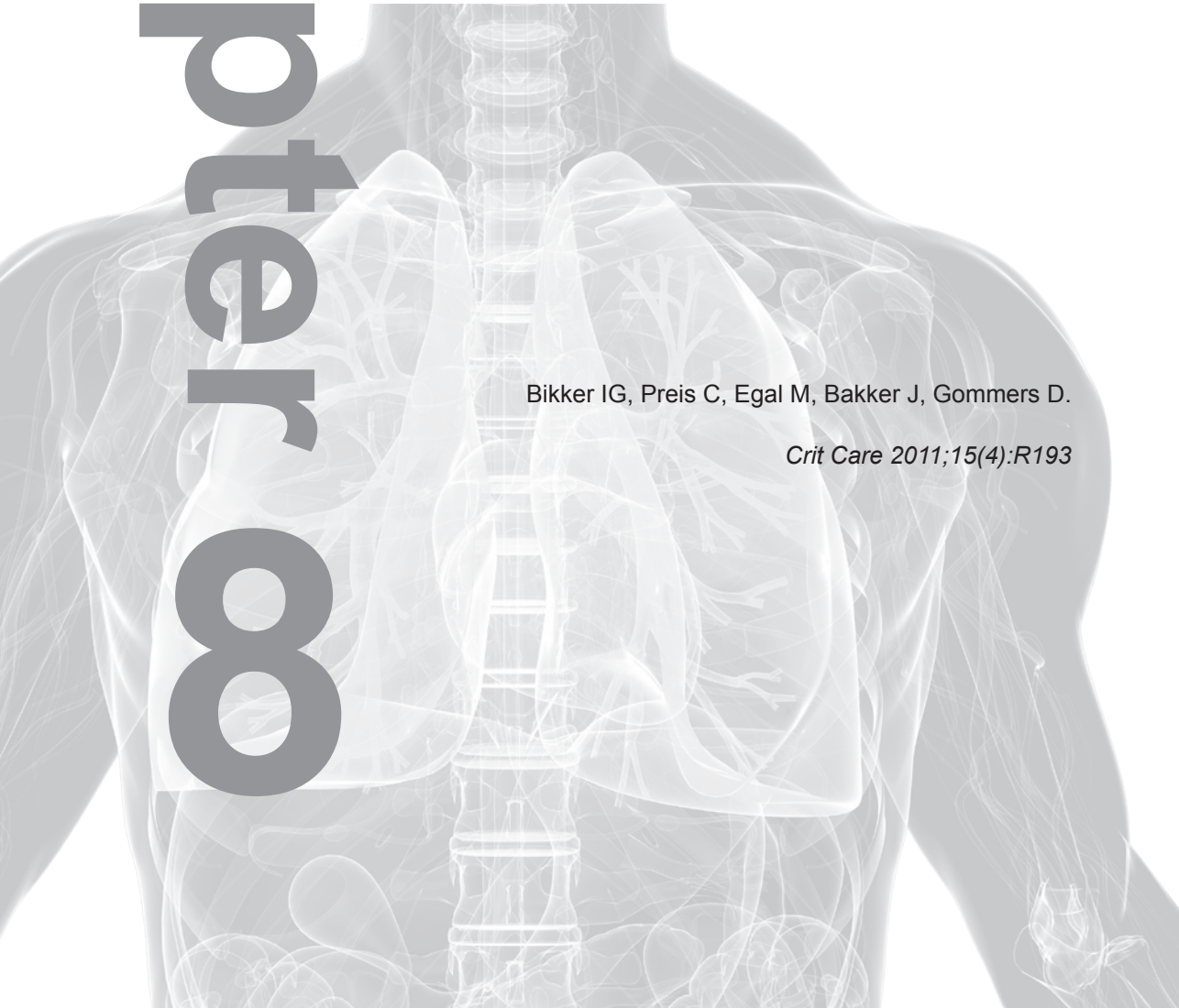

Bikker IG, Preis C, Egal M, Bakker J, Gommers D.

Crit Care 2011;15(4):R193

Abstract

Introduction:
Computed tomography of the lung has shown that ventilation shifts from dependent to nondependent lung regions. In this study, we investigated whether, at the bedside, electrical impedance tomography (EIT) at the cranial and caudal thoracic levels can be used to visualize changes in ventilation distribution during a decremental positive end-expiratory pressure (PEEP) trial and the relation of these changes to global compliance in mechanically ventilated patients.

Methods:
Ventilation distribution was calculated on the basis of EIT results from 12 mechanically ventilated patients after cardiac surgery at a cardiothoracic ICU. Measurements were taken at four PEEP levels (15, 10, 5 and 0 cm H_2O) at both the cranial and caudal lung levels, which were divided into four ventral-to-dorsal regions. Regional compliance was calculated using impedance and driving pressure data.

Results:
We found that tidal impedance variation divided by tidal volume significantly decreased on caudal EIT slices, whereas this measurement increased on the cranial EIT slices. The dorsal-to-ventral impedance distribution, expressed according to the center of gravity index, decreased during the decremental PEEP trial at both EIT levels. Optimal regional compliance differed at different PEEP levels: 10 and 5 cm H_2O at the cranial level and 15 and 10 cm H_2O at the caudal level for the dependent and nondependent lung regions, respectively.

Conclusions:
At the bedside, EIT measured at two thoracic levels showed different behavior between the caudal and cranial lung levels during a decremental PEEP trial. These results indicate that there is probably no single optimal PEEP level for all lung regions.

Introduction

Electrical impedance tomography (EIT) is a promising new tool for bedside monitoring of regional lung ventilation and changes in regional and global lung volume (1-3). EIT is a technique based on the injection of small electrical currents and voltage measurements using electrodes on the skin surface. Cross-sectional images are generated from these measurements, representing impedance change in a 5- to 10-cm-wide slice of the thorax. It is a radiation-free, non-invasive, portable lung imaging technique.

EIT can be performed at different craniocaudal levels of the thoracic cage, but the caudal thoracic level just above the diaphragm is of particular importance because atelectasis due to mechanical ventilation can be expected most at this level. On the basis of computed tomography (CT), it is known that the dorsal and dependent lung regions are most susceptible to alveolar collapse and recruitment (4). Therefore, these lung regions would benefit most from individualized positive end-expiratory pressure (PEEP) settings, and consequently most EIT studies have been performed at the caudal thoracic level in the dependent lung regions (5,6). However, conflicting results have been found between regional lung parameters measured with EIT (6-8) and those measured with global lung parameters, such as compliance and end-expiratory lung volume (EELV) (9,10). In a previous study, we found that tidal impedance variation measured at one thoracic level was not equal to tidal volume, and we speculated that this might be due to derecruitment (9). As derecruitment occurs most prominently in the dorsal lung regions above the diaphragm, the relation between global lung parameters and the results of regional lung parameters measured with EIT would be dependent on the measurement location. However, the relation between ventilation distributions in the cranio-caudal axis has not yet been studied with EIT.

Therefore, in this study, we evaluated whether ventilation distribution measured by EIT, as well as the relation between EIT regional compliance and global dynamic compliance, differs between cranial and caudal thoracic levels in response to decremental PEEP steps.

Materials and methods

Following approval by the local institutional human investigations committee, patients were enrolled in this study after we obtained their written informed consent. The study data were collected during an ongoing study which investigated lung condition and the response to PEEP before, during and after cardiothoracic surgery. The study population consisted of 12 mechanically ventilated patients in a cardiothoracic ICU. Exclusion criteria for participation in the study were pneumothorax, severe airflow obstruction due to chronic obstructive pulmonary disease (defined as forced expired volume in one second or vital capacity below predicted value minus two standard deviations), thoracic deformations and severe cardiovascular instability.

Study protocol

After the surgical procedure and after the patient's arrival at the cardiothoracic ICU, measurements were taken during the warm-up period following the surgical procedure. During this period, all patients were fully sedated and ventilated in pressure-controlled mode without any signs of spontaneous breathing activity. Prior to this protocol, hypovolemia was corrected by the anesthesiologist. All patients were in the supine position.

After a stabilization period of 15 minutes, 2 silicone EIT belts, each with 16 integrated cardiographic electrodes, were placed around the thoracic cage (Fig. 1). In all patients, EIT was measured at a caudal level and a cranial thoracic level during decremental PEEP steps according to the study protocol. One belt was placed at the highest possible thoracic level, just under the armpits, at the third or fourth intercostal space. The second belt was placed just below the nipples at the sixth or seventh intercostal space. The belts were connected to a single EIT device (EIT evaluation kit 2; Dräger, Lübeck, Germany) in an alternating fashion. EIT data were generated by application of a small alternating electrical current of 5 mA at 50 kHz.

PEEP was increased to 15 cm H_2O, and a recruitment maneuver with peak inspiratory pressure (PIP) of 40 cm H_2O and PEEP of 20 cm H_2O was applied for 40 seconds. After a steady state of 15 minutes at 15 cm H_2O PEEP, PEEP was decreased stepwise from 15 to 10 cm H_2O, then to 5 cm H_2O and, if clinically acceptable, to 0 cm H_2O. Each PEEP was applied for 15 to 20 minutes. The driving pressure (PIP minus PEEP) was kept constant at all used PEEP levels. Before the end of each PEEP level, EIT was measured at both levels

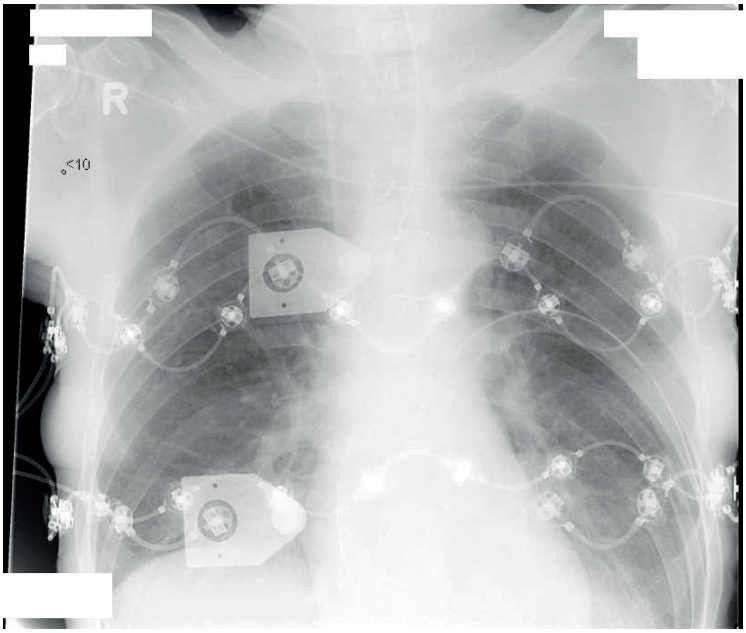

Figure 1 Chest X-ray of one of the studied patients showing the cranial (upper) and caudal (lower) electrical impedance tomography belt. X-ray taken at 5 cm H_2O positive end-expiratory pressure (PEEP).

during a two-minute period, and hemodynamic and ventilatory parameters were recorded. Pressure-controlled ventilation was used specifically to enable the evaluation of regional compliance independently of other lung regions. Dynamic compliance was calculated by dividing expiratory tidal volume measured at the Y-piece of the Engström Carestation ventilator (GE Healthcare, Madison, WI, USA) by the constant driving pressure set for each patient. In addition, arterial blood gas analysis was performed (i-STAT MN300 System; Abbott Point of Care, Inc., Princeton, NJ, USA) to calculate the ratio of partial pressure of oxygen to fraction of inspired oxygen at each PEEP level.

EIT analysis

EIT data were stored and analyzed offline on a personal computer. The EIT scans consist of images showing impedance with a 32 × 32 color-coded matrix relative to the lowest impedance recorded during the PEEP trial (relative ΔZ). The difference between relative ΔZ at the end of inspiration and expiration is defined as tidal impedance variation. Tidal impedance variation was visualized on functional EIT (fEIT) images, which showed tidal impedance variation per pixel (32 high × 32 width matrix) averaged over one minute (Fig. 2).

EIT regional compliance was calculated by dividing the tidal impedance variation by the driving pressure (11). The concept of regional compliance measured with EIT is possible because of the proportional relation between local impedance and local volume changes (7). Pressure-controlled ventilation was used specifically to enable the evaluation of regional compliance independently of other lung regions.

For analysis of the regional distribution of ventilation, the EIT images were subdivided into two symmetrical non-overlapping layers from the ventral to dorsal orientation, defined as regions of interest (ROIs). This was done in a different fashion for the measurements recorded at the cranial and caudal thoracic levels based on the anatomical position of lung tissue (Fig. 2). At the caudal level, each of these ROIs, from line 3 to 30, was 14 × 32 pixels. At the cranial level, each of these ROIs, from line 3 to 22, was 10 × 32 pixels. In addition, to minimize influences from the diaphragm, we selected smaller upper and lower ROIs of each of the four horizontal lines (4 × 32 pixels) at the center of the above described upper and lower ROIs. This was done at both the caudal and cranial levels.

Distribution of EIT tidal ventilation in a ventral to dorsal direction was expressed according to the center of gravity index (12). Change in global tidal impedance was divided into two equal ROIs, dorsal and ventral, each accounting for 50% of the EIT image. The center of gravity was calculated by dividing the dorsal tidal impedance variation by the total tidal impedance variation.

Volume changes were calculated by dividing changes in end-expiratory lung impedance by the ratio of tidal impedance variation to tidal volume. As this ratio differs between PEEP levels, it was averaged between successive PEEP levels to calculate lung volume changes between successive PEEP levels (for example, from baseline 5 to 15 cm H_2O or from 15 to 10 cm H_2O).

Statistical analysis

Statistical analysis was performed with the GraphPad version 5.0 software package (GraphPad Software, Inc., San Diego, CA, USA). Unless stated otherwise, results are expressed as means ± standard deviations for normally distributed data and medians ± interquartile ranges for non-normally distributed data. The Shapiro- Wilk normality test was used to evaluate the distribution of all data. The Friedman test for the one-way analysis of variance for repeated measures was used to study the change at the decremental PEEP steps of the center of gravity index, ratio of tidal impedance variation to tidal volume, dynamic compliance and arterial oxygenation. For all comparisons, $p < 0.05$ was considered significant considered significant.

Results

Table 1 presents the physiologic and demographic data of the study population. Dynamic compliance and arterial oxygenation data are shown in Table 2.

Table 1. Patient characteristics

	Data
Number of patients	12
Females/males	3/9
Age (years)	69.6 ± 9.4
Height (m)	1.72 ± 0.08
Body weight (kg)	78.8 ± 12.3
Baseline PEEP (cm H_2O)	5.0 ± 0.0

Data are means ± standard deviations

Table 2. Arterial oxygenation, compliance and ventilator settings during decremental PEEP steps

	PEEP (cm H_2O)				
Measurement	Baseline 5	15	10	5	0
Compliance (mL/cm H_2O)	52.9 ± 9.6	60.2 ± 9.2	63.0 ± 8.6	57.9 ± 7.8	41.2 ± 7.4[b]
PaO_2/FiO_2 ratio (kPa)	39.9 ± 15.7[b]	64.5 ± 13.7	61.9 ± 14.8	47.5 ± 14.4[c]	28.8 ± 11.2[d]
Ventilatory mode	PCV	PCV	PCV	PCV	PCV
I:E ratio	1:1	1:1	1:1	1:1	1:1
Driving pressure (cm H_2O)	10 ± 2	10 ± 2	10 ± 2	10 ± 2	10 ± 2
Respiratory rate (breaths/minute)	15 ± 1	15 ± 1	15 ± 1	15 ± 1	15 ± 1
Tidal volume (mL)	491 ± 54	591 ± 120	615 ± 103	565 ± 91	403 ± 88

Data are means ± standard deviations unless otherwise indicated. Significance compared to 15 cm H_2O: [b]<0.01, [c]<0.05, [d]<0.001.

Figure 2 shows the fEIT images averaged over one minute in one representative patient at 15, 10, 5 and 0 cm H_2O PEEP at both thoracic levels. During the decremental PEEP trial, the area of ventilation increased at the cranial level but decreased at the caudal level (Fig. 2).

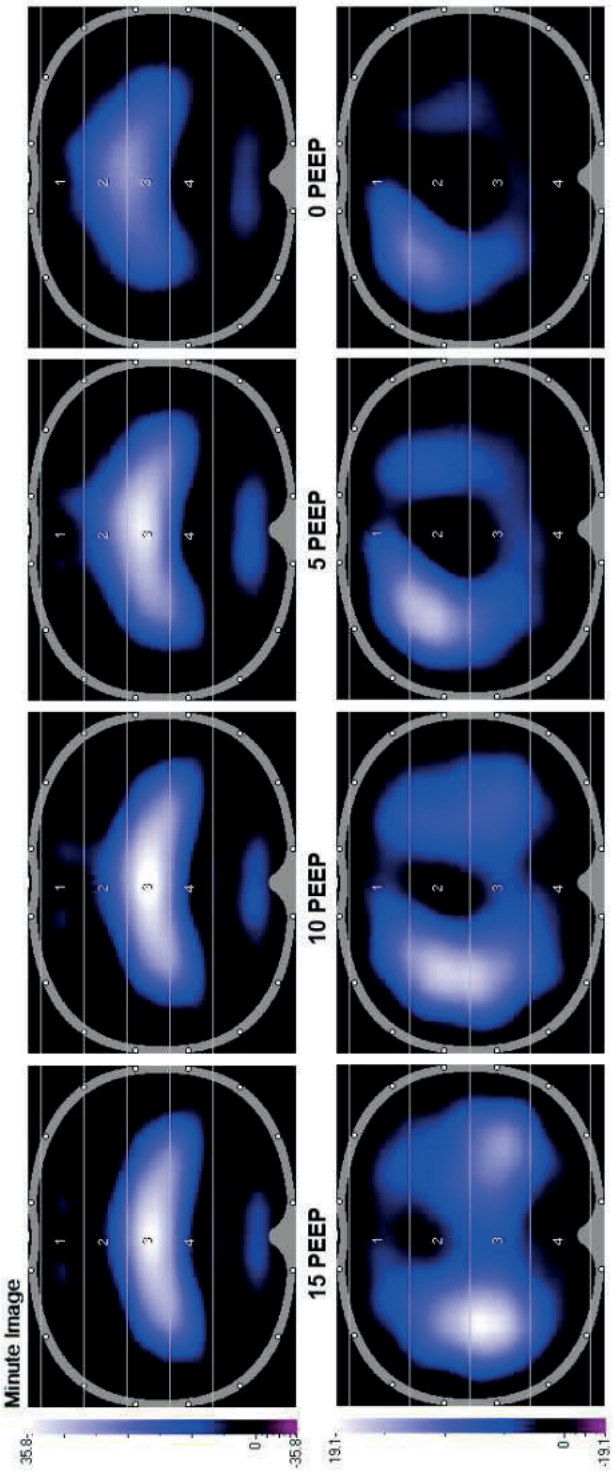

Figure 2: Images of ventilation distribution at a cranial (top row) and caudal (bottom row) thoracic lung levels at the different decremental positive end-expiratory pressure (PEEP) steps in a representative patient. Images were obtained by averaging tidal impedance distribution over one minute. The regions of interest (ROIs) used in the present study are displayed at both levels and defined according to the anatomical position of lung tissue. Nondependent lung regions: 1 and 2. Dependent lung regions: 3 and 4

The regional compliance of the two ROIs at both thoracic levels is shown in Figure 3 at each decremental PEEP step. The total regional compliance of both ROIs decreased at the caudal level during the decremental PEEP trial, whereas it increased initially at the cranial level after PEEP was lowered from 15 to 10 cm H_2O. At the caudal level, regional compliance decreased rapidly during the decremental PEEP steps. At the cranial level, the tidal impedance variation increased in the nondependent ROI and decreased in the dorsal ROI during the decremental PEEP steps.

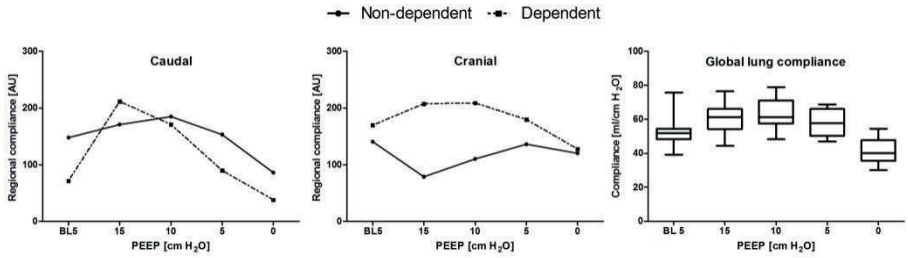

Figure 3 Dynamic compliance (right) and regional compliance measured at a caudal (left) and cranial (middle) thoracic lung levels at dependent orientation (dorsal) and nondependent orientation (ventral) regions of interest (ROIs). Regional compliance was calculated by dividing the electrical impedance tomography (EIT) tidal impedance variation by the applied driving pressure. Box and whisker plots: 95%, 75%, 50%, 25% and 5%. AU: arbitrary units.

Both the tidal impedance variation and the tidal volume decreased at the decremental PEEP steps, but the ratio of tidal impedance variation divided by tidal volume decreased at the caudal level and increased at the cranial level during the decremental PEEP trial (Fig. 4A). In addition, the center of gravity index decreased at both lung levels during the decremental PEEP trial, which means that tidal impedance variation decreased at the dorsal lung region and decreased less, or even increased, at the ventral lung regions after lowering the PEEP (Figure 4C).

The ratio of tidal impedance variation divided by tidal volume from the small ROIs, to minimize diaphragm influence, is shown in Fig. 4B. It also decreased at the caudal level and increased at the cranial level during the decremental PEEP trial, but the changes were smaller compared to the original ROIs, which were designed to cover all anatomical lung tissue.

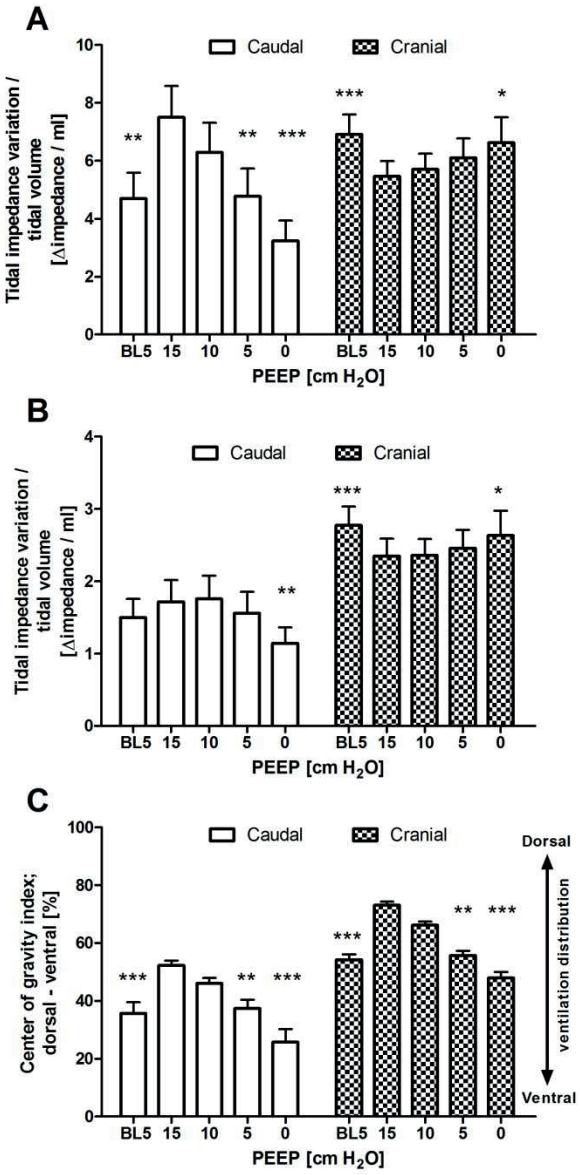

Figure 4: Tidal impedance variation divided by tidal volume obtained from (A) regions of interest (ROIs) to include all anatomical lung tissue and from ROIs selected to minimize caudal diaphragmatic influence (ROI: 4 × 32 pixels) (B). Panel C shows center of gravity index. Data are presented as means + standard errors of the mean. Significance compared to 15 cm H_2O positive end-expiratory pressure (PEEP): * $p < 0.05$, ** $p < 0.01$, *** $p < 0.001$.

Lung volume changes compared to baseline are shown in Figure 5, calculated from both caudal and cranial EIT measurement levels. The rate of EELV decrease was non-significantly different between the caudal and cranial levels. At the caudal level, the rate increased, whereas at the cranial level, the rate of lung volume loss decreased during the decremental PEEP steps.

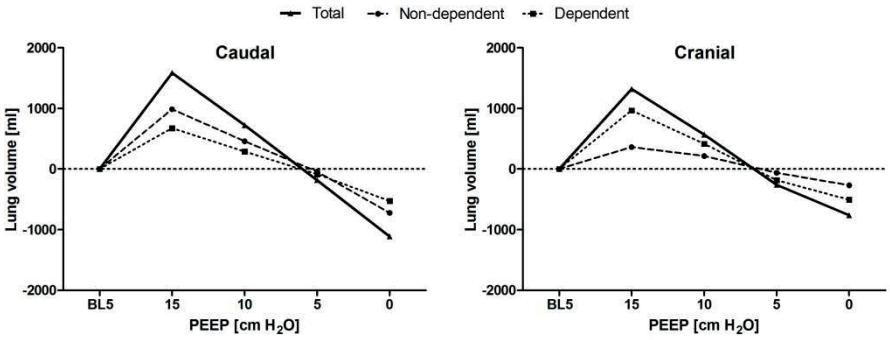

Figure 5: End-expiratory lung volume (EELV) calculated from end-expiratory impedance changes. Values are relative to baseline 5 cm H_2O positive end-expiratory pressure (PEEP), which was set at 0.

Discussion

In this study, the center of gravity index measured with EIT decreased at both the cranial and caudal thoracic levels during a decremental PEEP trial, whereas tidal impedance variation divided by tidal volume decreased at the caudal level and increased at the cranial level. This indicates that during a decremental PEEP trial, ventilation distribution not only shifted from the dorsal to ventral direction, but also from the caudal to cranial direction during mechanical ventilation in post-cardiac surgery patients.

To the best of our knowledge, this study is the first to investigate ventilation distribution using EIT at multiple levels in mechanically ventilated patients at the bedside. Both the tidal impedance variation and the tidal volume decreased at the decremental PEEP steps, but the ratio of tidal impedance variation divided by tidal volume decreased at the caudal level and increased at the cranial level during the decremental PEEP trial (Fig. 4). Multiple CT studies have shown a highly correlated linear relation between local air and impedance distribution (6-8), suggesting that local ventilation decreases more at the caudal level that at the cranial level. It becomes clear that the dorsal-dependent lung regions just above

the diaphragm are the areas with most potential for lung collapse and loss of ventilation at lower PEEP levels. This particular area was measured with EIT with the caudal belt placed just below the nipples at the sixth or seventh intercostal space. However, at this level, the effects of the diaphragm's entering into the middle of the EIT eclipse also can contribute to the major decrease in tidal impedance variation. When smaller ROIs were selected, tidal impedance variation still decreased, but to a lesser degree. In addition, we have shown that the center of gravity decreased during the decremental PEEP trial, which means that tidal impedance variation decreased more at the dorsal lung region and decreased less, or even increased, at the ventral lung region after PEEP was lowered (Fig. 3 and 4). The impedance shift from the dorsal to ventral lung region during the decremental PEEP steps was due to the onset of more collapse at the dorsal site than at the ventral site at the PEEP levels applied, as shown by the individual impedance changes in the different ROIs (Fig. 3). This finding is in agreement with the common understanding that ventilation distribution is gravity- dependent, as shown by CT (4). At the cranial level, tidal impedance variation even increased after the PEEP level was lowered from 15 to 10 cm H_2O and increased further after the PEEP level was lowered in the most ventral ROIs (Fig. 3). This finding can be explained by the reduction in overdistention in the nondependent lung parts in the upper part of the lung. This means that applying a PEEP level of 15 cm H_2O was too high for the cranial site but not for the caudal site, indicating that the optimal PEEP level is different for these sites.

Regional compliance, as calculated by regional impedance changes divided by the pressure amplitude (11,12), showed different ventilation distribution behavior in response to the decremental PEEP steps at both studied lung levels (Fig. 3). In our study, because driving pressure was kept constant in each patient during the decremental PEEP steps, the tidal impedance variation can be regarded as regional compliance. In this study, the behavior of the global dynamic compliance was similar to the regional compliance at the cranial level but not at the caudal level (Fig. 3). Both global compliance and total regional compliance at the cranial level increased initially after lowering PEEP from 15 to 10 cm H_2O PEEP, whereas both global and total regional compliance decreased during the next PEEP steps (Fig. 4). For decremental PEEP steps, this finding is explained by the classical finding that compliance increases as a result of the release of overdistended alveoli until collapse increases and lowers the compliance. This has been described in detail previously by Suarez-Sipmann et al. (13). Inspection of the individual regional compliance behavior of the different ROIs showed different PEEP levels at which the regional compliance is maximal (Fig. 3). This finding

means that there is no single optimal PEEP for the whole lung. This principle was previously proven with pressure impedance curves in lavaged pigs by Kunst et al. (14) and explained in an excellent review by Hickling (15). In those studies, multiple pressure impedance curves in the dorsal to ventral direction were generated from an inspiratory pressure-volume curve, and different lower and upper inflection points were found. However, only the dorsal to ventral direction was studied. In the present study, we have also shown, on the basis of EIT in patients at the bedside, that this is true in the caudal to cranial direction. Our study results are also in agreement with a recent CT study of acute respiratory distress syndrome patients by Caironi et al. (16), who also found different optimal PEEP values in the cranio-caudal direction to counteract the different superimposed pressures calculated by CT. The different superimposed pressure levels on each lung section are one of the most important explanations for the difference in optimal PEEP levels, as we found in the present study. Especially in the dorsal and caudal lung regions, the weight of the heart and edematous lung tissue in respiratory failure will cause atelectasis and surfactant depletion.

We calculated EELV changes at both the caudal and cranial lung levels. Both levels showed a comparable pattern, but the rate of lung volume loss differed non-significantly during the decremental PEEP steps. This finding could be explained by increased lung volume due to atelectasis at the basal part of the lung at lower PEEP levels. However, calculation of lung volume changes on the basis of regional EIT measurement calibrated with a global lung parameter (tidal volume) does have limitations. In our former study, we showed that EIT-based lung volume calculation does not correlate well with lung volume measured using a multibreath nitrogen washout technique (9). Also, the use of a global lung parameter (for example, tidal volume) with unpredictable distribution limits these calculations. Furthermore, this study shows that ventilation distribution during PEEP changes can vary not only in a ventral to dorsal direction but also in a cranial to caudal direction. Therefore, calculations made using regional lung impedance data can be used only as an indication of global lung volume changes. In addition, when calculating lung volume during PEEP steps on the basis of EIT and tidal volume, it is necessary to calculate the mean impedance to volume ratio from the high and low PEEP levels, as this ratio is not constant when PEEP is changed.

The present study was performed in patients after cardiothoracic surgery because these patients demonstrate a uniform lung condition and are highly responsive to PEEP. We earlier showed that using a PEEP strategy combined with recruitment maneuvers in patients after cardiothoracic surgery, lung volume could be preserved, inflammatory reaction could be reduced and increase in right ventricular

afterload could be minimized (17-19). Several factors are known to affect lung function postoperatively, including cardiopulmonary bypass (which is known to release inflammatory mediators), mechanical ventilation and mechanical compression of the left lung during the surgical procedure itself (20).

EIT-based measurements taken at multiple thoracic levels have some inherent methodological issues. Because of the position and shape of the thoracic cage and lungs, not all lung regions can be studied. In this study, we positioned the cranial EIT belt at the highest possible level, just under the armpits, taking measurements at a lung level just above the hilus (Fig. 1). The most caudal belt was positioned just under the nipples at the sixth or seventh intercostal space, so that measurements were taken just above the diaphragm (Fig. 1). At this level, the diaphragm could enter the EIT eclipse and thereby change the amount of lung volume during PEEP steps. This would be especially true in critically ill patients who are known to have reduced EELV (21) and at high and low PEEP levels. In our study, we tried to avoid these effects by selecting smaller ROIs away from the middle of the EIT eclipse, where the effects of the diaphragm are most likely. The tidal impedance variation to tidal volume ratio still decreased, but it was lower compared to the ROIs covering all anatomical lung tissue (Fig. 4B). Also, the heart moves upward and sideways as PEEP decreases, thereby taking more space within the left portion of the electrode plane, as can be anticipated from Figure 2. Furthermore, the EIT device used in the present study measures an eclipse with a central diameter of 5 to 10 cm. Moreover, the distance between the two belts was about 10 cm, indicating that almost all of the accessible lung tissue for EIT was measured with both belts. Although techniques for three-dimensional (3D) measurement of impedance are under development (22-24), they are not yet available in clinical practice. On the basis of the findings of the present study, measurement of ventilation distribution in the cranial to caudal direction with 3D EIT would provide additional information, although the most caudal region would still provide the most clinically relevant information in the ICU population.

Conclusions

On the basis of the findings of this study, ventilation distribution shifts not only from the dorsal to ventral region but also from the caudal to cranial level during decremental PEEP. Also, in the mechanically ventilated patients in our study, the PEEP level at which regional compliance was maximal differed for the dependent and nondependent lung regions as well as for the caudal and cranial lung levels, suggesting that no single optimal PEEP exists for all lung regions. The clinical implications of these findings are that, during clinical PEEP titration, one has to realize that the results are dependent on the measurement location. Also, a lung-monitoring system (for example, EIT) at the bedside is a prerequisite to finding the optimal balance in finding the best ventilatory settings. Further, EIT measurements taken at two thoracic levels, that is, the caudal and cranial parts of the lung, provides additional information for monitoring ventilation distribution during mechanical ventilation in the whole lung.

Key messages

• Ventilation distribution changes measured using EIT during a PEEP trial were comparable to CT, but the EIT monitoring measurements were taken at the bedside.
• The optimal PEEP level differs between lung regions: from the cranial to caudal region and from the ventral to dorsal region.
• To monitor ventilation distribution during a PEEP trial, EIT measurements should be taken in the caudal and cranial parts of the lung.
• If EIT is measured at a caudal lung level during high and low PEEP steps, the results can be influenced by the diaphragm's entering the EIT eclipse.

References

1. Frerichs I, Dargaville PA, Dudykevych T, Rimensberger PC. Electrical impedance tomography: a method for monitoring regional lung aeration and tidal volume distribution? *Intensive Care Med* 2003; 29: 2312-6.
2. Putensen C, Wrigge H, Zinserling J. Electrical impedance tomography guided ventilation therapy. *Curr Opin Crit Care* 2007; 13: 344-50.
3. Zhao Z, Steinmann D, Frerichs I, Guttmann J, Moller K. PEEP titration guided by ventilation homogeneity: a feasibility study using electrical impedance tomography. *Crit Care* 2010; 14: R8.
4. Gattinoni L, Caironi P, Pelosi P, Goodman LR. What has computed tomography taught us about the acute respiratory distress syndrome? *Am J Respir Crit Care Med* 2001; 164: 1701-11.
5. Bikker IG, Leonhardt S, Reis MD, Bakker J, Gommers D. Bedside measurement of changes in lung impedance to monitor alveolar ventilation in dependent and non-dependent parts by electrical impedance tomography during a positive end-expiratory pressure trial in mechanically ventilated intensive care unit patients. *Crit Care* 2010; 14: R100.
6. Meier T, Luepschen H, Karsten J, Leibecke T, Grossherr M, Gehring H, et al. Assessment of regional lung recruitment and derecruitment during a PEEP trial based on electrical impedance tomography. *Intensive Care Med* 2008; 34: 543-50.
7. Victorino JA, Borges JB, Okamoto VN, Matos GF, Tucci MR, Caramez MP, et al. Imbalances in regional lung ventilation: a validation study on electrical impedance tomography. *Am J Respir Crit Care Med* 2004; 169: 791-800.
8. Frerichs I, Hinz J, Herrmann P, Weisser G, Hahn G, Dudykevych T, et al. Detection of local lung air content by electrical impedance tomography compared with electron beam CT. *J Appl Physiol* 2002; 93: 660-6.
9. Bikker IG, Leonhardt S, Bakker J, Gommers D. Lung volume calculated from electrical impedance tomography in ICU patients at different PEEP levels. *Intensive Care Med* 2009; 35: 1362-7.
10. Markhorst DG, Groeneveld AB, Heethaar RM, Zonneveld E, van Genderingen HR. Assessing effects of PEEP and global expiratory lung volume on regional electrical impedance tomography. *J Med Eng Technol* 2009; 33: 281-7.
11. Costa EL, Borges JB, Melo A, Suarez-Sipmann F, Toufen C, Jr., Bohm SH, et al. Bedside estimation of recruitable alveolar collapse and hyperdistension by electrical impedance tomography. *Intensive Care Med* 2009; 35: 1132-7.
12. Luepschen H, Meier T, Grossherr M, Leibecke T, Karsten J, Leonhardt S. Protective ventilation using electrical impedance tomography. *Physiol Meas* 2007; 28: S247-S260.
13. Suarez-Sipmann F, Bohm SH, Tusman G, Pesch T, Thamm O, Reissmann H, et al. Use of dynamic compliance for open lung positive end-expiratory pressure titration in an experimental study. *Crit Care Med* 2007; 35: 214-21.
14. Kunst PW, Bohm SH, Vazquez dA, Amato MB, Lachmann B, Postmus PE, et al. Regional pressure volume curves by electrical impedance tomography in a model of acute lung injury. *Crit Care Med* 2000; 28: 178-83.
15. Hickling KG. Reinterpreting the pressure-volume curve in patients with acute respiratory distress syndrome. *Curr Opin Crit Care* 2002; 8: 32-8.
16. Caironi P, Cressoni M, Chiumello D, Ranieri M, Quintel M, Russo SG, et al. Lung Opening and Closing During Ventilation of Acute Respiratory Distress Syndrome. *Am J Respir Crit Care Med* 2009.

17. Reis Miranda D, Gommers D, Struijs A, Dekker R, Mekel J, Feelders R, et al. Ventilation according to the open lung concept attenuates pulmonary inflammatory response in cardiac surgery. *Eur J Cardiothorac Surg* 2005; 28: 889-95.

18. Reis Miranda D, Struijs A, Koetsier P, van Thiel R, Schepp R, Hop W, et al. Open lung ventilation improves functional residual capacity after extubation in cardiac surgery. *Crit Care Med* 2005; 33: 2253-8.

19. Reis Miranda D, Klompe L, Mekel J, Struijs A, van Bommel J, Lachmann B, et al. Open lung ventilation does not increase right ventricular outflow impedance: An echo-Doppler study. *Crit Care Med* 2006; 34: 2555-60.

20. Carvalho EM, Gabriel EA, Salerno TA. Pulmonary protection during cardiac surgery: systematic literature review. *Asian Cardiovasc Thorac Ann* 2008; 16: 503-7.

21. Bikker IG, van Bommel J, Dos Reis MD, Bakker J, Gommers D. End-expiratory lung volume during mechanical ventilation: a comparison to reference values and the effect of PEEP in ICU patients with different lung conditions. *Crit Care* 2008; 12: R145.

22. Graham BM, Adler A. Electrode placement configurations for 3D EIT. *Physiol Meas* 2007; 28: S29-S44.

23. Xu G, Wang R, Zhang S, Yang S, Justin GA, Sun M, et al. A 128-electrode three dimensional electrical impedance tomography system. *Conf Proc IEEE Eng Med Biol Soc* 2007; 2007: 4386-9.

24. Metherall P, Barber DC, Smallwood RH, Brown BH. Three-dimensional electrical impedance tomography. *Nature* 1996; 380: 509-12.

Chapter 6

Global and regional parameters to visualize the 'best' PEEP during a PEEP trial in a porcine model with and without acute lung injury

Bikker IG, Blankman P, Specht P, Bakker J, Gommers D.

Minerva Anestesiol 2013 Sep;79(9):983-92.

Abstract

Background:
Setting the optimal level of positive end-expiratory pressure (PEEP) in critically ill patients remains a matter of debate. 'Best' PEEP is regarded as minimal lung collapse and overdistention to prevent lung injury. In this study, global and regional variables were evaluated in a porcine model to identify which variables should be used to visualize 'best' PEEP.

Methods:
Eight pigs (28-31 kg) were studied during an incremental and decremental PEEP trial before and after the induction of acute lung injury (ALI) with oleic acid. Arterial oxygenation, compliance, lung volume, dead space, esophageal pressure and electrical impedance tomography (EIT) were recorded at the end of each PEEP step.

Results:
After ALI, 'best' PEEP was comparable at 15 cm H_2O between regional compliance of the dorsal lung region by EIT and the global indicators: dynamic compliance, arterial oxygenation, alveolar dead space and venous admixture. After ALI, the intratidal gas distribution was able to detect regional overdistention at 15 cm H_2O PEEP. 'Best' PEEP based on transpulmonary pressure was lower and no optimal level could be found based on lung volume measurements alone. In addition, the recruitment phase significantly improved end-expiratory lung volume, PaO_2, venous admixture and regional and global compliance, both in ALI and the 'healthy' lung.

Conclusion:
Most of the evaluated parameters indicate comparable 'best' PEEP levels. However, a combination of these parameters, and especially EIT-derived intratidal gas distribution, might provide additional information. The application of lung recruitment was beneficial in both ALI and the 'healthy' lung.

Introduction

Although mechanical ventilation is essential for the survival of most patients with respiratory failure admitted to the intensive care unit (ICU), it can exacerbate lung damage and may even be the primary factor in acute lung injury (ALI) (1). Protective ventilatory strategies have been introduced to attenuate ventilator-induced lung injury, including reduction of tidal volume and prevention or minimization of lung collapse and overdistention by optimal setting of the positive end-expiratory pressure (PEEP) (2-4). However, large clinical trials comparing high vs. low PEEP with fixed low tidal volume were unable to demonstrate differences in mortality. Even a meta-analysis could only demonstrate a significant difference in the subgroup with ARDS patients, in favor of higher PEEP protocols (5). Therefore, endpoints other than mortality are needed to guide PEEP settings in individual patients.

Currently, PEEP setting is often guided by global lung parameters such as arterial oxygenation, global compliance and dead space ventilation (3;6;7). PEEP is generally only increased after increased oxygen requirements following the ARDSnet protocol; however, this may also lead to overdistention in some of these patients (3;8). The highest dynamic compliance obtained from a decremental PEEP titration has been proposed as a tool to find an optimal balance between the mechanical forces acting on the lung and set ‘best’ PEEP (6;7;9). However, global indicators are not specific for regional lung collapse or overdistention and, especially in patients with respiratory failure, the lung may be atelectatic or consolidated in the dependent regions (10). Talmor et al. used transpulmonary pressures measured with an esophageal balloon to set the ‘best’ PEEP, aiming at preventing alveolar collapse by counterbalancing the gravitational force of the dependent lung with an equal or higher PEEP level than the measured intra-thoracic pressure (11). In addition, electrical impedance tomography (EIT), a real-time imaging method, provides a cross-sectional image of the ventilated lung and is able to monitor regional ventilation distribution (12-14). Using this method, our group has shown the possibility to differentiate between collapse and overdistention during a PEEP trial in mechanically ventilated patients (15;16). In addition, Lowhagen et al. introduced the EIT parameter 'intratidal gas distribution' to monitor the effect of PEEP on gas distribution to optimize PEEP in ARDS patients (14).

Therefore, in a porcine model before and after the induction of ALI, this study evaluates global and regional variables to identify which parameters should be used to describe ‘best’ PEEP. Another aim is to establish whether EIT

parameters have additional value over the existing parameters in order to describe the 'best' PEEP.

Materials and Methods

Ethics Statement

The study was approved by the Erasmus MC Animal Experimental Committee (Permit nr. 142-08-01) and conducted in accordance with the National Guidelines for Animal Care and Handling. The entire experiment was performed under midazolam and fentanyl anesthesia. After completion of the experiment, animals were sacrificed with pentobarbital overdose. All efforts were made to minimize suffering.

Animal preparation and data acquisition

(A more extensive description is available as an online supplement)

In eight Yorkshire/Landrace pigs (28-31 kg) anesthesia was induced and venous access established. Cervical tracheotomy was performed and the pigs were connected to the EVITA XL ventilator (Dräger Medical, Lubeck, Germany). Both an arterial and pulmonary artery thermodilution catheter were placed.
Respiratory variables were monitored with the NICO (Novametrix, Wallingford, CT, USA), the LUFU system for end-expiratory lung volume (EELV) measurements (Dräger Medical, Lubeck, Germany), the Bicore 2 for esophageal pressures (Cardinal Health, Palm Springs, CA) and with EIT (EIT evaluation kit 2, Dräger, Lübeck, Germany). The EIT data were analyzed offline, using special software (EITdiag, Dräger Medical, Lubeck, Germany), EIT images were subdivided into two symmetrical non-overlapping ventral to dorsal oriented layers defined as regions of interest (ROI).

Acute lung injury model

Oleic acid (OA) administration is a well-studied model of induction of ALI (17). The mechanism is probably mainly due to a direct toxic effect on the endothelial wall. Grotjohan et al. described a titrated approach (mean dose 0.12 ml/kg) which resulted in a stable, reproducible model of ALI, with increased shunt fraction, decreased compliance, increased lung weight and alveolar edema in all lung lobes on chest X-ray (18). Hemodynamically, they observed decreased blood pressure and increased pulmonary artery pressure, mainly caused by vasoconstriction of pulmonary muscular arteries. The authors recommended a

stabilization period of at least 30 min after the last OA injection (18), whereas we applied a 90-min period.

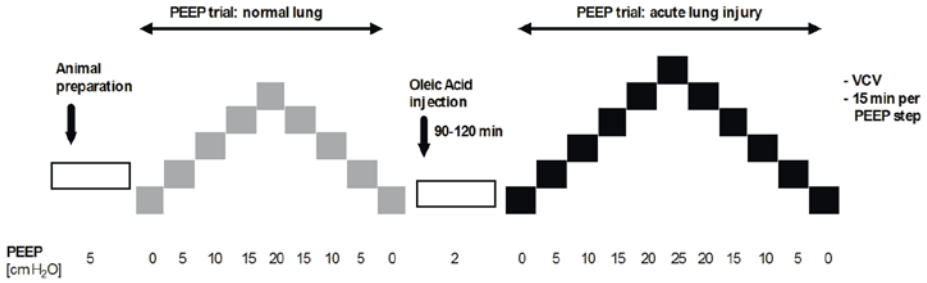

Figure 1: Schematic drawing of the ventilatory procedures throughout the experiment. Increases and decreases of positive end-expiratory pressure (PEEP). The highest applied PEEP step was considered as the recruitment maneuver, 20 cm H_2O before and 25 cm H_2O after the induction of acute lung injury with oleic acid. VCV; volume controlled ventilation.

Experimental protocol

Ventilatory procedures throughout the experiment are shown in Figure 1. The animals were ventilated in volume-controlled mode. Tidal volume was set at 8 ml/kg, respiratory rate adjusted to a $PaCO_2$ of 4.5-6.0 kPa and the inspiratory to expiratory ratio was 1:2. The FiO_2 was set at 0.8 to obtain adequate levels of blood gases even after induction of ALI and to minimize the development of resorption atelectasis. These settings were kept constant throughout the experiment. Ventilation was started at a PEEP of 5 cm H_2O.

After completion of the surgical protocol and the set-up of all necessary equipment, a stabilization period of at least 30 min followed. Baseline values were recorded and the PEEP was stepwise increased by 5 cm H_2O from 0 to 20 and then decreased in the same manner to 0. Each step lasted for about 15 min. Severe ALI was induced by OA injection (OA C18H34O2 Boom BV, Meppel, the Netherlands) (0.14±0.03 ml/kg) into the right atrium with the PEEP set at 2 cm H_2O. Each animal received a bolus of 0.1 ml/kg injected over 20 min to obtain a PaO_2 below 10 kPa, if necessary additional injections were given to reach this target. During OA injection a continuous infusion (0.02-0.28 mcg/kg/min) of norepinephrine (100 mcg/ml, Centrafarm Services BV, Etten-Leur, The Netherlands) through the ear vein was given to maintain a stable mean arterial pressure. After a steady state of at least 1.5 h after the induction of ALI,

measurements were repeated during a PEEP trial from 0 to 25 cm H_2O PEEP and again decremental steps to 0 cm H_2O PEEP, in the same manner as before ALI. The highest PEEP level during each trial was considered as the recruitment phase. During the PEEP trials, norepinephrine was administered to maintain a stable perfusion pressure; no additional fluid boluses were used to avoid fluid overload during the decremental PEEP steps.

At baseline and at the end of each step during the PEEP trials the following variables were obtained: airway and esophageal pressures during an inspiratory and expiratory hold of 5 s, arterial and mixed venous blood gases, volumetric capnography and EIT recordings; also, EELV was measured by changing the FiO_2 from 0.8 to 0.6 and from 0.6 to 0.8. In addition, hemodynamic and ventilatory data were obtained.

In the present study, 'best' PEEP was defined for each individual parameter, aiming at the lowest amount of lung collapse and, if possible, an optimum between lung collapse and lung overdistention. Therefore, maximum EELV, (regional) compliance and PaO_2, the lowest venous admixture and dead space just before a significant increased value, and transpulmonary pressures equal to or exceeding zero during end expiration were defined as 'best' PEEP.

Statistical analysis

Statistical analysis was performed with Graphpad software package (Graphpad software Inc. San Diego, USA). Results are expressed as mean □ SD for normal distributed data and median + interquartile range (IQR) for not normally distributed data. The Shapiro-Wilk normality test was used to evaluate the distribution of all data. Changes of EELV, PaO_2, venous admixture, dead space and regional and global compliance were evaluated by the Wilcoxon test. Correlation between dynamic and static compliance was evaluated using Pearson's correlation. *P*-values < 0.05 were considered statistically significant.

Table 1: Hemodynamic variables during the PEEP trials, before and after induction of acute lung injury (ALI)

PEEP (cm H_2O)	0	5	10	15	20	25	20	15	10	5	0
Before ALI											
CO (L/min)	4.4 (2.0)	4.6 (2.3)	4.2 (1.7)	3.9 (1.9)	3.3 (1.7)			3.4 (1.4)	3.7 (1.3)	4.1 (0.9)	4.7 (1.0)
HR (bpm)	85 (27)	86 (39)	91 (33)	90 (56)	107 (69)			110 (64)	99 (52)	87 (34)	91 (24)
MAP (mmHg)	92 (21)	87 (29)	94 (24)	85 (28)	88 (6)			83 (29)	90 (20)	97 (25)	105 (19)
CVP (mmHg)	4 (8)	5 (8)	7 (8)	9 (4)	10 (8)			9 (9)	8 (7)	7 (8)	6 (9)
PAP (mmHg)	16 (10)	16 (6)	19 (8)	20 (8)	23 (9)			22 (9)	20 (9)	19 (10)	20 (8)
Lactate (mmol/L)	0.7 (1.1)	0.6 (0.8)	0.7 (0.7)	0.6 (1.0)	0.6 (1.0)			0.7 (1.0)	0.7 (0.7)	0.6 (0.5)	0.6 (0.5)
Norepinephrine (mcg/kg/min)	0.00 (0.00)	0.00 (0.00)	0.00 (0.00)	0.02 (0.12)	0.10 (0.25)			0.05 (0.15)	0.00 (0.05)	0.00 (0.00)	0.00 (0.00)
After ALI											
CO (L/min)	4.2 (1.1)	4.3 (3.0)	4.1 (2.7)	3.9 (1.5)	3.3 (0.9)	2.8 (0.9)	2.6 (0.6)	3.0 (1.8)	3.5 (1.9)	3.9 (1.6)	5.2 (1.5)
HR (bpm)	128 (53)	129 (86)	127 (45)	131 (30)	151 (55)	169 (75)	163 (75)	167 (67)	151 (45)	152(46)	163 (25)
MAP (mmHg)	86 (28)	91 (25)	97 (24)	100 (22)	81 (25)	79 (27)	81 (25)	84 (43)	91 (28)	89 (31)	78 (36)
CVP (mmHg)	4 (6)	7 (7)	8 (7)	8 (7)	10 (7)	10 (7)	9 (7)	7 (7)	6 (8)	6 (8)	6 (7)
PAP (mmHg)	48 (13)	40 (9)	42 (10)	38 (12)	36 (13)	37 (14)	35 (10)	31 (9)	41 (13)	41 (11)	45 (12)
Lactate (mmol/L)	0.8 (0.7)	0.8 (0.6)	0.9 (0.5)	0.9 (0.4)	1.0 (0.5)	1.1 (0.6)	0.9 (0.6)	0.9 (0.7)	1.0 (0.7)	0.9 (0.7)	1.4 (1.1)
Norepinephrine (mcg/kg/min)	0.12 (0.23)	0,08 (0.10)	0.07 (0.07)	0.08 (0.08)	1.12 (0.37)	0.32 (0.55)	0.25 (0.57)	0.12 (0.37)	0.12 (0.35)	0.12 (0.22)	0.12 (0.53)

Data are presented as mean (SD); CO, cardiac output; HR, heart rate; MAP, mean arterial pressure; CVP, central venous pressure; PAP, pulmonary artery pressure

Results

Hemodynamic data during the PEEP trial are given in Table1.

The effect of PEEP on the global lung parameters is shown in Figure 2. The induction of ALI led to a significant decrease in EELV, dynamic compliance and arterial oxygenation, and to a significant increase in both dead space and venous admixture at the corresponding PEEP level. Dynamic compliance was highly correlated with the static compliance of the respiratory system (p <0.001, r=0.97, R_2=0.94).

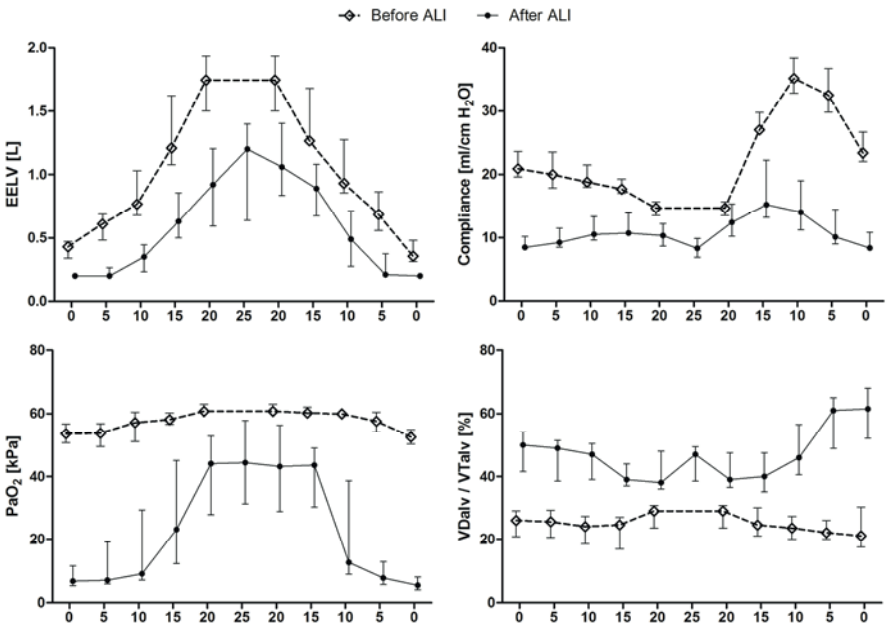

Figure 2: End-expiratory lung volume (EELV), dynamic compliance, the ratio between alveolar dead space to alveolar tidal volume (VDalv/VTalv) and PaO2 are shown at each positive end-expiratory pressure (PEEP) step. The highest applied PEEP step was considered as the recruitment maneuver, 20 cm H_2O before and 25 cm H_2O after the induction of acute lung injury (ALI) with oleic acid. Data are presented as median with interquartile range.

Best PEEP values are presented in Table 2. Before and after ALI, EELV had its maximum at the highest PEEP level directly after a recruitment maneuver (Fig. 2). Between identical PEEP levels before and after recruitment, EELV was significantly higher at PEEP 15, 10 and 5 cm H_2O before ALI and at PEEP 20, 15 and 10 cm H_2O after ALI (Fig. 2). Dynamic compliance was maximal at PEEP level of 10 cm H_2O before ALI and at 15 cm H_2O after ALI (Fig. 2). After ALI, alveolar dead space showed a significant increase after decreasing PEEP from 10 to 5 cm

H_2O (Fig. 2). Before and after ALI, PaO_2 was maximum at the highest PEEP level (Fig. 2). Between identical PEEP levels before and after recruitment, PaO_2 was significantly higher at PEEP 15, 10 and 5 cm H_2O before ALI, and at PEEP 20 and 15 cm H_2O after ALI (Fig. 2). Venous admixture was minimum at the highest PEEP level and showed a significant increase after decreasing the PEEP level from 15 to 10 cm H_2O, and during the subsequent PEEP steps before and after ALI.

Table 2: Best PEEP values for the different parameters, before and after induction of acute lung injury (ALI)

	Definition	Before ALI	After ALI
End-expiratory lung volume	Highest	20	25
PaO_2	Highest	5	15
Venous admixture	Lowest	15	15
Alveolar dead space fraction	Lowest	5	15
Compliance (global)	Highest	10	15
EIT regional compliance			
- ventral	Highest	5	0
- dorsal	Highest	10	15
EIT intratidal gas distribution		5	10
Transpulmonary pressure	End expiratory ≥ 0	5	10

All values are expressed in cm H_2O PEEP; PaO_2, arterial oxygen tension; EIT, electrical impedance tomograpy

Transpulmonary pressures during an inspiration and expiration hold at the studied PEEP levels are shown in Figure 3. During expiration, transpulmonary pressure was zero at 5 cm H_2O PEEP before ALI and at 10 cm H_2O PEEP after ALI (Fig. 3). During decremental PEEP steps, lower inspiratory transpulmonary pressures were required to maintain constant tidal volumes at the decremental PEEP steps, as compared to the equal incremental PEEP steps. This was not present in the expiratory curves (Fig. 3).

Regional compliance calculated from the EIT in the dorsal to ventral orientated ROIs is shown in Figure 4. Higher regional compliance, caused by decreased inspiratory pressures while maintaining equal tidal volumes, was found with decreasing PEEP. This was observed especially before ALI, and was more pronounced for the dorsal region (Fig.4). The maximal regional compliance for the dorsal region during the decremental PEEP trial after the recruitment maneuver

was 10 cm H_2O before ALI, and 15 cm H_2O after ALI (Fig. 4). The contribution of the dependent lung regions to the inspiration increased at higher PEEP levels.

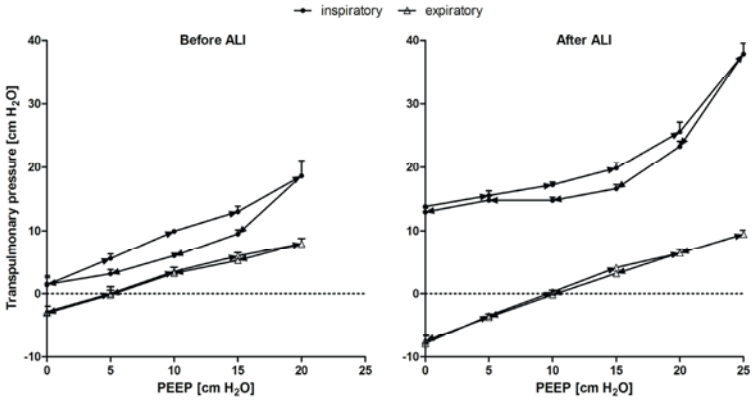

Figure 3: Transpulmonary pressures during inspiration and expiration holds at the applied PEEP levels, before (left panel) and after (right panel) the induction of acute lung injury (ALI) with oleic acid. Transpulmonary pressure was calculated by subtracting the esophageal pressure from the airway pressure. Solid dots represent inspiratory values and open triangles represent expiratory values. Data are presented as mean + standard error of the mean.

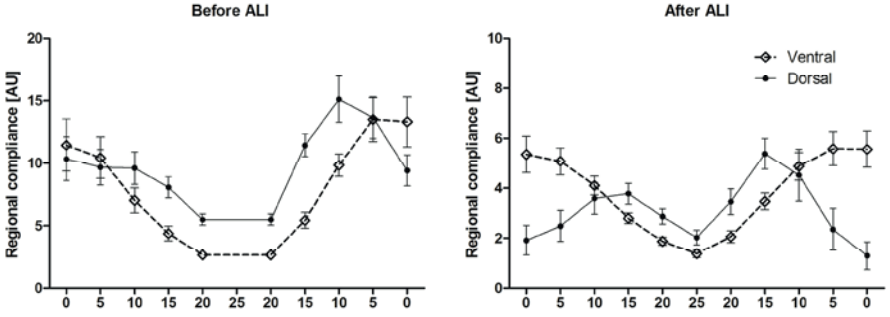

Figure 4: Regional compliance in the ventral and dorsal regions of interest at the applied PEEP levels, before and after the induction of lung injury (ALI) with oleic acid. Regional compliance was calculated by dividing tidal impedance variation by the applied driving pressure. Data are presented as mean + standard error of the mean.

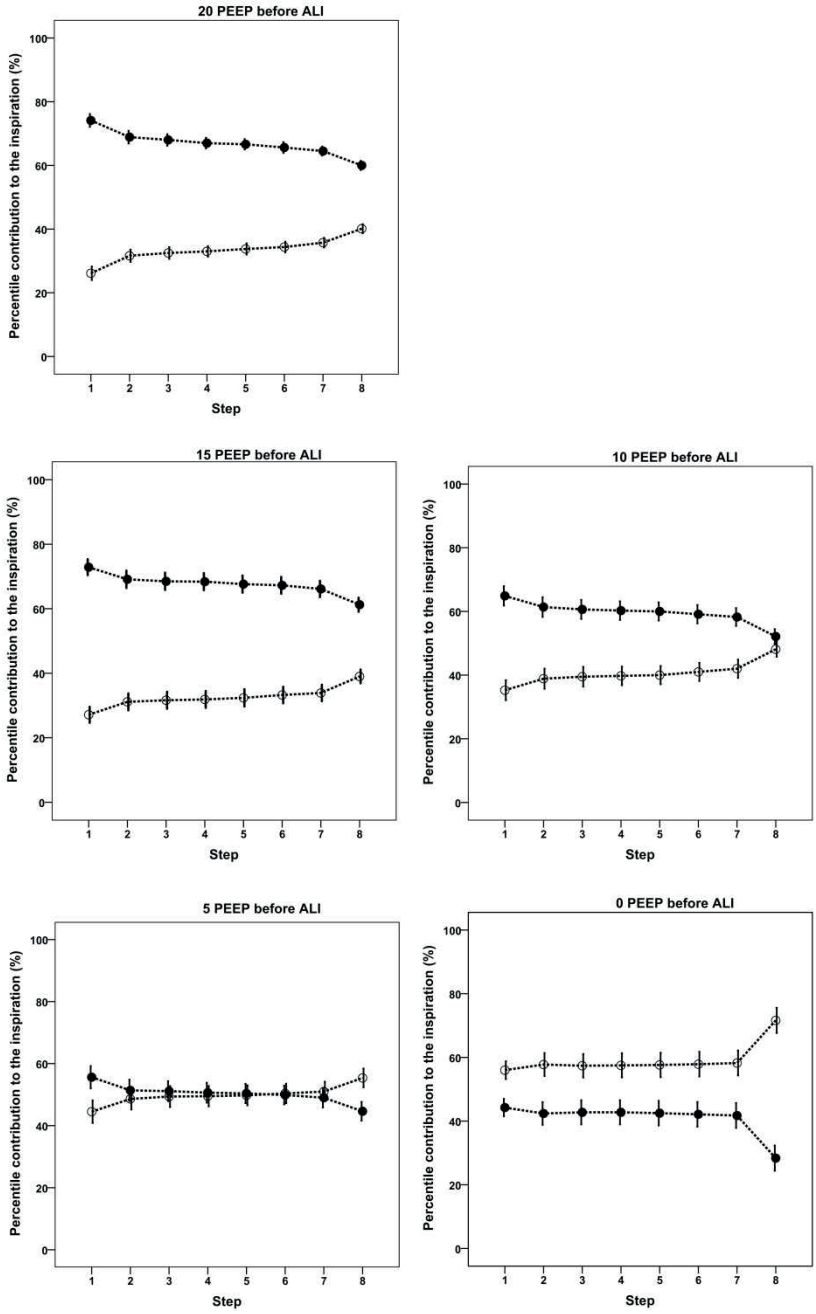

Figure 5a: Data are shown as mean ± SE. Intratidal gas distribution before acute lung injury (ALI). *Solid line* = non-dependent lung region; *dashed line* = dependent lung region

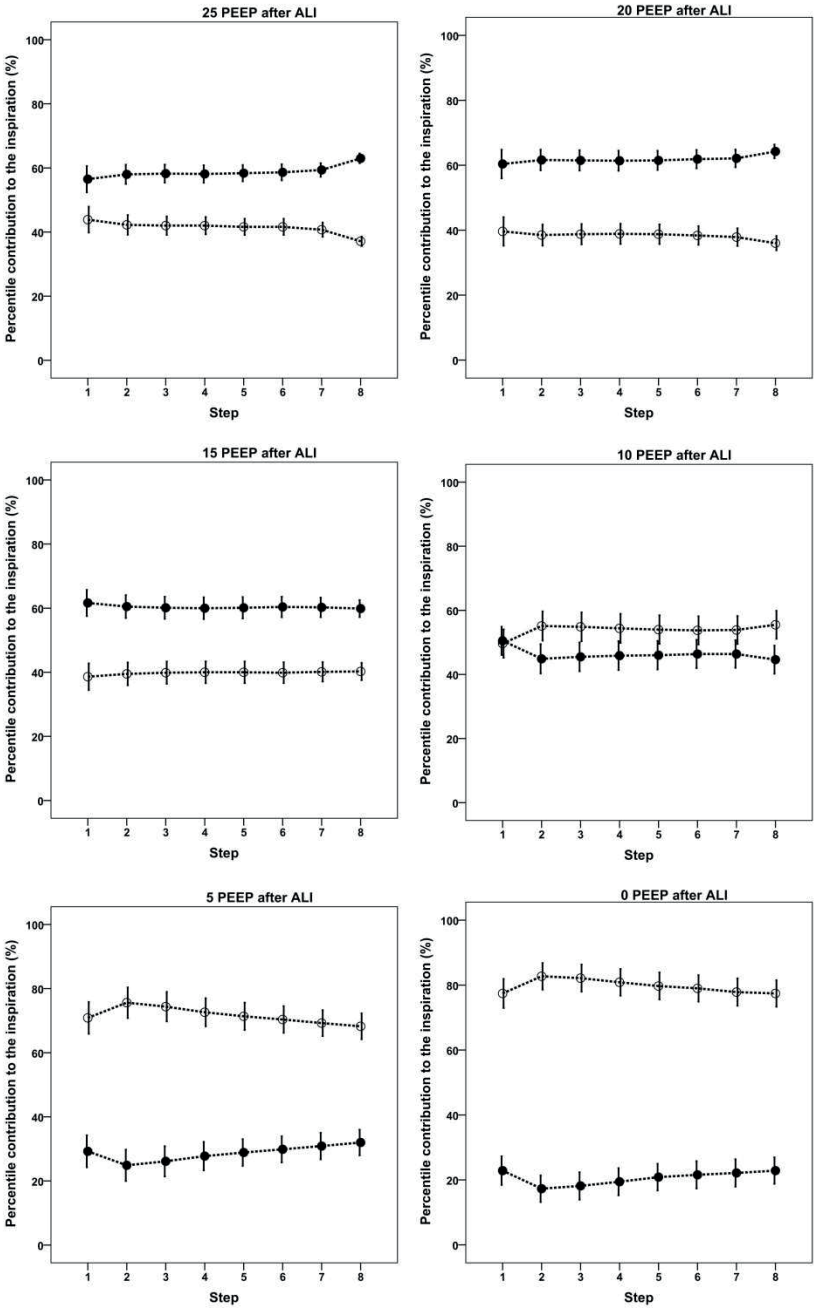

Figure 5b: Data are shown as mean ± SE. Intratidal gas distribution after acute lung injury (ALI). *Solid line* = non-dependent lung region; *dashed line* = dependent lung region.

Intratidal gas distribution (Fig. 5) shows a significantly different contribution of the dependent and non-dependent regions to the inspiration for each PEEP step after ALI. Also, before ALI, the intratidal gas distribution showed a significant difference between both regions at each PEEP level, except during 5 cm H_2O. At this latter PEEP level, there was a cross-section between the dependent and non-dependent lung region before induction of ALI (Fig. 5). This cross-section indicates the moment at which the non-dependent lung region becomes overdistended, which occurred between 15 and 10 cm H_2O after induction of ALI.

Discussion

In an experimental model of ALI, 'best' PEEP was comparable between regional compliance of the dependent lung region by EIT and the global indicators: dynamic compliance, arterial oxygenation, alveolar dead space and venous admixture. The 'best' PEEP based on transpulmonary pressure was lower in this experimental setting of ALI. The EIT derived intratidal gas distribution was able to identify the onset of overdistention.

In 2000 it was already known that mechanical ventilation with low tidal volume (6 ml/kg) was superior to high tidal volume (12 ml/kg) in patients with ALI or ARDS (1). High tidal volume ventilation in the presence of atelectasis, as seen in patients with ALI/ARDS, leads to overdistention of the 'healthy' aerated lung regions causing barotrauma and volutrauma, and this provokes biotrauma due to lung inflammation with the release of cytokines and mediators. This inflammatory response is called ventilator-induced lung injury and leads to a higher mortality rate (1-3). Studies applying higher PEEP levels showed improved oxygenation and compliance but were unable to further reduce the mortality rate (2, 7). Two meta-analysis studies (including ≥ 3500 patients with ALI or ARDS) reported that a moderate level of PEEP (around 9 cm H_2O) is superior in patients with ALI, whereas high PEEP levels (around 15 cm H_2O) are superior in patients with ARDS (9, 10). Higher PEEP may increase the risk of hyperinflation and a compromise must be found between PEEP-induced alveolar recruitment and prevention of hyperinflation. Also, Gattinoni et al. found extremely variable amounts of potential recruitable lung tissue on CT scanning and this was strongly associated with the response to PEEP (19). Therefore, one should not use a universal level of PEEP but rather the 'best' PEEP level that the individual patient needs at a specific time.

This implies constant re-evaluation of the individual ventilator settings, and the need for an optimal parameter to apply the 'best' PEEP.

Several studies investigated the 'best' PEEP setting during standardized PEEP steps in various forms of lung conditions in both experimental and human subjects (6;7;20;21). Maisch et al. studied 20 anesthetized patients with healthy lungs during incremental and decremental steps of 5 cm H_2O PEEP and compared EELV, arterial oxygenation, compliance and a modified dead space calculation (6). The authors concluded that, in these patients without lung disorders, compliance and dead space were able to detect lung collapse and overdistention and therefore are suitable to guide 'best' PEEP settings (6). In the present study, the lung condition before ALI is comparable to the study of Maisch et al. and the results are similar, except for dead space. In the present study, dead space increased from 15 to 20 cm H_2O, whereas no significant changes occurred thereafter (Fig. 2). This may be due to the influence of shunt with increased $PaCO_2$ in the dead space calculations. Suarez-Sipmann et al. (7) and Carvalho et al. (20), who studied, respectively, lung lavage induced ALI and OA-induced ALI during decremental PEEP steps, showed that compliance was a good parameter to guide 'best' PEEP. Also in the present study, dynamic compliance increased significantly during the decremental PEEP trial after the recruitment phase.

In this study we also evaluated the relation between regional and global parameters and whether they provide additional information. Costa et al. (22) and Meier et al. (23) demonstrated that EIT can be used to monitor regional compliance. In our study, we calculated the regional compliance for each pixel in the EIT matrix and divided them into ventral and dorsal ROIs. As the studied pigs were ventilated in volume-controlled mode with constant tidal volume, a change in regional impedance was caused by a change in the driving pressure and a spatial change in tidal volume distribution between PEEP steps. Others also described the change in tidal volume distribution with EIT and CT scanning in a ventral to dorsal manner during PEEP change (10;15;24). In our study, regional compliance decreased as a result of the increased driving pressure after ALI. The optimal value differed not only before and after the induction of lung injury, but also between the dorsal to ventral ROIs. In the dependent lung parts the optimum value increased from 10 to 15 cm H_2O PEEP after the induction of lung injury. A study by Lowhagen et al. showed that the relatively new parameter 'intratidal gas distribution' (which divides regional tidal impedance into eight iso-volume parts) was able to identify intratidal regional recruitment and overdistention (14). These authors showed that the contribution of the dependent lung regions to the inspiration increases at higher PEEP levels. This is also seen in the present study

for both lung conditions. In the present study we could identify the onset of overdistension, but this was only for one slice of the lung. EIT might be a practical new tool for optimal PEEP setting, especially as an adjunct to existing parameters.

Esophageal pressures were recorded during inspiration and expiration holds to calculate the transpulmonary pressure. Pelosi et al. studied the relation between esophageal pressure and the actual pleural pressure at three ventral to dorsal thoracic levels, in six supine dogs with OA respiratory failure (25); esophageal pressure underestimated the dorsal pleural pressure by about 4 cm H_2O and overestimated the ventral pleural pressure by about 6 cm H_2O. This was confirmed in the present study in which the 'best' PEEP based on transpulmonary pressure was 5 cm H_2O lower compared to the other parameters.

An important finding of the present study is that a recruitment maneuver in combination with PEEP, both before and after the induction of ALI, significantly improved EELV, PaO_2, venous admixture and regional and global compliance (Figs. 2 and 3). This means that not only patients with respiratory failure, but also patients with 'healthy' lungs benefit from a recruitment maneuver in conjunction with an adequate PEEP level. This is in agreement with the study of Maisch et al. in which a recruitment maneuver during PEEP titration, combined with a PEEP of 10 cm H_2O improved EELV, PaO_2, compliance and dead space in anesthetized, intubated patients just before surgery (6). Although the stable animal model used in the present study showed a high potential for lung recruitability (as evidenced by changes in shunt fraction), the extent of lung recruitability may differ from that in ARDS patients (19). Potential limitations of this study are the use of relatively large PEEP steps of 5 cm H_2O. Although this enabled measurement in both normal and injured lungs, a PEEP trial with smaller steps is more suitable to identify the 'best' PEEP in an individual patient. We did not use a formal recruitment maneuver, but used phases of recruitment and regarded the highest used PEEP as the recruitment maneuver; these levels resulted in high inspiratory and transpulmonary pressures exceeding most conventional recruitment maneuvers. Also, we did not use CT scanning to identify hyperinflation and alveolar collapse; however, the application of the highest and lowest PEEP levels in the present study has clearly been shown on CT scanning to induce lung overdistention and lung collapse, respectively (7;20).

Conclusion

In this experimental model of ALI, parameters that describe only lung volume, such as EELV, are inappropriate to indicate 'best' PEEP level. The EIT derived parameter, intratidal gas distribution, was able to indicate at which PEEP level overdistention of the non-dependent lung started; however, this was only for one slice of the lung. Therefore, we believe that the combination of parameters might provide important additional information. Best PEEP should prevent lung collapse and also overdistention; therefore, a combination of parameters should resemble both of these physiological principles. Finally, this study indicates that the application of a recruitment maneuver might be of benefit not only in ALI, but also in a healthy lung.

Key messages

- Most of the physiological parameters indicate comparable 'best' PEEP levels. In this animal study, after lung injury 'best' PEEP was found at 15 cm H_2O for most parameters. In healthy lungs, the 'best' PEEP ranged from 5 to 15 cm H_2O.
- Evaluating the best PEEP level with regional compliance (EIT) in supine patients might result in different optimal pressures, depending on the ventral to dorsal position.
- The EIT parameter 'intratidal gas distribution' was able to indicate the onset of overdistention; this parameter might provide additional useful information when combined with the existing parameters
- Application of a lung recruitment phase was beneficial in both the injured and in the 'healthy' lung.

Methods supplement

Animal preparation

In eight healthy female crossbred Yorkshire/Landrace pigs (28-31 kg) anesthesia was induced with an intramuscular injection of 2.5 mg/kg azaperon (Stresnil 40 mg/ml, Janssen Pharmaceutical, Beerse, Belgium), 30 mg/kg ketamine (Ketalin 100 mg/ml, Ceva Sante Animale BV Maassluis, the Netherlands) and 1 mg/kg midazolam (Dormicum 5 mg/ml, Roche Nederland BV, Woerden, the Netherlands). After induction, the pigs were placed in supine position on a thermo-controlled operation table to maintain body temperature. Intravenous access was obtained by cannulation of an ear vein; anesthesia was maintained with a combination of intravenous infusion of midazolam (1-2 mg/kg/h) and sufentanil (0.01-0.02 mg/kg/h; Sufenta forte 0.05 mg/ml Janssen-Cilag BV, Tilburg, the Netherlands). Muscle relaxation was obtained with infusion of pancuronium bromide (0.15-0.35 mg/kg/h; pavulon 2 mg/ml, NV Organon, Oss, the Netherlands). Through a midline cervical tracheotomy, an endotracheal tube (9.0 Fr) was placed in the trachea. After tracheotomy the pigs were connected to the EVITA XL ventilator (Dräger Medical, Lubeck, Germany).

A catheter was inserted through the right carotid artery for measurement of arterial blood pressure and sampling of blood. A pulmonary artery thermodilution catheter (PAC) (7.5 Fr Edwards Lifesciences, Irvine CA, USA) was inserted through the right jugular vein in the pulmonary artery for the continuous measurement of cardiac output, central venous pressure (CVP), pulmonary artery pressure (PAP), mixed venous hemoglobin oxygen saturation (SvO_2) and central body temperature. The position of the PAC was guided by pressure waveforms, while passing the heart. All catheters for measuring blood pressure were flushed with normal saline containing a low dose of heparin (5 IU/ml; Leo Pharma BV, Breda, the Netherlands) to avoid clotting in the catheters. A catheter was also placed in the urinary bladder to avoid urine retention.

Monitoring equipment

Airway pressure, flow, volume and volume-based capnography were sampled continuously during the experiment (NICO, Novametrix, Wallingford, CT, USA) and dead space was calculated with the Bohr-Enghoff equation. End-expiratory lung volume (EELV) was measured with the LUFU system (Dräger Medical, Lubeck, Germany) connected to the EVITA XL ventilator, which is described in detail elsewhere (26;27). Esophageal pressures were measured with the SmartCath® esophageal catheter connected to the Bicore 2 (Cardinal Health,

Palm Springs, CA, USA). The esophageal balloon was inserted to a depth of 50 cm from the incisors and filled with 1 ml of air. Placement was confirmed by the increase of cardiac artefacts as the balloon was withdrawn from the stomach. Electrical impedance measurements were performed at each step in the protocol during 2 min with a silicone belt with 16 integrated electrocardiographic electrodes placed around the thoracic cage at a juxtadiaphragmatic level, connected with an EIT device (EIT evaluation kit 2, Dräger, Lübeck, Germany). EIT data were generated by application of a small alternating electrical current of 5 mA at 50 kHz.

EIT analysis

EIT data were stored and analyzed offline using special software (EITdiag, Dräger, Lübeck, Germany). The EIT scans consist of images of impedance with a 32 x 32 color-coded matrix relative to the lowest impedance during the PEEP trial (rel. ΔZ). The difference between rel. ΔZ at the end of inspiration and expiration is defined as tidal impedance variation. This tidal impedance variation is visualized in the functional EIT (fEIT) image, which contains tidal impedance variation per pixel (32 x 32 matrix) averaged over 1 min. For analysis of the regional compliance, the EIT images were subdivided into two symmetrical non-overlapping ventral to dorsal oriented layers defined as regions of interest (ROI). Regional compliance was calculated following equation 1.

The intratidal gas distribution (Fig. 5a + 5B) is calculated according to the study of Lowhagen et al. (14). The inspiratory part of the global tidal impedance variation (TIV) curve was divided in eight equal volume sections. The corresponding time points are translated to the regional TIV curves. In this way the contribution from both lung regions to the inspiration can be calculated.

$$regional\ compliance = \frac{\sum tidal\ impedance\ \mathrm{var}iation\ (AU)}{driving\ pressure\ (cm\ H_2O)}$$

Equation 1

References

1. Ricard JD, Dreyfuss D, Saumon G. Ventilator-induced lung injury. Curr Opin Crit Care 2002; 8: 12-20.
2. Amato MB, Barbas CS, Medeiros DM, Magaldi RB, Schettino GP, Lorenzi-Filho G, et al. Effect of a protective-ventilation strategy on mortality in the acute respiratory distress syndrome. N Engl J Med 1998; 338: 347-54.
3. ARDSnet. Ventilation with lower tidal volumes as compared with traditional tidal volumes for acute lung injury and the acute respiratory distress syndrome. The Acute Respiratory Distress Syndrome Network. N Engl J Med 2000; 342: 1301-8.
4. Guerin C. The preventive role of higher PEEP in treating severely hypoxemic ARDS. Minerva Anestesiol 2011; 77: 835-45.
5. Briel M, Meade M, Mercat A, Brower RG, Talmor D, Walter SD, et al. Higher vs lower positive end-expiratory pressure in patients with acute lung injury and acute respiratory distress syndrome: systematic review and meta-analysis. JAMA 2010; 303: 865-73.
6. Maisch S, Reissmann H, Fuellekrug B, Weismann D, Rutkowski T, Tusman G, et al. Compliance and dead space fraction indicate an optimal level of positive end-expiratory pressure after recruitment in anesthetized patients. Anesth Analg 2008; 106: 175-81.
7. Suarez-Sipmann F, Bohm SH, Tusman G, Pesch T, Thamm O, Reissmann H, et al. Use of dynamic compliance for open lung positive end-expiratory pressure titration in an experimental study. Crit Care Med 2007; 35: 214-21.
8. Grasso S, Stripoli T, De Michele M, Bruno F, Moschetta M, Angelelli G, et al. ARDSnet ventilatory protocol and alveolar hyperinflation: role of positive end-expiratory pressure. Am J Respir Crit Care Med 2007; 176: 761-7.
9. Bikker IG, van Bommel J, Dos Reis MD, Bakker J, Gommers D. End-expiratory lung volume during mechanical ventilation: a comparison to reference values and the effect of PEEP in ICU patients with different lung conditions. Crit Care 2008; 12: R145.
10. Gattinoni L, Caironi P, Pelosi P, Goodman LR. What has computed tomography taught us about the acute respiratory distress syndrome? Am J Respir Crit Care Med 2001; 164: 1701-11.
11. Talmor D, Sarge T, Malhotra A, O'Donnell CR, Ritz R, Lisbon A, et al. Mechanical ventilation guided by esophageal pressure in acute lung injury. N Engl J Med 2008; 359: 2095-104.
12. Blankman P, Gommers D. Lung monitoring at the bedside in mechanically ventilated patients. Curr Opin Crit Care 2012; 18: 261-6.
13. Frerichs I, Dargaville PA, Dudykevych T, Rimensberger PC. Electrical impedance tomography: a method for monitoring regional lung aeration and tidal volume distribution? Intensive Care Med 2003; 29: 2312-6.
14. Lowhagen K, Lundin S, Stenqvist O. Regional intratidal gas distribution in acute lung injury and acute respiratory distress syndrome--assessed by electric impedance tomography. Minerva Anestesiol 2010; 76: 1024-35.
15. Bikker IG, Leonhardt S, Reis MD, Bakker J, Gommers D. Bedside measurement of changes in lung impedance to monitor alveolar ventilation in dependent and non-dependent parts by electrical impedance tomography during a positive end-expiratory pressure trial in mechanically ventilated intensive care unit patients. Crit Care 2010; 14: R100.
16. Bikker IG, Preis C, Egal M, Bakker J, Gommers D. Electrical impedance tomography measured at two thoracic levels can visualize the ventilation distribution changes at the bedside during a decremental positive end-expiratory lung pressure trial. Crit Care 2011; 15: R193.

17. Sum-Ping ST, Symreng T, Jebson P, Kamal GD. Stable and reproducible porcine model of acute lung injury induced by oleic acid. Crit Care Med 1991; 19: 405-8.

18. Grotjohan HP, van der Heijde RM, Jansen JR, Wagenvoort CA, Versprille A. A stable model of respiratory distress by small injections of oleic acid in pigs. Intensive Care Med 1996; 22: 336-44.

19. Gattinoni L, Caironi P, Cressoni M, Chiumello D, Ranieri VM, Quintel M, et al. Lung recruitment in patients with the acute respiratory distress syndrome. N Engl J Med 2006; 354: 1775-86.

20. Carvalho AR, Jandre FC, Pino AV, Bozza FA, Salluh J, Rodrigues R, et al. Positive end-expiratory pressure at minimal respiratory elastance represents the best compromise between mechanical stress and lung aeration in oleic acid induced lung injury. Crit Care 2007; 11: R86.

21. Tusman G, Suarez-Sipmann F, Bohm SH, Pech T, Reissmann H, Meschino G, et al. Monitoring dead space during recruitment and PEEP titration in an experimental model. Intensive Care Med 2006; 32: 1863-71.

22. Costa EL, Borges JB, Melo A, Suarez-Sipmann F, Toufen C, Jr., Bohm SH, et al. Bedside estimation of recruitable alveolar collapse and hyperdistension by electrical impedance tomography. Intensive Care Med 2009; 35: 1132-7.

23. Meier T, Luepschen H, Karsten J, Leibecke T, Grossherr M, Gehring H, et al. Assessment of regional lung recruitment and derecruitment during a PEEP trial based on electrical impedance tomography. Intensive Care Med 2008; 34: 543-50.

24. Kunst PW, de Vries PM, Postmus PE, Bakker J. Evaluation of electrical impedance tomography in the measurement of PEEP-induced changes in lung volume. Chest 1999; 115: 1102-6.

25. Pelosi P, Goldner M, McKibben A, Adams A, Eccher G, Caironi P, et al. Recruitment and derecruitment during acute respiratory failure: an experimental study. Am J Respir Crit Care Med 2001; 164: 122-30.

26. Maisch S, Boehm SH, Weismann D, Reissmann H, Beckmann M, Fuellekrug B, Meyer A, Schulte Am EJ. Determination of functional residual capacity by oxygen washin-washout: a validation study. Intensive Care Med. 2007; 33: 912-6.

27. Weismann D, Reissmann H, Maisch S, Fullekrug B, Schulte J. Monitoring of functional residual capacity by an oxygen washin/washout; technical description and evaluation. J Clin.Monit.Comput. 2006; 20: 251-60.

Chapter 10

End-expiratory lung volume-guided PEEP setting in mild acute respiratory distress syndrome: a randomized controlled trial

Blankman P, Bikker IG, Gommers D.

Submitted

Chapter 11

Summary and conclusions

Samenvatting en conclusie

Summary and conclusions

Mechanical ventilation remains an important, but also potentially hazardous, part of treatment in the intensive care unit (ICU). **Chapter 1** provides a short overview and brief history of mechanical ventilation, and describes the associated adverse events. Mechanical ventilation not only affects the lung, but can also influence the whole body due to the release of inflammatory mediators. Over the years, various protective ventilation strategies have been developed; one of these is the open lung concept (OLC), which aims at minimal lung damage by opening up collapsed alveoli with a recruitment maneuver. To prevent collapse of the recruited alveoli an optimal level of positive end-expiratory pressure (PEEP) has to be applied, which prevents both collapse and alveolar overdistention.

The work presented in this thesis studied this optimal level of PEEP, as well as other promising techniques, that might be helpful during clinical decision-making. These techniques include measurement of end-expiratory lung volume (EELV), use of electrical impedance tomography (EIT), and measurement of lung inhomogeneity.

EELV might be a valuable tool to optimize respiratory settings in mechanically ventilated patients. EELV represents the functional residual capacity (FRC) of the mechanically ventilated patient. Historically, although it was possible to measure EELV in ventilated patients, it remained difficult and impractical due to the bulky, costly and invasive equipment required. The study In **Chapter 2** investigated whether a novel, non-invasive nitrogen washout/washin technique was able to perform stable EELV measurements. In addition, baseline EELV measurements were performed in adult ICU patients without lung disorders, primary lung disorders (e.g. pneumonia) and/or secondary lung disorders (e.g. acute lung injury associated with abdominal sepsis). We found that EELV was markedly lower in all groups compared to predicted sitting FRC. In addition, it was shown that PEEP-induced changes in EELV not only represent recruitment or derecruitment, but are also the result of inflation or deflation of already ventilated lungs. Therefore, EELV alone is not the 'magic bullet' but, in combination with compliance, can provide additional information to optimize the ventilator settings.

In **Chapter 3** we studied this non-invasive, nitrogen washout/washin technique in pediatric patients undergoing cardiac surgery. The feasibility and precision of this device was evaluated in hospitalized children. It was found that the ICU ventilator with an in-built nitrogen washout/washin EELV technique could measure EELV with precision and could easily be used for mechanically ventilated pediatric patients.

Therefore, in **Chapter 4** we studied optimization of EELV using an alveolar recruitment strategy (ARS) and maintaining lung volume with adequate PEEP in children undergoing cardiac surgery for congenital heart disease. Mechanical ventilation with PEEP in children is known to decrease pulmonary blood flow and thereby cardiac output. A progressive fall in cardiac output occurs when increasing PEEP higher than 6 cm H_2O. This might be explained by overdistention of aerated lung areas in the presence of atelectatic lung areas. With this in mind, an open lung ventilation strategy was investigated in pediatric patients undergoing cardiac surgery for congenital heart disease. It was found that the use of 8 cm H_2O PEEP in combination with ARS resulted in a significant increase in the compliance and EELV, and a decrease in the $PaCO_2$ – $PetCO_2$ difference, compared to 8 cm H_2O PEEP without ARS and to controls ventilated with zero PEEP. No significant differences between the three strategies were found for heart rate, mean arterial pressure, and right atrial pressure.

Besides EELV measurements, the wash-out curve can be used to study ventilation inhomogeneity. In **Chapter 5** we describe an oxygen sensor that is used to measure EELV and a computer program (available at the bedside) that was used to compare six well-established indexes of ventilatory inhomogeneity calculated from the oxygen washout curve. The oxygen washout curves were provided by the rapid oxygen sensor of the LUFU EELV measurement system. Inhomogeneity was tested in a porcine model before and after induction of acute lung injury (ALI) at four different levels of PEEP. Six indexes were assessed: lung clearance index, mixing ratio, Becklake index, multiple breath alveolar mixing inefficiency, moment ratio and pulmonary clearance delay. The moment ratio and the lung clearance index appeared to be the most favorable for integration with oxygen washout curves as judged by high precision and agreement with earlier findings. Studies are currently in progress to evaluate the indexes in critically ill patients.

EIT is an exciting and promising technique to monitor regional ventilation distribution real-time at the bedside. The technique is based on the injection of small currents and voltage measurements using electrodes on the skin surface generating cross-sectional images representing impedance change in a slice of the thorax. EIT can be used to calculate impedance differences based on global or tidal lung volume. Earlier studies suggested a linear relationship between Δimpedance and Δvolume, which enables accurate calculation of dynamic EELV changes based on impedance changes. In **Chapter 6** we studied this relationship and found a significant but low correlation and moderate agreement between ΔEELV and change in lung volume calculated from the ΔEELI. Also, the amount of

impedance for each mL of tidal volume differed between patients and also varied at different PEEP levels. This was explained by the non-homogenous distribution of lung ventilation. Therefore, in critically ill patients, it was concluded that the assumption of a linear relationship between a change in global tidal impedance and tidal volume should not be used to calculate EELV.

Functional EIT (fEIT) images, or ventilation distribution maps, are ideal for real-time lung monitoring before and directly after a change in ventilator setting. These fEIT images contain the tidal impedance variation for each pixel of the EIT matrix, creating an image of ventilation distribution. In **Chapter 7** fEIT images displaying tidal breathing were examined in 14 ICU patients with or without lung disorders. Images made before a reduction in PEEP were subtracted from those recorded after each PEEP step, to evaluate regional increase/decrease in tidal impedance in each EIT pixel. Using this technique at the bedside for the individual patient, we found that EIT could clearly visualize improvement and loss of ventilation in dependent and non-dependent lung parts after decreasing PEEP in patients both with and without lung disorders. This methodology has now been implemented in the software of the clinically available EIT equipment and can be used to evaluate clinical therapies (e.g. change in PEEP or tidal volume, prone positioning).

Normally EIT is measured at a single caudal thoracic level just above the diaphragm. This level is of particular importance because most atelectasis due to mechanical ventilation can be expected at this level. In **Chapter 8** ventilation distribution was calculated at two different levels in 12 mechanically ventilated patients after cardiac surgery. Measurements were taken at four PEEP levels, at both the cranial and caudal lung levels. We found that tidal impedance variation divided by tidal volume significantly decreased on caudal EIT slices, whereas this measurement increased on the cranial EIT slices. The dorsal-to-ventral impedance distribution, expressed according to the center of gravity index, decreased during the decremental PEEP trial at both EIT levels. Optimal regional compliance differed at different levels of PEEP. It was concluded that in these patients there is a shift from caudal to cranial and from dorsal to ventral during a decremental PEEP trial.

In **Chapter 9** all available and clinically used global and regional variables were evaluated in a porcine model to identify which variable should be used to visualize ‘best’ PEEP. Currently, the PEEP setting is often guided by global lung parameters such as arterial oxygenation, compliance, or dead space ventilation. However, global indicators are not specific for regional overdistention, especially in the non-dependent part. Incremental and decremental PEEP trials were performed in pigs before and after the induction of ALI with oleic acid. Arterial oxygenation,

compliance, lung volume, dead space, esophageal pressure and EIT were recorded. It was found that the intratidal gas distribution based on EIT was able to detect regional overdistention and the 'best' PEEP could be estimated by even distribution of tidal ventilation between the dependent and non-dependent lung parts. It was concluded that most of the evaluated parameters indicate comparable 'best' PEEP levels, but a combination of these parameters, and especially EIT-derived intratidal gas distribution, might provide additional information.

Although ventilatory strategies with reduction of tidal volumes have shown to improve mortality in ARDS patients, large clinical trials comparing high vs. low PEEP show conflicting results. Therefore, it is recommended to use PEEP levels tailored to the individual patient, with adequate monitoring to minimize the risk of overstretching of the 'healthy' alveoli. In **chapter 10** we studied in a single-site randomized controlled trial, a ventilatory protocol aiming at normalizing EELV by changing the PEEP levels after lung recruitment. This strategy was compared to the ARDSnet protocol, in which the level of PEEP is based on the amount of FiO_2 used to achieve a peripheral saturation of 88-93%. 37 ALI/ARDS patients according to the New Berlin criteria were included. After initiation of the protocol, PEEP had to be increased in the intervention group to achieve the predicted supine EELV and was slightly decreased in the control group. The PaO_2/FiO_2 ratio remained unchanged in the control group but showed a significant increase in the intervention group during the study time period. No significant differences were found in ventilator-free days and length of stay at the ICU between the two groups. It was concluded that an EELV-guided PEEP strategy was able to restore predicted EELV in patients with mild ARDS and resulted in significantly increased arterial oxygenation but at a higher PEEP level compared to the FiO_2-PEEP table.

In summary, this thesis presents the results of studies aiming at the improvement of bedside PEEP settings to prevent additional lung injury during the challenging task of mechanical ventilation. It is clear that low tidal volume should not only be used in patients with acute respiratory distress syndrome (ARDS) but also in non-ARDS patients on the ICU, and even during mechanical ventilation in the operation room. However, the application of PEEP remains a matter of debate. Our results clearly demonstrate that EELV alone is not the appropriate parameter; the combination of EELV and a lung homogeneity index might be promising but has not yet been tested in patients. In addition, because the intratidal gas distribution based on EIT was able to detect regional overdistention, we believe this could be a promising parameter to describe 'best' PEEP. However, additional studies are required to confirm these results in patients both with and without ARDS.

Samenvatting en conclusie

Mechanische longbeademing blijft een onmisbaar, maar ook potentieel schadelijk deel van intensive care (IC) zorg. In **hoofdstuk 1** geven we een kort overzicht en beschrijving van de geschiedenis van mechanische longbeademing. Ook worden hier belangrijke bijwerkingen beschreven. Mechanische longbeademing beïnvloedt niet alleen de long, maar ook het hele lichaam door vrij zetting van inflammatoire mediatoren. In het verleden zijn beschermende longbeademings strategieën ontwikkeld. Een hiervan is het “Open Long Concept”, wat zicht richt op minimale longschade door het openen van samengevallen longblaasjes (alveoli) met een recruitment manoeuvre. Om het weer samenvallen van deze alveoli te voorkomen , moet een optimaal niveau van positief eind expiratie druk (PEEP) worden gebruikt. Dit voorkomt het samenvallen en tegelijkertijd alveolaire overrekking. Dit proefschrift bestudeert deze optimale PEEP en veelbelovende technieken die klinische beslissingen hierin kunnen ondersteunen. Eind expiratoir long volume (EELV) metingen, Elektrische impedantie tomografie (EIT) en long inhomogeniteit werden bestudeerd.

EELV zou een belangrijk middel kunnen zijn om beademings instellingen te kunnen optimaliseren in beademde patiënten. EELV is de functionele residuaal capaciteit (FRC) van de beademde patiënt. Het was eerder al mogelijk om deze FRC te meten in beademde patiënten. Echter, het bleef moeilijk en onpraktisch omdat grote, kostbare en invasieve apparatuur noodzakelijk was. In **hoofdstuk 2** onderzochten we of een nieuwe, non invasieve stikstof uitwas methode in staat was om stabiele EELV metingen te verrichten. Ook voerden we referentie EELV metingen uit in volwassen IC patiënten zonder longafwijkingen, met primaire longafwijkingen (bijv. longontsteking) en secondaire longafwijkingen (bijv. acuut long falen veroorzaakt door buik sepsis). We vonden dat EELV in alle groepen beduidend verlaagd was vergeleken met het voorspelde zittend FRC gebaseerd op referentie waarden. Ook zagen we dat PEEP geïnduceerde EELV veranderingen niet alleen recruitment of de-recruitment betekenden, maar ook het resultaat waren van inflatie of deflatie van al geventileerde alveoli. Daarom moet EELV op zichzelf niet gezien worden als de ‘magic bullet’, echter in combinatie met long compliantie geeft het aanvullende informatie om beademings instellingen te optimaliseren.

In **hoofdstuk 3** bestuderen we deze non invasieve stikstof uitwas methode in pediatrische patiënten die een cardio chirurgische ingreep ondergaan. We beoordeelden de toepasbaarheid en precisie van deze techniek in kinderen. We vonden hierbij dat dit IC beademingstoestel met ingebouwde stikstof uitwas techniek, EELV met precisie kon meten en dat het gemakkelijk gebruikt kon worden in beademde pediatrische patiënten.

Hierdoor konden we deze techniek in **hoofdstuk 4** gebruiken om een alveolaire recruitment strategie (ARS) te onderzoeken. We bestudeerden de optimalisatie van het EELV door deze ARS en het behouden van long volume met een adequaat niveau PEEP in pediatrische patiënten die een cardio chirurgische ingreep ondergingen voor aangeboren hartafwijkingen. Long beademing met PEEP in kinderen staat bekend omdat het de pulmonale bloed flow en daardoor het hartminuut volume verlaagt. Een progressief dalend hartminuutvolume treedt op bij PEEP hoger dan 6 cm H_2O. Dit zou verklaard kunnen worden door overrekking van al geventileerde alveoli in samenhang met tegelijkertijd samengevallen long gebieden. Daarom onderzochten we een open long beademing strategie (ARS) bij kinderen tijdens hartchirurgie voor aangeboren afwijkingen. We vonden dat het gebruik van 8 cm H_2O PEEP in combinatie met ARS resulteerde in significant hogere compliantie, EELV en een verlaagd $PaCO_2$ – $PetCO_2$ verschil, vergeleken met zowel 8 cm H_2O PEEP zonder ARS, als beademing zonder PEEP. We vonden geen significante verschillen in hartslag, gemiddelde arteriële bloeddruk en rechter atrium druk tussen de drie strategieën.

Naast EELV metingen kan de uitwas curve ook worden gebruikt om ventilatie inhomogeniteit weer te geven. In **hoofdstuk 5** beschrijven we het gebruik van een zuurstof sensor, ontworpen om EELV te meten. Een bedside beschikbaar computer programma werd gebruikt om zes eerder bekende inhomogeniteit indexen te vergelijken die berekend werden uit de zuurstof uitwas curve. Deze zuurstof uitwas curves werden gemeten door de snelle zuurstof sensor van het LUFU eind expiratoir longvolume meetsysteem. Inhomogeniteit werd gemeten in een varkens model voor en na het induceren van acute long schade (ALI) op vier verschillende PEEP niveaus. Zes indexen werden vergeleken: de lung clearance index (LCI), mixing ratio, Becklake index, multiple breath alveolar mixing inefficiency, moment ratio en de pulmonary clearance delay. De moment ratio en LCI index bleken het meest geschikt voor integratie met zuurstof uitwas curves gezien de hoge precisie en overeenkomst met eerder gepubliceerde bevindingen. Onderzoek volgt om deze indexen in ernstig zieke patiënten te beoordelen.

Elektrische impedantie tomografie (EIT) is een veelbelovende techniek om regionale long ventilatie verdeling real-time aan het bed te meten. EIT is een techniek die gebaseerd is op de injectie van elektrische micro stroom en microvoltage metingen met elektrodes op het huidoppervlak. Dit kan vervolgens omgezet worden in dwars doorsnede beelden die impedantie veranderingen laten zien in een doorsnede van de thorax. EIT kan worden gebruikt om impedantie veranderingen te berekenen op basis van teug of globaal longvolume. Eerdere studies suggereerden een lineaire relatie tussen Δimpedantie en Δvolume, wat

accurate berekeningen mogelijk maakt van dynamische EELV veranderingen gebaseerd op impedantie. In **hoofdstuk 6** bestudeerden we deze relatie en vonden dat er een significante, maar lage relatie en gemiddeld agreement was tussen Δ EELV en verandering in longvolume berekend uit Δ long impedantie. Ook de hoeveelheid impedantie per ml teugvolume varieerde tussen patiënten en op verschillende PEEP niveaus. Dit werd verklaard door niet homogeen verdeelde long ventilatie. Daarom kan in ernstig zieke patiënten de aanname van een lineaire relatie tussen globaal teug impedantie en teugvolume niet worden gebruikt om EELV te berekenen.

Functionele EIT (fEIT) beelden of ventilatie distributie beelden zijn zeer geschikt voor real-time long monitoring, zowel voor als direct na een beademings instelling verandering. Deze fEIT beelden bevatten de teug impedantie waarden voor elke pixel van de EIT matrix, waarbij een beeld van ventilatie verdeling wordt gevormd. In **hoofdstuk 7** werden fEIT beelden met daarin de teugvolume informatie onderzocht in 14 IC patiënten met of zonder longafwijkingen. Beelden gemaakt voor stapsgewijze verlaging in PEEP werden in mindering gebracht op deze gemeten na de PEEP stap, om hiermee regionale veranderingen in teug impedantie te evalueren per EIT pixel. Door middel van deze techniek aan het bed van de individuele patiënt, vonden wij dat EIT duidelijk verbetering of verlies in ventilatie in zowel dependent als non-dependent long gebieden kan weergeven tijdens PEEP verandering in patiënten met of zonder longafwijkingen. Deze methodiek is nu geïmplementeerd in een klinisch beschikbaar EIT meetsysteem en kan worden gebruik om klinisch handelen te evalueren (bijv. PEEP of teug verandering, buikligging).

Normaal wordt EIT gemeten op een enkel caudaal thoracaal niveau net boven het diafragma. Dit niveau is het meest interessant, aangezien dit niveau het meest gevoelig is voor atelectase gedurende long beademing. In **hoofdstuk 8** werd ventilatie distributie berekend op twee verschillende thoracale niveaus in 12 beademde patiënten na cardiale chirurgie. Metingen werden verricht op vier PEEP niveaus, op zowel een caudaal als craniaal thoracaal long niveau. We vonden dat teugimpedantie verandering gedeeld door teugvolume significant verminderde op caudale EIT doorsnedes, waarbij deze waarde toenam op de craniale thoracale EIT doorsnedes. De dorsaal naar ventrale ventilatie verdeling, gemeten met de center of gravity index, verminderde gedurende de stapsgewijze PEEP verlaging op beide EIT niveaus. Optimale regionale compliantie verschilde op verschillende PEEP niveaus. We concludeerden dat er een verschuiving van caudaal naar craniaal en van dorsaal naar ventraal is tijdens stapsgewijze PEEP titratie in deze patiënten.

In **hoofdstuk 9**, werden alle beschikbare en klinisch gebruikte globale en regionale variabelen geëvalueerd in een varkensmodel om te onderzoeken welke variabele gebruikt dient te worden om de optimale PEEP te bepalen. Momenteel wordt de PEEP instelling meestal bepaald op basis van globale long parameters zoals arteriële oxygenatie, compliantie of dode ruimte ventilatie. Echter, deze globale parameters zijn niet specifiek voor regionale alveolaire overrekking, zeker in de non-dependent long gebieden. In 8 varkens werd een stapsgewijze PEEP verhoging en verlaging verricht voor en na het induceren van longschade met oliezuur (oleïne). Arteriële oxygenatie, compliantie, long volume, dode ruimte, oesofagiale druk en elektrische impedantie werden gemeten. We vonden dat de intratidale gas verdeling gebaseerd op EIT metingen in staat was om regionale alveolaire overrekking te meten en de optimale PEEP geschat kon worden door gelijke verdeling van regionale teug ventilatie tussen dependent en non-dependent long gebieden. Geconcludeerd werd dat de meeste geëvalueerde parameters vergelijkbare optimale PEEP lieten zien, echter een combinatie van deze, en met name de intratidal gas verdeling, aanvullende informatie kan laten zien.

Beademings strategieën waarbij het teugvolume gereduceerd werd, laten een verbeterde overleving zien in ARDS, echter grote onderzoeken die hoge versus lage PEEP vergeleken, lieten conflicterende resultaten zien. Daarom wordt aanbevolen om een PEEP niveau te gebruiken, welke aan de individuele patiënt aangepast is, met adequate monitoring om het risico op overrekking van gezonde alveoli te minimaliseren. In **hoofdstuk 10** onderzoeken we in een gerandomiseerd onderzoek een beademingsprotocol gericht op het normaliseren van EELV door het PEEP niveau te wijzigen na long recruitment. Dit protocol werd vergeleken met het ARDSnet protocol. Hierin is het PEEP niveau gebaseerd op de FiO_2 noodzakelijk om een perifere saturatie van 88-93% te halen. 37 ALI/ARDS patiënten volgens the New Berlin criteria werden geïncludeerd. Na start van het protocol moest de PEEP in de interventiegroep worden verhoogd om de voorspelde liggende EELV te bereiken, de PEEP werd licht verlaagd in de controlegroep. De PaO_2/FiO_2 ratio bleef onveranderd in de controlegroep, echter steeg significant in de interventie groep gedurende de studie periode. Geen significante verschillen warden gevonden tussen beademingsvrije dagen en duur van IC opname tussen beide groepen. Geconcludeerd werd dat een EELV gestuurde PEEP strategie in staat was om het voorspelde EELV in milde ARDS te herstellen en resulteerde in significant verbeterde arteriële oxygenatie, echter hier was een hoger PEEP niveau voor noodzakelijk vergeleken met de FiO_2-PEEP tabel

Dit proefschrift presenteert de resultaten van diverse onderzoeken gericht op de verbetering van bedside PEEP instelling, gedurende de uitdagende taak van mechanische longbeademing om verdere longschade te voorkomen. Uit eerder onderzoek blijkt dat lage teugvolumes niet alleen in ARDS patiënten gebruikt moeten worden, maar ook in niet-ARDS patiënten op de IC, als gedurende mechanische longbeademing in de operatiekamers. Echter het gebruik en instelling van PEEP blijft een gebied van onderzoek en discussie. Uit onze resultaten blijkt dat EELV alleen niet de juiste parameter is om PEEP in te stellen. Een long inhomogeniteits index, eventueel gecombineerd met EELV, is veelbelovend maar nog niet onderzocht in klinische patiënten. De intratidale gas verdeling gebaseerd op EIT was in staat om regionale alveolaire overrekking te detecteren en lijkt hierom een veelbelovende parameter om de optimale PEEP te bepalen. Verdere onderzoeken zijn nodig om deze resultaten in patiënten met of zonder ARDS te bevestigen.

Dankwoord

Klaar! Eindelijk, na zo'n 8 jaar geleden te zijn begonnen aan deze klus. De totstandkoming van dit proefschrift zou niet mogelijk zijn geweest zonder hulp van de vele mensen die mij geholpen en gesteund hebben. Een aantal wil ik in het bijzonder bedanken.

Allereerst mijn promotor, **Prof. Dr. Diederik Gommers**. Beste Diederik, jou inspirerende visie was de reden om samen met je aan dit project te beginnen. Al in 2004 kwam ik op mijn zoektocht naar een interessant afstudeeronderzoek binnen de Anesthesiologie bij jou uit. Ook toen ging het om beademing en FRC. Je aanbod om weer met deze materie bezig te zijn, kon ik dan ook niet laten gaan. Het waren leerzame en interessante jaren. Ik heb veel van je geleerd! Ik kijk uit naar je oratie.

Prof. Dr. Jan Bakker. Beste Jan, bedankt voor het bieden van de mogelijkheid om dit onderzoek te verwezenlijken op deze mooie Intensive Care.

Prof. dr. Can Ince. Beste Can, bedankt voor het zitting nemen in de leescommissie. Je gedachten en kennis van de fysiologie zorgden voor een zeer waardevolle en aanvullende kijk op IC beademing.

Prof. Dr. Robert Jan Stolker en **Prof Dr. Jozef Kesecioglu**, bedankt voor het zitting nemen in de leescommisie. Beste Robert Jan, dank voor al je adviezen in de afgelopen opleidingsjaren.

Alle **intensivisten,** en in het bijzonder **Jasper van Bommel, Bart van den Berg, Ben van der Hoven, Christine Groeninx en Willy Thijsse**. Bedankt voor alle hulp, begeleiding en gesprekken over beademing en atelectase. Zonder jullie praktische hulp en kennis was het niet gelukt.

Dinis dos Reis Miranda, bedankt voor alle hulp in de afgelopen jaren en in het bijzonder voor het begeleiden van mijn afstudeer onderzoek en de hulp bij de eerste stapjes binnen de statistiek. Ik kon met jou de meest veelzijdige en interessante onderzoeken doen.

Mijn paranimf, jaren lange kamergenoot en goede vriendin **Eva Klijn**. Het onderzoek op de IC werd er veel leuker, levendiger, leerzamer en soms ook roeriger op, nadat je ook begon met jouw onderzoek. Je eerlijke en directe kijk, leidde tot veel verhelderende en weleens stevige gesprekken. Ik hoop dat we snel bij je verdediging kunnen zijn!

Beste **Paul**, het duurde even voor onze samenwerking op gang kwam, ook omdat ik fysiek al van de afdeling weg was. Maar daarna ontstond een uitmuntende samenwerking. Bedankt voor al je hulp. Erg veel waardering voor wat je als student en coassistent hebt weten te bereiken. Ik hoop dat ik je hierbij kon helpen. Succes met het laatste deel van je promotie.

Beste **Michel**, je wist mij, (maar ook Eva) toch voor te zijn. Het was erg leuk om de kamer te delen. Ik heb veel van je gedrevenheid geleerd. Veel succes met je opleiding!

Thierry Scohy en **Carsten Preis,** het was altijd weer ontzettend leuk om met jullie onderzoek te doen. De samenwerking met jullie als ervaren thorax anesthesiologen was erg leerzaam en leverden naast uren bij de volwassen en pediatrische patiënten, ook de mooiste resultaten op.

Een buitengewoon boeiende periode was de tijd op de experimentele afdeling van de Anesthesiologie en Intensive Care. **Patricia Specht** en collega's, bedankt voor al jullie hulp tijdens mijn kamer vullende onderzoektijd.

Mijn collega onderzoekers op de IC, Beste **Tim, Alex, Mo** en alle anderen, dank voor de hulp, gezelligheid en samenwerking.

Beste **Wim Holland**, bedankt voor al je inzet, zelfs na je pensioen. Je visie en de ingewikkelde Matlab programma's waren onvergetelijk.

Onderzoek met nieuwe apparatuur die nog volop in ontwikkeling is, gaat niet zonder een goede samenwerking en technische ondersteuning vanuit de ontwikkelaar. Speciaal wil ik **Luc Bormans** en **Eckhard Teschner** bedanken. Beste Luc, je gedrevenheid en liefde voor beademing was indrukwekkend, bedankt voor alle gesprekken die we hierover konden voeren. Dear Eckhard, Thank you for all your support in those years and the opportunity to work with all these exciting new technologies.

Onderzoek op de Intensive Care, en dan ook aan het bed maken een nauwe samenwerking met de **IC verpleegkundigen, fellows en arts-assistenten** noodzakelijk. Bedankt voor de praktische hulp en vooral jullie geduld! Ook wil ik graag **Koos Jabaai** bedanken voor alle hulp.

Laraine Visser, bedankt voor al het werk en alle correcties, om dit boekwerk en de artikelen te verbeteren.

Alle collega **arts-assistenten, stafleden en anesthesiemedewerkers binnen de Anesthesiologie**, bedankt voor alle gezelligheid, samenwerking, begeleiding en tips!

Alle **vrienden** en mijn **familie,** met in het bijzonder **mijn ouders, broers en zussen.** Bedankt voor de aandacht, de gezelligheid, de goede zorgen, geduld,

en nog veel meer belangrijke dingen. **Pieter**, ik ben erg blij dat ik je kon vragen paranimf te zijn en dat je mij wilt ondersteunen tijdens mijn verdediging.

En als laatste de allerbelangrijkste, **lieve Mariska, Erik en Lars**, jullie zijn alles voor mij. Bedankt voor jullie geduld in de afgelopen jaren.

Curriculum Vitae

Ido Geert Bikker is op 14 oktober 1981 geboren te Noordeloos. Na het voltooien van het VWO in 2000, studeerde hij geneeskunde aan de Erasmus Universiteit te Rotterdam. In 2004 behaalde hij het doctoraal examen en in 2007 het Arts examen. Hierna startte hij met promotie onderzoek op de Intensive Care afdeling van het Erasmus Medisch Centrum te Rotterdam onder begeleiding van Prof. Dr. D. Gommers. Vanaf april 2010 tot heden is hij in opleiding tot Anesthesioloog met als opleider Prof. Dr. R.J. Stolker in het Erasmus Medisch Centrum. Vanaf januari 2015 tot heden is hij zich aan het sub specialiseren binnen de Pijngeneeskunde. Samen met Mariska heeft hij 2 fantastische kinderen; Erik en Lars.

Publications

1. Bikker IG, van BJ, Reis MD, Bakker J, Gommers D. End-expiratory lung volume during mechanical ventilation: a comparison with reference values and the effect of positive end-expiratory pressure in intensive care unit patients with different lung conditions. *Crit Care* 2008; 12: R145.
2. Scohy TV, Bikker IG, Hofland J, de Jong PL, Bogers AJ, Gommers D. Alveolar recruitment strategy and PEEP improve oxygenation, dynamic compliance of respiratory system and end-expiratory lung volume in pediatric patients undergoing cardiac surgery for congenital heart disease. *Paediatr Anaesth* 2009.
3. Bikker IG, Leonhardt S, Bakker J, Gommers D. Lung volume calculated from electrical impedance tomography in ICU patients at different PEEP levels. *Intensive Care Med* 2009; 35: 1362-7.
4. Bikker IG, Scohy TV, Ad JJCB, Bakker J, Gommers D. Measurement of end-expiratory lung volume in intubated children without interruption of mechanical ventilation. *Intensive Care Med* 2009; 35: 1749-53.
5. Bikker IG, Leonhardt S, Reis MD, Bakker J, Gommers D. Bedside measurement of changes in lung impedance to monitor alveolar ventilation in dependent and non-dependent parts by electrical impedance tomography during a positive end-expiratory pressure trial in mechanically ventilated intensive care unit patients. *Crit Care* 2010; 14: R100.
6. Bikker IG, Preis C, Egal M, Bakker J, Gommers D. Electrical impedance tomography measured at two thoracic levels can visualize the ventilation distribution changes at the bedside during a decremental positive end-expiratory lung pressure trial. *Crit Care* 2011; 15: R193.
7. Bikker IG, Blankman P, Specht P, Bakker J, Gommers D. Global and regional parameters to visualize the 'best' PEEP during a PEEP trial in a porcine model with and without acute lung injury. *Minerva Anestesiol* 2013; 79: 983-92.

8. Blankman P, Bikker IG, Gommers D. End-expiratory lung volume-guided PEEP setting in mild acute respiratory distress syndrome: a randomized controlled trial. *Under review: Critical Care.*

9. Blankman P, Hasan D, Bikker IG, Gommers D. Stress and strain calculations at the bedside using non-invasive FRC measurements in mechanically-ventilated ICU patients. *Under review: Acta Anaesthesiologica Scandinavica*.

10. Bikker IG, Gommers D. FRC meting bij beademde patiënten. Optimale beademing door middel van 'bedside long monitoring'.Intensive Care Capita Selecta 2008; 1: 15-22.

11. Gommers D, Bikker IG. FRC measurements in order to optimize PEEP. A practical guide to improve measurements with the Engström Carestation. GE FRC Appliguide 2010.

PhD Portfolio

Name PhD student: Bikker IG Erasmus MC Department: Intensive Care Research School: COEUR	
	Year
General academic skills	
Biomedical English Writing and Communication	2009
Research skills	
Biostatistics, Erasmus winter programme	2008
Introduction clinical research	2008
Weekly research meetings	2008
	2009
In-depth courses	
Intensive Care research	2009
Presentations	
"*FRC-meting noodzakelijk om PEEP in te stellen?*", Vught	2007
"Bedside lung monitoring: EIT & VRI", Refereeravond Intensive Care, Rotterdam	2008
"Longvibraties in beeld: Vibration Response Imaging", Zwolle	2008
"Longvibraties in beeld: Vibration Response Imaging", Veldhoven	2009
"Longvibraties in beeld: Vibration Response Imaging", Symposium inspiration at work, Rotterdam	2009
"Longvibrations envisioned: Vibration Response Imaging", Zweden,	2009
"Effect of PEEP on lung function pediatric cardiac surgery", Research Seminar, intensive Care, Rotterdam	2009
"FRC and ventilatory inhomogeneity" Intensive Care research, Rotterdam	2009
"PEEP and lung function pediatric cardiac surgery", Dept Anesthesiology.	2010
International conferences	
ARF Rotterdam	2007
ISICEM Brussel	2007
ISICEM Berlijn	2008
ISICEM Brussel	2008
ISICEM Lissabon	2008
ISICEM Brussel	2009
ISICEM Wenen	2009
Poster presentation, International conferences	
ARF Rotterdam, "FRC measurements during mechanical ventilation in different types of lung disorders."	2007
ISICEM Brussel, "Functional residual capacity measurement during mechanical ventilation in order to find the optimal positive end-expiratory pressure"	2007

ISICEM Brussel, “FRC measurements during mechanical ventilation in ICU patients”	
ISICEM Lissabon: “Can end-expiratory lung impedance change be used to calculate end-expiratory lung volume adequately during PEEP change?”	2008
ISICEM Lissabon: “EELV is reduced in mechanically ventilated critically ill patients”	2008
ISICEM Brussel: “Measurement of EELV without interruption of mechanical ventilation in pediatric patients”	2008
ISICEM Brussel: “Effect of PEEP on regional ventilation monitored by EIT in mechanically ventilated ICU patients”	2009
ISICEM Wenen, “The TV index: a new index of ventilation inhomogeneity based on oxygen washout curves”	2009
ISICEM Brussel, “Electrical impedance tomography at two thoracic levels provides detailed information about ventilation distribution in the cranial to caudal direction”	2009
ISICEM Brussel, “ISICEM Brussel, “Transpulmonary pressure and ventilation distribution measured with EIT during a PEEP trial in porcine acute lung injury”	2010
	2010
Seminars and workshops	
Research seminar, pulmonary circulation	2007
Research seminar, novel aspects of ICR	2009
Research seminar, Intensive Care	2009
Supervising Master’s theses	
P. Blankman	2011
M. Egal	2009